Investigation of mouse embryonic stem cell pluripotency using a miniaturized platform for high-throughput screenings in 2D or 3D

Zur Erlangung des akademischen Grades eines

DOKTORS DER NATURWISSENSCHAFTEN

(Dr. rer. nat.)

von der KIT-Fakultät für Chemie und Biowissenschaften

des Karlsruher Instituts für Technologie (KIT)

genehmigte

DISSERTATION

von

Tina Tronser

aus

Pforzheim, Deutschland

1. Referent: Priv.-Doz. Dr. Pavel Levkin

2. Referent: Prof. Dr. Martin Bastmeyer

Tag der mündlichen Prüfung: 19. April 2018

Abstract

Stem cells possess unique properties, like the ability to self-renew and the potential to differentiate into various cell types of the whole organism, making them highly valuable for multiple research fields, such as tissue engineering, pharmaceutical research, transplantation and regenerative medicine. However, long-term *in vitro* maintenance of the cell stemness remains challenging and the underlying mechanisms are still not fully understood. *In vivo* stemness and the regulation of the stem cell development is influenced by multiple cues such as the interaction with neighboring cells, the surrounding extracellular matrix and soluble factors, demonstrating the complexity of the stem cell microenvironment. Based on these findings, current research is focused on the development of artificial systems and substrates that mimic this *in vivo* complexity in order to maintain the undifferentiated state of stem cells *in vitro*. Furthermore, high-throughput screening of stem cells is crucial to gain more insights into the underlying mechanisms as well as to identify compounds and factors maintaining stemness. However, limited availability and expandability of stem cells restricts the use of microtiter plates (96- and 384- well plates) for high-throughput screening of stem cells emitting the urge for miniaturized platforms.

Therefore, the objective of this PhD work was to employ and establish artificial substrates that enable culture and maintenance of stem cells using their biochemical, structural and mechanical properties. These artificial substrates and culture systems should simplify culture and further enable high-throughput screenings of stem cells, while maintaining their undifferentiated and pluripotent state. In this work I used a transgenic mouse embryonic stem cell line, stably expressing GFP fused to the pluripotency gene Oct 4 (mESC Oct4-eGFP), allowing direct read-out of the differentiation state of these cells using fluorescence microscopy or flow cytometry.

In the first part, a nanofibrous material, namely bacterial cellulose derived from *Komagataeibacter xylinus,* was applied for the culture of mouse embryonic stem cells proving its potential in maintaining stemness under short-term as well as long-term culture conditions (17 days) while reducing the culture requirements and significantly facilitating conventional culture of mouse embryonic stem cells. This positive effect on maintenance of stemness could be attributed to the structural properties of the bacterial cellulose such as its high surface roughness and porosity.

In the second part of the thesis, the highly chemically defined porous poly(2-hydroxyethyl methacrylate-*co*-ethylene dimethacrylate) (HEMA-EDMA) was exploited to generate a miniaturized platform enabling culture and screening of mouse embryonic stem cells in defined nano- and microliter droplets (80 nL – 25 µL), whilst maintaining their undifferentiated state for up to 72 h. This phenomenon was based on the dual-functionality of the polymer´s micro-nanorough surface topography: maintaining the undifferentiated state of the mouse embryonic stem cells as shown in a previous work (Jaggy *et al.*, 2015). The microroughness and porosity enabled the generation of hydrophilic and superhydrophobic areas exhibiting completely opposite wettabilities, which, in turn, permit spontaneous, pipetting-free formation of an array of microdroplets *via* the effect of discontinuous dewetting.

In the third part of the project, a miniaturized platform, Droplet Microarray, was employed to develop a novel method for the facile single-step formation of high-density arrays of stem cell-based embryoid bodies. Since embryoid bodies are three-dimensional stem cell aggregates that recapitulate the early embryonic development, this approach can be used for high-throughput screening of cells in 3D microenvironments. I used this methodology to perform a high-throughput screening of 774 FDA-approved drugs to identify compounds affecting embryonic development or embryotoxicity.

To conclude, the ability of two artificial substrates, bacterial cellulose and poly(2-hydroxyethyl methacrylate-*co*-ethylene dimethacrylate) (HEMA-EDMA), to maintain the undifferentiated state of mouse embryonic stem cells based on their surface topography and to facilitate conventional culture methods was demonstrated. Further, the potential of the Droplet Microarray for high-throughput screenings of stem cells under conditions of prolonged inhibition of stem cells' spontaneous differentiation was demonstrated. These materials can both be useful for applications in the field of stem cell research, pharmacological testing and tissue engineering.

Zusammenfassung

Stammzellen weisen einzigartige Eigenschaften, wie die Fähigkeit zur Selbsterneuerung und das Potenzial sich in eine Vielzahl von Zelltypen zu differenzieren, auf. Aufgrund dieser Fähigkeiten sind sie in Forschungsgebieten wie "Tissue Engineering", pharmazeutischer Forschung, Transplantations- und regenerativer Medizin von großer Bedeutung. Jedoch ist die Langzeit-Erhaltung dieser Fähigkeiten (stemness) anspruchsvoll und die zugrundeliegenden Mechanismen sind noch nicht vollständig bekannt. *In vivo* werden Stammzellen in einem komplexen System aus vielen unterschiedlichen Faktoren, wie Interaktion mit benachbarten Zellen, extrazellulärer Matrix und löslichen Faktoren, beeinflusst. Ein Fokus der aktuellen Forschung liegt daher in der Entwicklung von Systemen und Substraten, welche diese Komplexität imitieren und somit den undifferenzierten Zustand der Stammzellen *in vitro* erhalten. Zusätzlich werden innerhalb der Forschung Hochdurchsatz-Screenings durchgeführt, um einen tiefergehenden Einblick der Differenzierung zugrundeliegenden Mechanismen zu erhalten sowie Wirkstoffe zu identifizieren, die die Stammzellentwicklung regulieren. Dabei limitieren die begrenzte Verfügbarkeit und Vermehrbarkeit der Stammzellen die Möglichkeit konventionelle Mikrotiterplatten (96- und 384-well Platten) für Hochdurchsatz-Screenings von Stammzellen zu verwenden, wodurch die Notwendigkeit miniaturisierter Plattformen erkennbar wird.

Die Zielsetzung dieser Promotion war somit die Etablierung und Anwendung artifizieller Substrate für die Kultivierung von Stammzellen, welche die Stammzellidentität durch ihre biochemischen, strukturellen und mechanischen Eigenschaften erhalten, die Kultivierung von Stammzellen vereinfachen und zudem Hochdurchsatz-Screenings an Stammzellen ermöglichen. Die hier verwendete Zelllinie ist eine embryonale Stammzelllinie aus der Maus, welche GFP, das an das Pluripotenzgen Oct 4 gekoppelt ist, stabil exprimiert und somit eine direkte Auswertung der Differenzierung der mausembryonalen Stammzellen mittels Fluoreszenzmikroskopie ermöglicht.

Im ersten Teil dieser Arbeit wurde ein nanofibrilläres Material, eine aus *Komagataeibacter xylinus* gewonnene bakterielle Zellulose, für die Kultivierung von mausembryonalen Stammzellen verwendet. Es konnte gezeigt werden, dass dieses Material das Potenzial aufweist, die Stammzellidentität unter Kurzzeit- und

Langzeit-Kultivierung (17 Tage) zu erhalten aufweist und die Stammzellkultivierung somit durch Reduzierung der Anforderungen signifikant vereinfacht. Dieser positive Effekt konnte dabei auf die strukturellen Eigenschaften, wie Oberflächenrauheit und Dicke der bakteriellen Zellulose zurückgeführt werden.

Im zweiten Teil wurde das chemisch hoch definierte, poröse poly(2-hydroxyethyl methacrylat-*co*-ethylen dimethacrylat) (HEMA-EDMA) verwendet, welches das Potenzial hat eine miniaturisierte Plattform zu generieren, die die Kultivierung und das Screening von Stammzellen in definierten Nano- und Mikrotropfen (80 nL -25 µL) bei zeitgleichem Erhalt des undifferenzierten Zustandes der Stammzellen bis zu 72 h ermöglicht. Dies basiert auf der doppelten Funktionalität der mikro-nanorauen Oberflächenstruktur des Polymers: Nämlich erstens auf dem Erhalt des undifferenzierten Zustandes der embryonalen Stammzellen, wie in Jaggy et al. bereits gezeigt (Jaggy *et al.*, 2015), und zweitens auf der Möglichkeit hydrophile und superhydrophobe Flächen zu generieren. Diese Flächen weisen Unterschiede in der Benetzbarkeit auf und durch den Effekt eines diskontinuierlichen Entnetzungsprozesses („discontinuous dewetting") wird innerhalb eines Schrittes ein aus mehreren Mikrotropfen bestehenden Array gebildet.

Im dritten Teil des Projektes wurde diese miniaturisierte Plattform, das Droplet Microarray, zur einfachen Herstellung eines dichten Arrays verwendet, das aus multiplen Embryoid Bodies besteht, die in den einzelnen Mikrotropfen getrennt voneinander vorliegen. Da Embryoid Bodies als dreidimensionale Stammzellaggregate die frühe Embryonalentwicklung rekapitulieren, ermöglichte die Nutzung dieser neuen Methode das Durchführen eines Hochdurchsatz-Screenings von 774 von der FDA zugelassenen Wirkstoffen und somit die Identifizierung von Wirkstoffen mit Auswirkungen auf die Embryonalentwicklung oder mit embryotoxischen Effekten.

Zusammenfassend konnte die Fähigkeit zweier artifizieller Substrate, nämlich bakterielle Zellulose und poly(2-hydroxyethyl methacrylat-*co*-ethylen dimethacrylat) (HEMA-EDMA), gezeigt werden den undifferenzierten Zustandes von mausembryonalen Stammzellen durch die Substrat-Oberflächenstruktur zu erhalten, sowie konventionelle Methoden der Stammzellkultivierung zu vereinfachen. Des Weiteren konnte das Potenzial des Droplet Microarray, Hochdurchsatz-Screenings an Stammzellen bei zeitgleicher Langzeitinhibierung deren Differenzierung durchzuführen, gezeigt werden. Abschließend kann gesagt werden, dass eine Anwendung beider hier

gezeigten Substrate in den Bereichen Stammzellforschung, pharmazeutischer Forschung und „Tissue Engineering" von großem Nutzen sein kann.

Table of Contents

List of Figures

List of Tables

List of Abbreviations

µM	micro Molar
BC	bacterial cellulose
BC-FD	bacterial cellulose - freeze dried
BC-RT	bacterial cellulose - room temperature dried
BC-W	bacterial cellulose - wet (never dried)
DMA	Droplet Microarray
DMEM	Dulbecco's Modified Eagle's Medium
EB	embryoid bodies
ECM	extracellular matrix
EDMA	ethylene dimethacrylate
ESC	embryonic stem cells
FDA	Food and Drug Administration
FP	filter paper
GFP	green fluorescent protein
HEMA	2-hydroxethyl methacrylate
HTS	high-throughput screening
LIF	leukemia inhibitory factor
MEF	mouse embryonic fibroblasts
mESC	mouse embryonic stem cells
Oct4	octamer 4 binding protein
PBS	phosphate-buffered saline
PI	propidium iodide
wt%	weight percent

1 Introduction

1.2 Stem cells and their potential for research

Over the last decades stem cells have gained high importance in biological research as they possess unique properties distinguishing them from other cell types. These properties, termed stemness, are the ability of self-renewal through repeated division and the potential to differentiate into various cell subtypes of the organism, thereby generating multiple tissues (Figure 1) (Kobel & Lutolf, 2010; Laustriat *et al.*, 2010; Seki & Fukuda, 2015). The differentiation potential in turn can range depending on the stem cell type, from multipotent stem cells (e.g. adult stem cells) with the ability to differentiate only into a subset of cells, to pluripotent stem cells (e.g. embryonic stem cells) with the potential to differentiate into all cells of the organism.

Stem cells can, as indicated above, be categorized into embryonic-, adult- and induced pluripotent stem cells, differing in their origin as well as in their capacity of self-renewal and differentiation (Figure 1) (Abdelalim & Turksen, 2016; Chagastelles & Nardi, 2011). Thereby adult stem cells can, depending on the type, be derived from various organs of the adult body (e.g. hematopoietic stem cells from the bone marrow) and exhibit a reduced ability in differentiation, generating only cell derivatives specific for their tissue of origin (Kondo *et al.*, 2003). Induced pluripotent stem cells (iPSCs) on the contrary are obtained from somatic cells by inducing four transcription factors (Oct 4, Sox2 (sex determing region Y-box 2), KLF4 (Krüppel-like factor 4), C-Myc) related to pluripotency and with this reprogramming the cells into an embryonic stem cell-like state (Seki & Fukuda, 2015; Takahashi & Yamanaka, 2006). The ability to induce pluripotency in somatic cells (e.g. fibroblasts), that was firstly achieved by Takahashi and Yamanaka in 2006 (Takahashi & Yamanaka, 2006), possesses the potential to revolutionize regenerative and personalized medicine by enabling and broaden therapeutic applications based on patient derived induced pluripotent stem cells. Based on this multiple advances have been made towards patient specific drug screening and *in vitro* disease models for degenerative diseases such as Parkinson's and Alzheimer's disease (Avior *et al.*, 2016; Gieseck *et al.*, 2015; Xiao *et al.*, 2016).

The first derived and *in vitro* cultured embryonic stem cells (ESCs) were from mouse origin and were isolated in 1981 by Evans and Kaufman (Evans & Kaufman, 1981). In

contrast the human ESCs (hESCs) were firstly derived in 1998 by Thomson et al. (Thomson *et al.*, 1998). Embryonic stem cells (ESCs) are, independent of their origin, derived from the inner cell mass of the early embryo in the blastocyst stage, which will be formed between embryonic day 3 and 4 (E3.0 - E4.0) in the mouse embryo or embryonic day 5 and 6 in the human embryo (Niakan *et al.*, 2012). As mentioned before ESCs have the ability of prolonged self-renewal and the potential to differentiate into all cells of the organism (pluripotency) (Evans & Kaufman, 1981; Martin, 1981; Thomson *et al.*, 1998). Due to these two properties, stem cells are attracting growing interest in functional tissue engineering, regenerative and transplantation medicine as well as in personalized medicine with promise for patient specific and therapeutic applications (Harink *et al.*, 2013; Kitambi & Chandrasekar, 2011; Nirmalanandhan & Sittampalam, 2009). However, stem cell research still faces several limitations that will have to be overcome before stem cells can be used to their full potential for therapeutic applications. As for example the underlying mechanisms for maintaining stemness and controlling differentiation of stem cells *in vitro* remain largely unknown. In order to enable culture of stem cells and maintenance of stemness, several environmental conditions must be carefully controlled and hence, a lot of effort is done in developing systems that mimic the environmental *in vivo* conditions to the best possible extent (Balikov *et al.*, 2017; Patel *et al.*, 2016; Titmarsh *et al.*, 2013). However, yet it remains elusive and challenging due to the great complexity of the cellular *in vivo* microenvironment and multitude of requirements important to maintaining stemness.
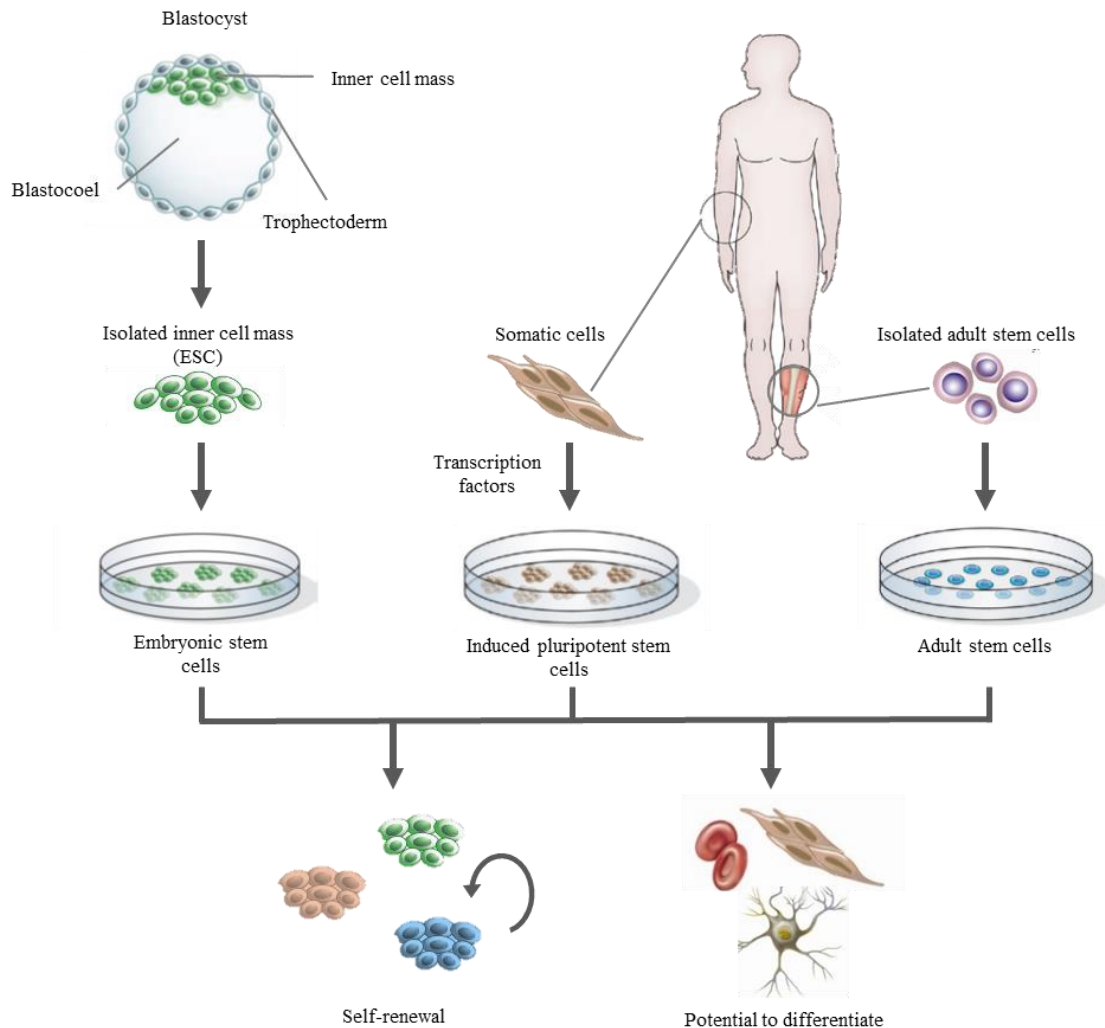
Figure 1. Schematic representation of stem cell types, their origin and unique properties. Modified from (Lutolf et al., 2009).

1.2 Embryonic stem cells and their niche

In vivo stem cells reside in a tightly controlled, tissue specific microenvironment that consists out of biochemical, mechanical and physical cues surrounding and influencing stem cell development. Besides intrinsic signals such as presence of regulatory proteins for cell division and gene expression, those extrinsic cues are needed to regulate stem cell fate and differentiation (Watt & Hogan, 2000). Especially during early embryonic development stem cells are interacting highly with the surrounding microenvironment. In case of ESCs the stem cell niche in the embryo is arranged as follows. The ESCs form the inner cell mass of the blastocyst, which is partially in contact with fluid in the adjacent, internal cavity called blastocoel (Figure 1) (Lanza, 2009). Both inner cell mass and blastocoel are in turn surrounded by the trophectoderm, which will form the extraembryonic tissue such as the placenta (Lodish *et al.*). Hence the ESCs are

influenced by neighboring cells, soluble factors and structural component of the extracellular matrix (ECM) (Figure 2) during embryonic development. Thereby the ESCs can, depending on their location within the inner cell mass, be in direct interaction with either trophectoderm cells and ESCs or ESCs alone.
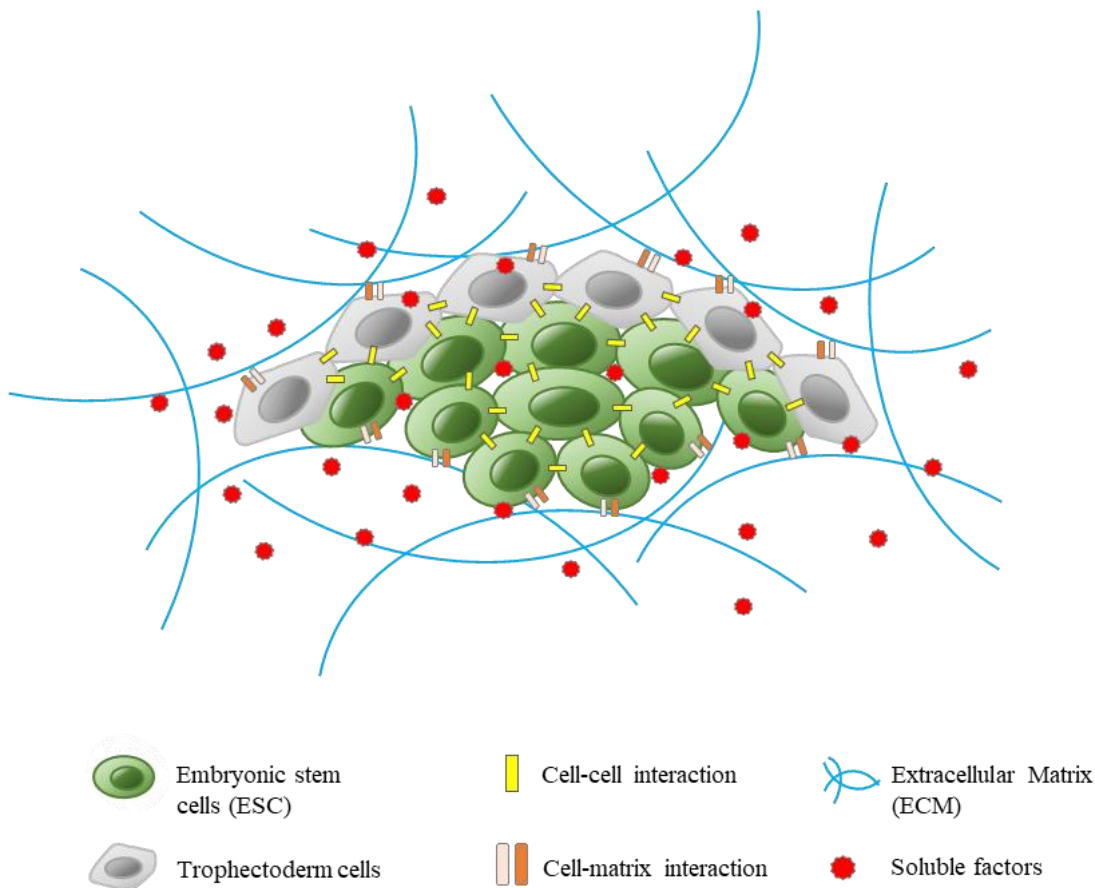
Figure 2. Schematic representation of the embryonic stem cell niche. ESCs are highly influenced through various environmental stimuli in the stem cell niche: 1) cell-cell interaction over E-Cadherin-β-Catenin binding with neighboring ESC or trophectoderm cells 2) cell-matrix interaction over integrin binding with ECM protein (e.g. collagen IV, laminin, fibronectin) 3) interaction with soluble factors (e.g. growth factors, cytokines, chemokines) 4) sensing of biophysical factors (e.g. stiffness, shear forces, structural and spatial arrangement).

These cell-cell interactions are mainly mediated over E-Cadherin-β-Catenin binding. In previous studies E-Cadherin proved to have, besides function in cell-cell binding, a stabilizing effect on functional LIFR (leukemia inhibitory factor receptor) by forming with it a ternary complex at the stem cell membrane which in turn, through binding of the extracellular ligand LIF (leukemia inhibitory factor) (Figure 3), results in improved maintenance of stemness and self-renewal (Pieters & van Roy, 2014). In general

binding of the cytokine LIF to the heteromeric receptor, that is composed of the low affinity LIFR and the subunit gp130, leads to JAK (Janus kinase) mediated activation of the STAT3 pathway by phosphorylation of its tyrosine residue, further leading to the activation of transcription factors (e.g. KLF4, Nanog) involved in stemness (Figure 3). Due to this LIF is considered to be a substantial soluble factor present in the mouse embryonic stem cell niche. However there are multiple other soluble factors, differing in their effect on stemness depending on the stem cell type and its residual niche. As for example human embryonic stem cells are not affected by LIF but are dependent on the presence of fibroblast growth factor (FGF) in their microenvironment (Theunissen *et al.*, 2014).
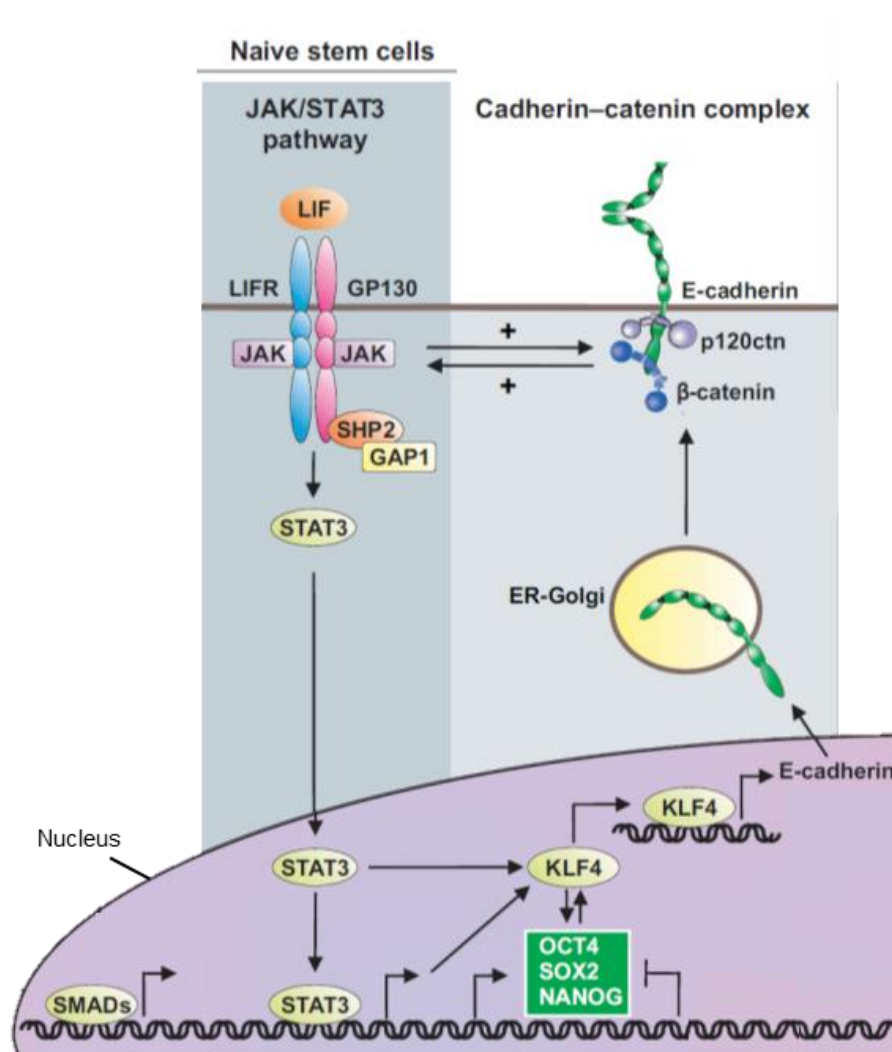
Figure 3. Interaction between E-Cadherin-β-Catenin mediated cell-cell interaction and LIF mediated signaling in ESCs. Modified from (Pieters & van Roy, 2014).

Another important cue, beside cell-cell interaction and influence over soluble factors, is the interaction with insoluble factors of the ECM, which is a fibrillary network

consisting out of proteins such as collagen, fibronectin and laminin interlaced with proteoglycans. Furthermore the stem cell can sense other signals, like the topography or stiffness of the ECM over this cell-surface interaction. Main mediator of this surface sensing is the heterodimeric transmembrane receptor integrin that can be composed of 18 α-chains and 8 β-chains (Sun *et al.*, 2012). This high diversity of integrin in turn leads to an increased recognition and cellular response to variances in the ECM. The stem cell binds over integrin to the ECM, which leads to formation of integrin clusters, so called focal adhesions. Intracellularly specific adaptor proteins such as talin, vinculin and α-actinin will bind to the cytoplasmatic tail of integrin subsequently converting the mechanical cues from the ECM into biophysical signals. This conversion, also known as mechanotransduction, occurs through changes in the cytoskeleton and activation of signaling cascades and transcription factors influencing cell fate and differentiation (Das *et al.*, 2014).

The *in vivo* microenvironment of embryonic stem cells is highly complex and though a lot of progress is done in developing systems mimicking the stem cell niche, maintenance of the undifferentiated state of stem cells *in vitro* still remains challenging and the underlying mechanisms are not fully understood. Certain environmental conditions that must be carefully controlled are required to enable stem cells to be cultured and stemness to be maintained *in vitro*. In case of mouse embryonic stem cells (mESCs), these requirements are appropriate culture medium supplemented with LIF, and passaging the cells regularly (every 2nd day) to prevent the induction of spontaneous differentiation through overgrowth (Efe & Ding, 2011; van der Sanden *et al.*, 2010). Another likewise important requirement to maintain mESC stemness is the stimulation of cell attachment to the surface, generally ensured via gelatin coating and mitotically inactivated mouse embryonic fibroblasts (MEFs). MEFs are furthermore known to secrete soluble factors into the culture medium and thereby contributing to the maintenance of stemness (Llames *et al.*, 2015). However, the use of MEFs for mESC cultures has several drawbacks, such as the need for purification steps and removal of the MEFs for experiments that require a pure population of stem cells. Moreover, the methods used for mitotic inactivation of MEFs are mainly based on mitomycin C treatment or gamma irradiation, both of which can have cytotoxic effects on stem cells due to residual mitomycin C and apoptosis of MEF cells. These limitations reveal the need for MEF-free culture systems to be developed suitable for the investigation, screening, and expansion of stem cells (Chen *et al.*, 2013; Higuchi *et al.*, 2014; Rodin *et*

al., 2014). All in all, the above-mentioned requirements demonstrate how laborious, costly, and time-consuming mESC cultures are, and despite precise control of the aforementioned prerequisites, inhibiting spontaneous differentiation of various stem cells including mESCs *in vitro* remains very difficult (Kobel & Lutolf, 2010; van der Sanden *et al.*, 2010).

1.3 Artificial substrates for regulation of stem cell differentiation

A lot of progress is being made in the development of artificial systems with better resemblance of the highly complex *in vivo* microenvironment, to enable improved maintenance of stemness and regulation of differentiation *in vitro*. Thereby research focus is the adjustment of individual niche factors at a time, in order to result in a better understanding of the underlying mechanism of differentiation.

1.3.1 Immobilization of proteins

Main approach in the design of such artificial substrates is the cell-surface interaction, known to be an important contributing factor in the stem cell niche, influencing self-renewal and differentiation (see Introduction 1.2). The first strategies to generate such highly defined chemical substrates enabling improved maintenance of stem cells under MEF-free conditions, were achieved through coating of conventional tissue culture plates (polystyrene plates) with ECM components. One example is the use of Matrigel, a gelatinous mixture composed of various ECM proteins such as collagen IV, laminin and fibronectin, enabling improved stem cell attachment by mimicking the niche ECM (Joddar & Ito, 2013). Not only in mixture but also individual ECM proteins such as gelatin or fibronectin have been used for stem cell culture in order to maintain stemness. Most commonly the individual ECM proteins are thereby spotted in a patterned fashion using contact or non-contact printing techniques (Ceriotti *et al.*, 2009; Ghaemi *et al.*, 2013). These spotting techniques further enable, by printing and immobilizing different ECM proteins, the investigation of variable protein combinations and their effect on cell adhesion and proliferation. Flaim et al. used this approach in their study in order to investigate the various ECM protein combinations on their potential to direct ESC differentiation toward the early hepatic fate as well as their influence on the maintenance of the *in vivo* function of hepatocytes (Flaim *et al.*, 2005). Furthermore the immobilization of cell adhesion molecules like E-Cadherin or signaling molecules are being employed (Nagaoka *et al.*, 2006) to promote stemness. Alberti et al.

exploited this potential to immobilize signaling molecules to deposit the molecules LIF (leukemia inhibitory factors) and stem cell factor (SCF) by covalently binding the molecules to a maleic anhydride copolymer (POMA-PEG7) surface (Alberti *et al.*, 2008), allowing maintenance of mESCs pluripotency for up to 2 weeks without further external addition of LIF.

1.3.2 Nanofibrous structures: bacterial cellulose

Besides direct attachment to the provided attachment sites of the surrounding substrate, stem cells can sense and be influenced through mechanical cues such as surface topography, porosity and the fibrillary structure (Moraes *et al.*, 2010; Zhou *et al.*, 2015a; Zonca *et al.*, 2013). One approach is the use of nanofibrous structures, which can be synthesized through electrospinning technology or naturally derived (Bhardwaj & Kundu, 2010; Jin *et al.*, 2017; Murphy *et al.*, 2014). By using the electrospinning technology it is possible to generate fine fibers from polymer solutions with diameters in the nano- and micrometer range. The electrospinning setup consists thereby of three major components: a high voltage supply, a spinneret and a grounded collecting plate. During the electrospinning process an electric charge of certain polarity is induced on the polymeric solution, which is subsequently accelerated in a charged jet towards the collector plate of opposite polarity, forming fibers (Figure 4A).

Cellulose is a natural nanofibrous structure originating from various plants, fungi, algae or aerobic bacteria. Especially bacterial cellulose (BC) is gaining high importance in stem cell research due to its biocompatibility. BC is most commonly synthesized under static culture conditions, generating a cellulose film at the liquid-air interface, as bacteria, in particular the aerobic bacterial strain *Komagataeibacter xylinus (KX)*, will intrinsically produce glucose chains that will get extruded and subsequently aggregate into nano- and microfibers further forming a web shaped network (Figure 4B) (Esa *et al.*, 2014; Shah *et al.*, 2013; Sulaeva *et al.*, 2015; Ullah *et al.*, 2016). With increasing cultivation time, the thickness of the film will continuously increase, until the bacteria will get trapped underneath the cellulose film and become less active due to high oxygen deficit (Shah *et al.*, 2013).
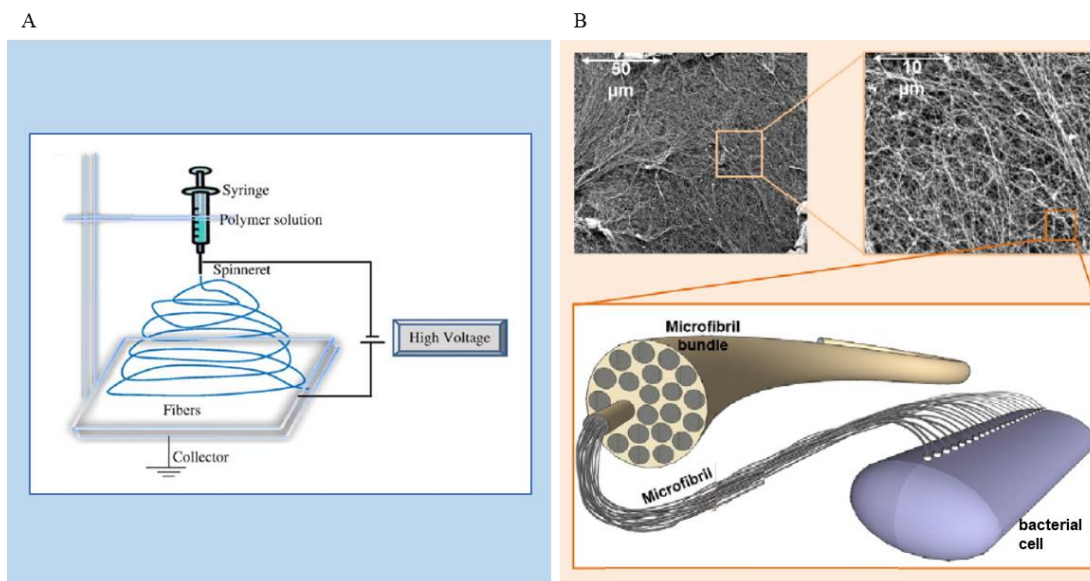
Figure 4. Graphical schematic of cellulose production. (A) Schematic representation of synthetical cellulose production using the electrospinning technique. Modified from (Bhardwaj & Kundu, 2010). (B) Schematic overview of structural organization of naturally derived bacterial cellulose (BC). Modified from (Sulaeva *et al.*, 2015)

Besides the mentioned biocompatibility BC possesses further advantages like its purity, due to lack of potential sources of toxicity like hemicellulose, lignin and pectin, other than in plant-derived cellulose (Sulaeva *et al.*, 2015; Ullah *et al.*, 2016). In addition BC exhibits high crystallinity, mechanical strength, high water holding capacity, permeability towards liquid and gases based on its porosity, broad chemical modifying ability, biodegradability and the ability of 3D molding during synthesis (Esa *et al.*, 2014; Jang *et al.*, 2017; Shah *et al.*, 2013; Sulaeva *et al.*, 2015). Furthermore the BC is highly adjustable in its structural and mechanical properties. The BC membrane thickness for example can be modulated by the cultivation time, and its porosity, roughness, and mechanical properties through its drying method (Shah *et al.*, 2013). In addition BC possesses the ability to generate controllably complex 3D structures, enabling the production of realistic tissue or scaffold material through combination with 3D printing techniques, microfluidics and electrospinning techniques (Ardila *et al.*, 2016; Pattinson & Hart, 2017; Sultana & Zainal, 2016; Yu *et al.*, 2016). Due to these numerous advantages BC finds wide application in tissue engineering, as skin substitute and as wound dressing material, exhibiting higher complement activation than conventional graft materials (Jin *et al.*, 2017; Mertaniemi *et al.*, 2016). In stem cell research BC has so far been applied as composite material, as for example by combining BC with hydroxyapatite, a natural occurring mineral containing calcium, in

order to mimic bone tissue and direct differentiation of stem cells seeded on these BC composite into the osteogenic lineage (Favi *et al.*, 2016; Huang *et al.*, 2017; Ran *et al.*, 2017). Furthermore studies showed morphological similarities between BC and the extracellular matrix protein collagen, indicating a comparable support in cell growth or even possible maintenance of the undifferentiated state of stem cells (Geisel *et al.*, 2016). Hence a positive effect on maintenance of stemness can be caused by the distinctive surface topography and fibrillary structure as well as through the mechanical strength of the BC.

1.3.3 Polymeric materials

Further artificial substrates influencing stem cell differentiation through their surface topography and stiffness are generated by application of polymeric materials. Hydrogels are such polymeric networks that can easily be produced and additionally modified in its stiffness and viscosity, enabling investigation of those parameters on stem cell differentiation. Hydrogels are mainly generated of poly(acrylamide) (PAAm) and poly(ethylene glycol) (PEG) (Murphy *et al.*, 2014; Viswanathan *et al.*, 2014), however further functionalization with ECM proteins is generally needed in order to promote cell-substrate interaction. As for example Gobaa et al. generated an array comprised of hydrogel microwells with varying substrate stiffness and shear moduli, but equal geometrical and biochemical properties. The stiffness of hydrogels was controlled by using three different PEG precursor concentrations leading to different levels of gel crosslinking. In addition, the hydrogels were functionalized with various combinations of different ECM proteins. This enabled the investigation of the effect of surface stiffness in combination with variable ECM proteins on mesenchymal stem cell (MSC) and neural stem cell (NSC) differentiation and enabled the characterization and identification of the optimal combinations suitable for stem cell culture and maintenance of stemness (Gobaa *et al.*, 2011). Other polymeric materials currently applied for stem cell culture further allow modulation of surface roughness, chemistry and wettability as for example varying combinations of acrylate monomers (Mei *et al.*, 2010). Thereby modulation of the surface topography can be achieved, in a highly reproducible and spatially controlled manner, through the use of lithographic techniques such as nanoimprinting, microcontact printing (μCP), electron-beam lithography or photolithography (Coyle *et al.*, 2016; Higuchi *et al.*, 2014; Nam *et al.*, 2011; Viswanathan *et al.*, 2014). Thereby these techniques enable generation of

nanostructures such as nanopits or nanopillars on the surface of the substrates. As for example, Hu et al. used electron-beam lithography creating a substrate of multiple nanograles and nanopillars that vary in their dimensions and distances between the individual structures, resulting in differential T-cell activation and proliferation based on the surface topography (Hu *et al.*, 2016). Also modulation of the surface roughness and topography can be done through varying the chemical composition of the used polymer mixture. In previous work a highly chemically defined poly(2-hydroxyethyl methacrylate-*co*-ethylene dimethacrylate) (HEMA-EDMA) substrate was generated by free radical photopolymerization exhibiting varying surface topographies (Jaggy *et al.*, 2015). By using varying ratios of the porogens, 1-decanol and cyclohexanol, precise control of the surface roughness was possible achieving substrates with smooth (Surface roughness (Sa) 2 ± 0.4 nm), nanorough (Sa 68 ± 30 nm) and micro-nanorough (Sa 919 ± 22 nm) surface topographies (Figure 5). These substrates were applied for stem cell culture and the effect of the respective surface topographies on mESC differentiation and stemness was investigated, showing significantly improved maintenance of mESC stemness on the micro-nanorough surface.
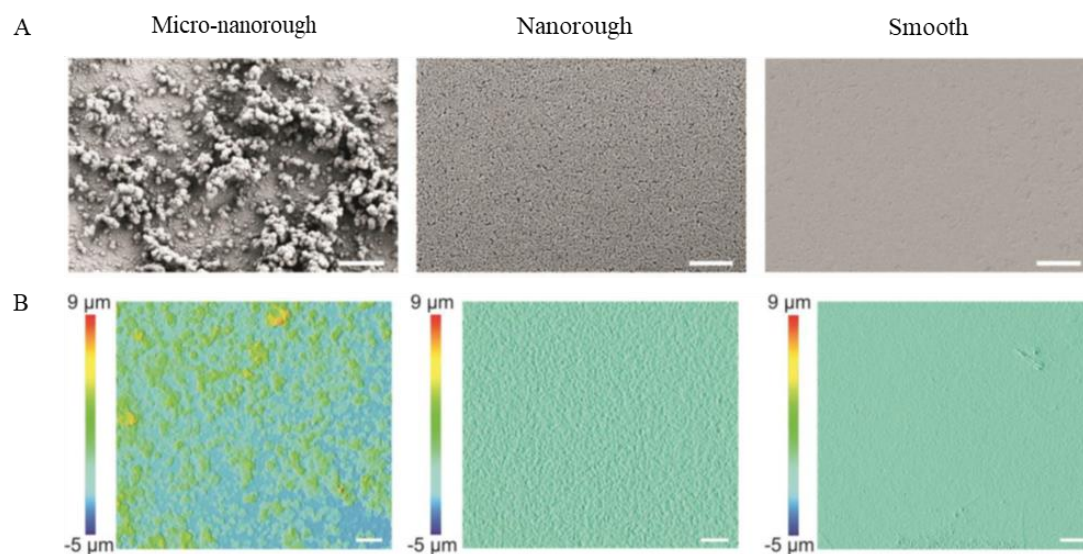
Figure 5. HEMA-EDMA substrate exhibiting varying surface topographies. (A) SEM images showing an overview of micro-nanorough, nanorough and smooth surface structure of the highly chemically defined HEMA-EDMA substrate. Scale bar 5 μm. (B) Surface roughness of the respective topographies imaged through optical profilometry. Scale bar: 20 μm for micro-nanorough and nanorough; 100 μm for smooth surface. Figure modified from (Jaggy *et al.*, 2015).

All the above mentioned approaches generating artificial substrates mimicking the *in vivo* microenvironment, enable culture of stem cells under highly defined and reproducible conditions whilst maintaining stemness and regulating differentiation.

1.3.4 Development of miniaturized platforms for stem cell applications

Further complicating stem cell research, next to the difficult maintenance of stemness *in vitro*, is the limited availability and restricted expandability of certain stem cells types, making the use of conventional culture and microtiter plates (96- and 384- well plates) almost impossible. Hence a lot of progress has so far been made in the fields of nanotechnology and engineering in developing methods to generate miniaturized platforms for stem cell applications such as screenings. This is addressed by both, improving commonly used methods and designing various novel approaches (Berthuy *et al.*, 2016). The new developed platforms are mainly based on the previously mentioned artificial substrates (see Introduction 1.3) to benefit on their potential in maintaining stemness due to a close resemblance of the *in vivo* microenvironment. An example of such a miniaturized platform based on the use of a fibrous material showing to have an effect on stem cell differentiation through mimicking structural composition of the natural stem cell niche was presented in the work of Deiss et al. They developed a patterned paper array through impregnation with Teflon, generating repelling barriers in the paper, and allowing precise deposition of cells and peptides in array format for screening applications (Deiss *et al.*, 2014).

As mentioned before, techniques widely applied for fabrication of microarray include contact or non-contact printing, and lithographic techniques (Kang *et al.*, 2010; Nam *et al.*, 2011). For instance, by using standard soft lithography, Zhang et al. developed a microarray, named SMARchip, for screening of stem cells containing 512 round wells with a diameter of 500 µm separated by superhydrophobic borders (Zhang *et al.*, 2016). A further approach of a miniaturized microarray created based on the property of extreme water repellency was developed by Feng et al. using photolithography to generate a patterned polymer microarray (Droplet Microarray) consisting of hydrophilic spots of different shapes and sizes ranging from 3000 to 1000 µm, separated by superhydrophobic borders, enabling spontaneous formation of multiple confined micro-reservoirs for culturing and screening of cells (Feng *et al.*, 2014; Popova *et al.*, 2015; Popova *et al.*, 2016). Along with possibility of dramatic miniaturization of screenings, these techniques allow for generation of arrays of spots with different chemical and physical properties. This is, as shown above, important for controlling microenvironment of stem cells during *in vitro* handling, enabling culture of stem cells

in xeno-free conditions and further expanding the applicability of stem cells for screening applications.

1.3.5 High-throughput screening of stem cells in 2D

Research focuses on characterizing the mechanisms underlying stem cell differentiation, as well as on identifying various compounds able to maintain stemness and inhibit spontaneous differentiation of stem cells using high-throughput screenings (HTS) (Gupta *et al.*, 2009; Williams *et al.*, 2008). HTS are most commonly performed using microtiter plates, as they enable parallel and simultaneous testing of multiple factors in formats ranging from 96 over 384 to 1536 experiments per plate (Ankam *et al.*, 2013). The use of microtiter plates for HTS, however, has several drawbacks and limitations. Performing large screens using microtiter plates (96-1536 well plates) is time consuming and laborious (Macarron *et al.*, 2011). First of all, it requires multiple pipetting steps and the use of expensive pipetting robotics. Second, it entails high consumption of expensive reagents and valuable cells resulting in high costs of experiments. Due to that reasons HTS of stem cells is not affordable for many laboratories. In addition to the financial aspect, the main limitation of using microtiter plates for screening stem cells is the limited availability and restricted expandability of these cells. This makes it difficult or sometimes impossible to perform large screens on some types of stem cells using conventional microtiter plates. It is especially critical in case of primary patient derived stem cells that are not just scarce in their amount, but also limited in time they could be cultured outside of the organism, due to rapid changes in their properties and responses during in vitro culturing (Lee-Thedieck & Spatz, 2014). To address these problems and be able to perform HTS without robotics and with minimal reagent and cell consumption, further miniaturization of screening compartments is required. Hence, the development of new miniaturized platforms for HTS of stem cells, requiring minute amount of cells and allowing for fabrication of customized scaffolds with defined chemical and physical properties, is in focus in the field of stem cell research. These miniaturized platforms for HTS, enabling cell numbers and the amount of compounds per experiment to be reduced, can make stem cell screening possible and cost-effective (Du *et al.*, 2016; Fernandes *et al.*, 2009; Jackman *et al.*, 1998). Thereby several screening approaches, such as screening for small molecules, proteins or biopolymers, are applied in order to elucidate the mechanisms underlying stem cell differentiation and to accelerate progress in compound

and drug discovery (Fernandes *et al.*, 2009). For example multiple HTS are being performed in order to identify compounds and small molecules that affect expansion of stem cells, self-renewal, maintenance of stemness or that enable directed differentiation of stem cells into a specific subtype of specialized cells (Gupta *et al.*, 2010). In the work of Williams et al. for instance, a screen of multiple small molecules was performed using murine skeletal muscle cells (C2C12) with the potential to differentiate in order to identify small molecules with effect on neuronal differentiation (Williams *et al.*, 2008). Furthermore multiple HTS on soluble factors are being conducted since, *in vivo,* stem cells are strongly influenced by soluble factors in their behavior and developmental fate. Chung et al. investigated the influence of the soluble factors: epidermal growth factor (EGF), fibroblast growth factor 2 (FGF2) and platelet-derived growth factor (PDGF) in a concentration-gradient-dependent manner on proliferation and differentiation of neural stem cells (NSCs) (Chung *et al.*, 2005).

A controlled environment is known to be a crucial factor in stem cell culture and expansion, as stem cells sense and react to various environmental conditions that can directly affect stemness, self-renewal and differentiation (Mei, 2012). The interaction of stem cells with environmental cues and conditions are versatile and include cell-surface and cell-cell interactions. Hence, to be able to regulate stem cell properties various materials are being investigated for their ability to influence the properties of stem cells and to create well-controlled substrates with defined chemical and physical properties for short and long term culture of stem cells (Ghaemi *et al.*, 2013). For this purpose miniaturized platforms are also widely used as they allow, in contrast to microtiter plates, simultaneous screening of large number of substrates and their combinations using minute amounts of cells. For instance, Mei et al. conducted a screening of 496 various combinations of different minor and major monomers by spotting acrylate monomer mixtures on glass substrate and culturing human embryonic stem cell (hESC) on it with the objective to identify suitable polymers supporting long-term culture and expansion of hESC (Mei *et al.*, 2010). In another study performed by Luo et al. self-assembled monolayers of alkanethiols, an easy adjustable substrate, was used for controlling the differentiation of human mesenchymal stem cells (hMSC). In this study 384 different combinations of alkanethiols were spotted on gold substrate to form an array of self-assembled monolayers for subsequent screenings with hMSCs (Luo & Yousaf, 2011).

Modulating the surface properties, such as topography, porosity, stiffness and geometry, can contribute to a better understanding of the effective factors and the underlying mechanisms of differentiation (Moraes *et al.*, 2010; Zhou *et al.*, 2015a; Zonca *et al.*, 2013). Several studies addressed and investigated the effect of surface topography on stem cell differentiation and expansion (Ankam *et al.*, 2013; Berthuy *et al.*, 2016; Simon & Lin-Gibson, 2011). Ankam et al. showed the fabrication of a multi architectural chip (MARC) containing various patterned topographies exhibiting different geometries and sizes in nano- to micrometer range in combination with various heights of PDMS layer (Ankam *et al.*, 2013). They used MARC to investigate the influence of surfaces with different properties on neural differentiation of hESCs and were able to find a combination of topographical features and biochemical cues that reduced the time of neuronal differentiation to 7 days compared to 20 days in conventional methods (Ankam *et al.*, 2013). Such miniaturized combinatorial screenings of surface properties in array format are used by an increasing number of research groups to advance and accelerate research progress by increasing effectiveness of screenings and reducing time and costs of experiments (Berthuy *et al.*, 2016; Simon & Lin-Gibson, 2011). In addition to array format, combinatorial screenings can be realized by using gradients like it was shown in the study of Clements et al. (Clements *et al.*, 2012). In this work, a platform with orthogonal gradients of porous silicon and cyclic RGD peptide was fabricated. Using this platform the authors investigated behavioral changes and attachment of MSCs upon the variable gradients and observed significant correlation between attachment of MSCs and density of silicon and cyclic RGD peptide on the surface with stronger correlation with peptide concentration.

Another widely used combination of environmental cues in stem cell screening is a joint investigation of influence of the stiffness of the surface and proteins such as ECM proteins on properties of stem cells (Gobaa *et al.*, 2015). In the work of Gobaa et al., the authors generated an array with dimensions of a standard microscope glass slide, comprised of hydrogel microwells of 450 μm size with varying substrate stiffness and shear moduli, but equal geometrical and biochemical properties. The stiffness of hydrogels was controlled by using three different PEG precursor concentrations leading to different levels of gel crosslinking. In addition, hydrogels were functionalized with 67 combinations of 11 different proteins, such as, for example, ECM protein fibronectin. By performing HTS of MSCs and neural stem cells (NSC) using this platform, the authors demonstrated the effect of surface stiffness in combination with

different proteins on stem cell differentiation, and were able to identify optimal combinations that supported self-renewal of stem cells (Gobaa *et al.*, 2011).

As mentioned before ECM proteins represent an important part of the stem cell niche; therefore, they are widely used in screenings searching for environmental cues promoting stem cell renewal, stemness or differentiation (Chien *et al.*, 2011). Beachley et al. developed a miniaturized 2D tissue model array consisting of 40 ECM microparticles, isolated and generated from 11 different porcine tissues, and spotted onto a glass substrate (Vince Z Beachley *et al.*, 2015). Proteomic analysis revealed that the fabricated ECM microparticles resembled to a high degree the ECM constitution from the respective tissue they were derived from. They used this tissue model array to conduct HTS of human adipose derived stem cells (hADCs) and investigate differentiation upon various tissue specific ECM combinations. For a better resemblance of the *in vivo* situation, the authors modified the 2D tissue model into a 3D system by inverting the array containing hASCs and ECM microparticles during culturing period and utilizing the method of "hanging drop" promoting formation of stem cell - tissue ECM spheroids. A similar effect of tissue specific ECM on hASCs differentiation was demonstrated in both 3D and 2D models. Several other studies also focused on developing 3D model systems for HTS of stem cells to enable better representation of natural microenvironment allowing for investigation on influence of niche components on stem cell fate in more *in vivo*-like conditions (Tarunina *et al.*, 2016; Zhang *et al.*, 2016).

1.3.6 High-throughput screening of stem cells in 3D

Various approaches are used to generate miniaturized 3D high-throughput platforms resembling a more physiological and natural environment and enabling further applications in compound screens, regenerative medicine, biomaterial and tissue engineering (Gaharwar *et al.*, 2016; Tong *et al.*, 2015). As for example the fabrication of scaffolds for 3D screening systems is based on using polymers, fibrous material, bioprinting techniques or hydrogels (Fernandes *et al.*, 2009; Floren & Tan, 2015; Neto *et al.*, 2014). 3D systems based on hydrogels cover investigation of the effect of compounds, small molecules, ECM proteins (Dumont *et al.*, 2014) as well as chemical and mechanical properties of the hydrogels on stem cell expansion (Raic *et al.*, 2014) and differentiation (Duffy *et al.*, 2016; Moraes *et al.*, 2010). Floren et al. developed a miniaturized 3D high-throughput platform based on the formation of fibrous hydrogel

that exhibits tunable properties such as elasticity, stiffness and geometry (Floren & Tan, 2015; Neto *et al.*, 2014). In addition, different combinations of ECM proteins were spotted in hydrogel array allowing the authors to create a screening platform for investigation of MSCs attachment, spreading and differentiation upon different combinations of ECM protein and substrate stiffness (Floren & Tan, 2015; Neto *et al.*, 2014).

The development and investigation of further approaches, scaffolds and materials for culturing and screening of stem cell in 3D environment led to the discovery and application of fibrous materials that were shown to have an effect on stem cell differentiation, probably through mimicking structural composition of the natural stem cell niche (Wang & Kisaalita, 2010).

Furthermore mimicking stem cell niche and microenvironment can be achieved through simulating cell-cell interactions by co-culturing different interdependent cell types (Tumarkin *et al.*, 2011). This approach was utilized in the work of Gracz et al., where the authors developed a microraft array (MRA), a miniaturized platform for the investigation of the interaction between intestinal stem cells (ISC) and Paneth cells that reside in a natural niche of ISC cells (Gracz *et al.*, 2015). Using MRA, the authors were able to show the direct effect of Paneth cells on formation of organoids derived from ISCs in a more in vivo like system.

1.3.6.1 Embryoid bodies for high-throughput screening

The use of embryoid bodies (EB) for screening applications is such a widely used example of a 3D culturing and screening model. EBs are 3D cell aggregates formed by pluripotent stem cells like ESCs. It has been shown that EBs recapitulate in many aspects early mammalian embryogenesis by differentiating into cells representing the three germ layers, and therefore, they represent a highly physiologically relevant model compatible with HTS applications (Vrij *et al.*, 2016; Warkus *et al.*, 2016). The primary three germ layers in the embryo are formed during the process of gastrulation, which approximately takes place from embryonic day 6.5 (E6.5) in the mouse embryo (Figure 6). Thereby the epiblast cells form a transient structure, known as primitive streak, and undergo transition giving rise to endo and mesoderm (Keller, 2005). Cells of the epiblast that do not pass through the primitive streak will give rise to the ectoderm. In case of EBs the first indication for differentiation was shown to be the formation of a

layer of primitive endoderm on the outer surface of the EB (Bratt-Leal *et al.*, 2009). However, the formation of a primitive streak like structure as well as the exact mechanism underlying and regulating the early induction of the germ layers within EBs are to date poorly understood. Within the three different germ layers, mesoderm derived cells develop into cells of the hematopoietic and vascular system, cardiac tissue and skeletal muscle cells. The endoderm lineage in particular gives rise to hepatocytes and pancreatic β-cells, whereas the ectoderm lineage gives rise to cell of the central nervous system as well as epithelial cells (Keller, 2005).
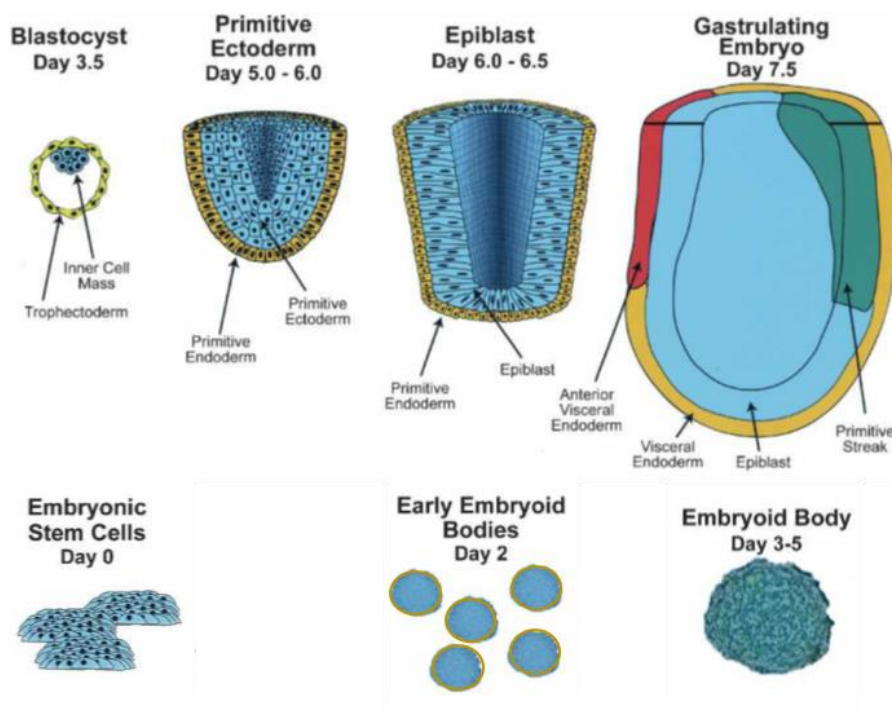
Figure 6. Schematic representation comparing the early stages of development in the embryo and embryoid bodies. Modified from (Keller, 2005).

Main methods applied for the EB formation are culture in "hanging drops" as well as in low adherence plates (Buesen *et al.*, 2004; Buesen *et al.*, 2009; Desbordes *et al.*, 2008). There ESCs are pipetted on the inner side of petri dish lid as "hanging drops" or into the particular wells of a low adherence plate, respectively (Corradi *et al.*, 2015; Warkus *et al.*, 2016). Both methods are thereby based on the culture of ESCs in suspension, allowing the formation of cell aggregates and spontaneous differentiation into EBs. In order to perform HTS using these methods the ESCs are, in a first step suspended in the respective compounds that are supposed to be tested during screening. Subsequently the individual ESC-compound solutions are pipetted either in the particular wells of the low adherence plate or in case of the "hanging drop" method in the lid of a petri dish that is

immediately turned afterwards to allow culture of the ESCs in "hanging drops" forming EBs (Corradi *et al.*, 2015; Warkus *et al.*, 2016). Hence, multiple pipetting steps are needed to perform HTS of compounds using these methods and in order to ensure parallel and simultaneous testing of multiple compounds the use of pipetting robotics is essential. Other technologies used for the formation of EBs, including culture of stem cells in bacterial grade dishes or spinner bioreactors, face disadvantages such as low homogeneity of formed EBs and reduced applicability for screenings due to high amounts of reagents needed (Kurosawa, 2007). Therefore the development of new technologies that enable HTS of EBs in low volumes and without the need for pipetting robotics as well as high size homogeneity of single EBs formed is important. For example, Vrij et al. fabricated a miniaturized platform enabling formation of EBs on a thermoformed Cyclic Oleofin copolymer (COP) film with low cell adhesion properties. Using this platform, the authors performed a screening of kinase inhibitors investigating its influence on differentiation of EB derived from mouse embryonic stem cells (Vrij *et al.*, 2016). Further approaches for creation of 3D HTS platforms mimicking *in vivo* environment are being realized through generation of organoids and tissue models (Horváth *et al.*, 2015; Jeon *et al.*, 2015) that allow for screening in a more natural and physiological system (Arai *et al.*, 2016; Nierode *et al.*, 2016). Additionally applying EBs in drug screening can help to identify compounds showing toxicity, increasing drug safety and reducing the use of premature *in vivo* testing during early stages of drug discovery.

1.4 Objective

Stem cells have gained more and more importance in fields like drug discovery, tissue generation and transplantation medicine, due to their potential of differentiating into vast subsets of cells and their ability of self-renewal. However long-term maintenance of these properties *in vitro* remains challenging and limited availability as well as restricted expandability of some stem cell types further complicate culture and screenings of stem cells using conventional tissue and microtiter plates (96- and 384-well plate). This emits the urge for miniaturized platforms allowing culture and screening of stem cells in order to identify compounds and factors promoting stem cell properties *in vitro*, further helping to elucidate the underlying mechanisms of differentiation. Thereby the use of artificial substrates with highly defined and reproducible biochemical properties proved to be beneficial.

Hence, the objective of this PhD work was to employ artificial substrates enabling the culture and maintenance of stem cells through their surface topography and roughness, simplifying stem cell culture and in case of the Droplet Microarray enabling high-throughput screening of stem cells. Therefore a transgenic mouse embryonic stem cell line, stably expressing eGFP fused to the pluripotency gene Oct 4 (mESC Oct4-eGFP) was used and with this allowing direct read-out of the differentiation state of the mESC Oct4-eGFP using fluorescence microscopy.

Two different artificial substrates were investigated for stem cell culture and their promoting effect on stemness; bacterial cellulose and a highly chemically defined porous poly(2-hydroxyethyl methacrylate-*co*-ethylene dimethacrylate) (HEMA-EDMA) respectively.

The bacterial cellulose that was used in the first part exhibits multiple properties such as high purity and biocompatibility demonstrating its applicability as artificial substrate for cell culture. Furthermore it is highly adjustable in its structural and mechanical properties, enabling precise modulation of its porosity, roughness and thickness. In addition the demonstrated morphological similarities between the bacterial cellulose and the *in vivo* occurring extracellular matrix protein collagen (Geisel *et al.*, 2016) indicate a comparable support in cell growth and a potential stemness promoting effect of the bacterial cellulose. Hence, the bacterial cellulose was employed in this work as it shows promising applicability for stem cell culture as defined, nanofibrous substrate that

allows precise modulation and regulation of its morphological and structural properties and based on this exhibits the potential for culture of stem cells in a precisely controlled microenvironment with ability for improved maintenance of stemness.

The highly chemically defined HEMA-EDMA substrate that was employed in the second and third part of this PhD project can be adjusted in its chemical composition further resulting in different surface topographies of variable roughness and porosity. Thereby the HEMA-EDMA's micro-nano surface topography was demonstrated to inhibit mESC differentiation, thus promoting the long-term maintenance of stemness under MEF-free conditions (Jaggy *et al.*, 2015). Furthermore the surface roughness is crucial to create the hydrophilic and superhydrophobic areas exhibiting various degrees of wettability, that enable spontaneous, pipetting-free formation of a miniaturized array of microdroplets via the effect of discontinuous dewetting. Therefore the aim in the second part of the project was to combine this dual-functionality of the HEMA-EDMA surface roughness to generate a miniaturized array of multiple droplets on a superhydrophobic-hydrophilic micropattern (Droplet Microarray) that enables high-throughput screening of stem cells and at the same time promotes the maintenance of stemness and inhibition of differentiation through its surface roughness without the need of MEFs. Thereby the Droplet Microarray allows for screening and identification of compounds and factors promoting stem cell properties *in vitro* in a chemically defined and controllable system.

Moreover, the objective in the third part of this work, was to employ the Droplet Microarray as a miniaturized platform for the facile formation of multiple, homogeneous embryoid bodies (EBs). Thereby as EBs closely resemble the *in vivo* situation by recapitulating the early embryonic development, using the Droplet Microarray as EB array enables screening and investigation in a more cellular complex system with closer resemblance to the *in vivo* microenvironment, resulting in biomedical more relevant results.

2 Material and Methods

2.1 Materials

2.1.1 Chemicals

Table 1. List of all chemicals

Name	Company
1-decanol	Sigma-Aldrich (Munich, Germany)
1H, 1H, 2H, 2H perfluorodecanethiol	Sigma-Aldrich (Munich, Germany)
2,2-dimetoxy-2-phenylacetophenone (DMPAP)	Sigma-Aldrich (Munich, Germany)
2-hydroxyethyl methacrylate (HEMA)	Sigma-Aldrich (Munich, Germany)
2-mercaptoethanol	Alfa Aesar (Massachusetts, USA)
3-(trimethoxysilyl)propyl methacrylate	AppliChem GmbH (Darmstadt, Germany)
4-(dimethylamino)pyridine (DMAP)	Merck KGaA (Darmstadt, Germany)
4-pentynoic acid	Sigma-Aldrich (Munich, Germany)
bovine gelatin	Sigma-Aldrich (Munich, Germany)
cyclohexanol	Sigma-Aldrich (Munich, Germany)
dichloromethane (DCM)	Merck KGaA (Darmstadt, Germany)
dimethyl sulfoxide (DMSO)	Carl Roth (Karlsruhe, Germany)
ethylene dimethacrylate (EDMA)	Sigma-Aldrich (Munich, Germany)
mitomycin C	Santa Cruz Biotechnology Inc. (Dallas, USA)
N,N'-diisopropylcarbodiimide (DIC)	Manchester Organics (Runcorn, UK)
porcine gelatin	Sigma-Aldrich (Munich, Germany)
ScreenWell FDA approved drug library V2	Enzo Life Sciences Inc. (New York, USA)
trichloro (1H, 1H, 2H, 2H-perfluorooctyl)silane	Sigma-Aldrich (Munich, Germany)

2.1.2 Media, buffer, solution

Table 2. List of used media, buffer and solutions

Name	Company
DMEM	Gibco Life Technologies GmbH (Darmstadt Germany)
100x Non-essential amino acids (NEAA)	Gibco Life Technologies GmbH (Darmstadt Germany)
Accutase	Invitrogen (California, USA)
PanSera ES (bovine Serum for stem cells)	PAN-Biotech GmbH (Aidenbach, Germany)
PBS	Thermo Fisher Scientific (Massachusetts, USA)
Penicillin/Streptomycin (Pen/Strep)	Gibco Life Technologies GmbH (Darmstadt Germany)
Trypsin-EDTA, 0.25%	Thermo Fisher Scientific (Massachusetts, USA)
α-MEM	Gibco Life Technologies GmbH (Darmstadt Germany)

2.1.3 Kits and primer

Table 3. List of used Kits and primer

Name	Company
InnuPrep Mini RNA Kit	AnalytikJena (Jena,Germany)
M-MLV RT Rnase (H-) point mutation	Promega (Wisconsin, USA)
Primer	Metabion international AG (Planegg, Germany)

2.1.4 Antibodies and cell stains

Table 4. List of all cell stains and antibodies

Name	Company
DAPI	Molecular Probes, Thermo Fisher Scientific Inc. (Massachusetts,USA)
donkey anti goat Cy3	Jackson Immunoresearch (West Grove, USA)
goat anti Brachyury	R&D Systems (Minneapolis, USA)
goat anti FoxA2 (HNF 3β)	R&D Systems (Minneapolis, USA)
goat anti rabbit Cy3	Jackson Immunoresearch (West Grove, USA)
Hoechst 33342	Molecular Probes, Thermo Fisher Scientific Inc. (Massachusetts,USA)
Propidium iodide (PI)	Invitrogen (California, USA)
rabbit anti β-III-Tubulin (TuJ1)	Sigma-Aldrich (Munich, Germany)

2.1.5 Cell lines

Table 5. List of the used cell lines and respective media

Name	Description	Source	Media
HEK293-LIF	HEK293 cells stably transfected with a leukemia inhibitory factor (LIF) expression plasmid	Prof. Dr. Martin Bastmeyer, KIT	α-MEM + 10% PanSera ES + 1% Pen/Strep
MEFs	mouse embryonic fibroblasts	Prof. Dr. Martin Bastmeyer, KIT	DMEM + 15% PanSera ES
mESC Oct4-eGFP	mouse embryonic stem cells expressing eGFP stably fused to Oct4	Prof. Dr. Martin Bastmeyer, KIT	+ 1% Pen/Strep + 1xNEAA + 0.1 mM 2-mercaptoethanol

2.1.6 Equipment

Table 6. List of used equipment

Name	Company
Guava easyCyte Flow Cytometer	Merck Millipore (Darmstadt, Germany)
Nanodrop 2000	Thermo Fisher Scientific (Massachusetts, USA)
OAI Model 30 UV lamp	OAI Instruments (San José,USA)
StepOnePlus Real-Time PCR System	Thermo Fisher Scientific (Massachusetts, USA)
CO_2 Incubator	
CB 160	Binder GmbH (Tuttlingen, Germany)
Heraeus BB15 CO2 Incubator	Thermo Fisher Scientific (Massachusetts, USA)
Clean bench	
BH-EN safety cabinet	Gelaire Pty Ltd. (Sydney, Australia)
ENVAIR ECO Air	ENVAIR Deutschland GmbH (Emmendingen, Germany)
Centrifuge	
Heraeus Labofuge 400R Centrifuge	Thermo Fisher Scientific (Massachusetts, USA)
MiniSpin Plus	Eppendorf AG (Hamburg, Germany)
Microscopes	
Keyence BZ9000	Keyence (Osaka, Japan)
Leica SPE confocal microscope	Leica Microsystems CMS GmbH (Mannheim, Germany)
Olympus IX81	Olympus Corporation (Tokyo, Japan)
Non-contact printer	
I-DOT One	Dispendix GmbH (Stuttgart, Germany)
sciFLEXARRAYER S11	Scienion AG (Berlin, Germany)

2.1.7 Consumables

Table 7. List of consumables

Name	Company
96 well PCR plate	Steinbrenner Laborsysteme (Wiesenbach, Germany)
CELLSTAR® Cell culture dishes	Greiner Bio-One International GmbH (Kremsmünster, Österreich)
CELLSTAR® Cell culture flasks	Greiner Bio-One International GmbH (Kremsmünster, Österreich)
CELLSTAR® Cell culture plates	Greiner Bio-One International GmbH (Kremsmünster, Österreich)
Cover slips	Carl Roth (Karlsruhe, Germany)
Filter paper Grade 1 Whatman^{TM}	GE Healthcare (Chicago, USA)
Nexterion® Glass B	SCHOTT Nexterion AG (Jena, Germany)
PCR tubes	Corning Inc. (Corning, USA)
qPCR sealing foil	Steinbrenner Laborsysteme (Wiesenbach, Germany)
Rotilabo®-syringe filter, sterile 0.22 µm	Carl Roth (Karlsruhe, Germany)

2.2 Cell culture

All cell culture and cell experiments were conducted, if not stated differently, under 37°C and 5% CO_2 atmosphere. The used media and media supplementation for the respective cell lines are listed in Table 5.

2.2.1 Production of leukemia inhibitory factor (LIF)

For the production of the cytokine leukemia inhibitory factor (LIF) HEK293 cells, stably transfected with a LIF expression plasmid, were cultured in a concentration of 1×10^6 cells/mL in α-MEM Medium. Following 48 h cultivation the supernatant was collected, centrifuged at 1200 rpm for 3 min, filtered using 0.22 µm sterile syringe filters and stored at -20°C for further use.

2.2.2 Culture and inactivation of mouse embryonic fibroblasts (MEFs)

Mouse embryonic fibroblasts (MEFs) were cultured on 75 cm^2 culture flasks that were previously coated with 0.1 wt% porcine gelatin in PBS for 30 min at RT followed by washing steps with PBS. In order to prevent uncontrolled growth of MEFs during subsequent co-culture with mESCs, the MEFs (80% confluency) were mitotically inactivated. Therefore the MEFs were incubated for 3 h at 37°C in presence of mitomycin C in PBS in a final concentration of 10 µg/mL, followed by thorough washing to remove any residual mitomycin C. The MEFs were transferred to 0.1 wt% porcine gelatin coated, 25 cm^2 culture flasks and kept for up to 1-3 days at 37°C, 5% CO$_2$ before co-cultured with mESCs.

2.2.3 Conventional routine culture of mouse embryonic stem cells (mESCs)

The transgenic mESC Oct4-eGFP line, stably expressing eGFP fused to Oct4 were cultured in 5 mL stem cell medium with 30 µL/mL LIF, on 0.1 wt% porcine gelatin in PBS precoated, 25cm^2 culture flasks containing mitotically inactivated MEFs. The cells were passaged every second day conducting the following steps: washing the mESC with PBS, detaching the cells from the culture flask by adding 0.25% Trypsin/EDTA for 3 min, resuspending them in fresh medium, centrifuging at 1200 rpm for 3 min and transferring mESCs in 1:3 ratio to a fresh gelatin coated culture flaks containing inactivated MEFs and stem cell medium with LIF supplementation. Only mESCs with a passage number below 20 were used in the cell experiments.

2.2.4 Preplating of mESCs

Before conducting the experiments the cell suspension had to be preplated in order to separate MEFs from mESC Oct4-eGFP. Therefore the cell suspension from the routine culture was transferred onto a non-coated petri dish in 5 mL stem cell medium with 30 µL/ml LIF and incubated for 30 min at 37°C and 5% CO$_2$. Due to slower cell adherence of mESCs than MEFs on non-coated surfaces, mESCs were collected in the supernatant while MEFs remained attached to the petri dish. Isolated mESCs were transferred onto a new 1 wt% gelatin-coated flask for use within the next 24 h or immediately employed in the respective cell concentration in the experiment. In order to adjust the cell concentration, the mESCs were counted using a Neubauer Chamber or Countess II Automated Cell counter and diluted appropriately.

2.3 Fabrication of stem cell culture substrates

2.3.1 Production of bacterial cellulose

Bacterial cellulose (provided by Dr. Anna Roig, Barcelona, Spain) is produced by bacterial strain *Komagataeibacter xylinus (KX)*. *KX* is cultured under static culture conditions in bacterial culture medium (20 g/L glucose, 5 g/L peptone, 5 g/L yeast extract, 1.15 g/L citric acid monohydrate and 6.8 g/L $Na_2HPO_4 \cdot 12H_2O$) for 5 days, generating a thin layer of bacterial cellulose (BC) at the liquid-air interface. BC was harvested, and cleaned in ethanol with subsequent transfer to DI water and boiled for 40 min. Following the cleaning and sterilization the BC was dried using different drying procedures to gain BC samples exhibiting different characteristics. The following samples were prepared and labelled in relation to their drying methods. BC-W: Never dried bacterial cellulose was stored after sterilization in DI water. BC-RT: Bacterial cellulose films were placed into chromatography paper between two glass slides and were dried at room temperature for 4 days. BC-FD: The bacterial cellulose films were plunge-freezed in chromatography paper with liquid nitrogen for 5 min following freeze-drying using LYOQUEST-85 freeze drier (Telstar) at -80 ° C, below 0.005 mbar for 12 h.

2.3.2 Seeding and culture of mESCs on bacterial cellulose

mESC Oct4-eGFP were seeded at the required concentration in a volume of 500 µL stem cell medium on the bacterial cellulose film in a 60 mm petri dish and allowed to settle for 90 sec. In order to reduce the displacement of cell suspension in wet bacterial cellulose samples (BC-W and BC-RT wet) during the seeding procedure excess water was aspirated from the wet BC samples before seeding. Following, 4.5 mL of stem cell culture medium and 30 µL/mL of LIF were added covering the bacterial cellulose film completely. The medium was changed every second day by transferring the bacterial cellulose film with mESC to a fresh 60 mm petri dish containing 5 mL culture medium and 30 µL/mL LIF.

2.3.3 Production of superhydrophobic-hydrophilic micropatterned substrates

The Nexterion® glass B slides were activated by immersion in 1M NaOH for 1h, followed by washing with DI water, immersion in 1M HCl for 30 min, followed by washing with DI water and drying. Glass slides were fluorinated by overnight incubation in 50 mbar with 30 µL trichloro (1H, 1H, 2H, 2H-perfluorooctyl)silane. Non-fluorinated, activated glass slides were modified with 20% v/v 3-(trimethoxysilyl)propyl methacrylate ethanol solution for 30 min. To prepare the nanoporous polymer surface, a mixture of 24 wt% 2-hydroxyethyl methacrylate (HEMA), 16 wt% ethylene dimethacrylate (EDMA), 12 wt% 1-decanol, 48 wt% cyclohexanol and 0.4 wt% 2,2-dimethoxy-2-phenylacetophenone (DMPAP) was placed on a fluorinated glass slide and covered it with a modified glass slide. To obtain a polymer surface of consistent thickness, 3.62 µm monodispersed silica beads were used. Polymerization took place under UV irradiation with 260 nm wavelength at 7 mW/cm^2 for 15 min. The glass slides were separated and the polymer layer on the modified glass slide was washed. A further increase in surface roughness was achieved by taping the polymer with adhesive tape. To modify the surface with alkyne, the slides were immersed in 45 mL cooled Dichloromethane (DCM), 111.6 mg 4-Pentynoic Acid, 56 mg of the catalyst DMAP and 180 µL N,N'-Diisopropylcarbodiimide (DIC) for 4 h while stirring. A 5% v/v 1H,1H,2H,2H-Perfluorodecanethiol acetone solution was applied on the polymer surface, covered with a photomask, and irradiated with 260 nm wavelength UV light 7mW/cm^2 for 1 min to generate a superhydrophobic pattern. To generate the superhydrophilic spots, the polymer surface was wetted with 10% v/v 2-mercaptoethanol in 1:1 water:ethanol solution, covered with a quartz slide and irradiated with 260 nm wavelength UV light 7mW/cm^2. Thereby this pattern of hydrophilic spots separated by superhydrophobic borders enables through application of an aqueous solution the formation of an array consisting of multiple separated microdroplets, subsequently named Droplet Microarray (DMA). The dimension hydrophilic spot (square spots) : superhydrophobic borders of the used pattern were 3 mm : 1 mm (DMA 3 mm); 1 mm : 0.5 mm (DMA 1 mm), respectively.

2.3.4 Seeding and culture of mESCs on superhydrophobic-hydrophilic micropatterned substrates

Prior to seeding of mESC Oct4-eGFP on the DMA, the array was sterilized using ethanol and dried under the cell culture bench. The DMA was coated using 2.2 wt% bovine gelatin in water at 37°C, 5% CO_2 for 1h, followed by a 45 min drying step. For the seeding procedure, the mESC Oct4-eGFP were applied at the required concentrations in a volume of 1.5 mL stem cell medium on the pattern of a pretreated DMA that was placed in a 100 mm petri dish and allowed to settle for 60 sec before removing any excess medium by slightly tilting the DMA. During this step only a fraction of cells of the initial cell concentration is trapped in the individual spots of the DMA 3 mm and 1 mm leading to different volumes per individual cells compared to the conventional culture. To prevent further evaporation during incubation in the cell incubator, a PBS wetted humidifying pad was placed in the lid of the petri dish.

2.4 Flow cytometry of mESCs

The mESC were seeded on the DMA as mentioned above and cultured for the respective time points (2 h, 24 h, 48 h and 72 h). Cells were detached from the DMA with Accutase, counted using a Neubauer Chamber and diluted to a cell concentration of 500-1000 cells/µL. The flow cytometric analysis was performed using Guava easyCyte Flow Cytometer and the corresponding software InCyte. Normalization of the individual samples was done to mESCs cultured under conventional conditions. For the analysis of the controls cells were cultured for 2 h, 24 h, 48 h and 72 h under conventional culture conditions, detached and preplated prior to measurement.

2.5 qPCR of mESCs

Cells were seeded and cultured on the DMA and under a set of different culture conditions for 2 h, 24 h, 48 h and 72 h. Following the detachment of the cells using trypsin, RNA was isolated using InnuPrep Mini RNA Kit. The samples' RNA concentrations were obtained using Nanodrop 2000. Samples were adjusted to 150 ng-1 µg RNA. cDNA was synthesized as follows: 1 µL random primer (200 ng/ µL) was added to each individual RNA sample and incubated for 5 min at

70°C. For 1st strand synthesis 4 µL 5x buffer, 2 µL dNTP (10 mM), 0.2 µL M-MLV RT Rnase ((H-) point mutation) and a respective volume of H_2O (final volume 22 µL per sample). As control to ensure the amplification process, samples were also processed without adding M-MLV RT Rnase. Samples were incubated for 10 min at 25°C, 60 min at 42°C, 10 min at 70°C and kept at 4°C for further processing (long term storage at -20°C). To confirm amplification and check for contamination with genomic DNA, a control PCR was conducted with 4 µL 5x buffer, 2 µL dNTP (2 mM), 1 µL each forward and reverse primer (GAPDH), 0.1 µL Go Taq G2 DNA Polymerase, 4 µL cDNA and respective volume H_2O (final volume 20 µL) (2 min 95°C, cycle 25-30 [30 sec 95°C, 30 sec 68°C, 1 min 72°C], 5 min 72°C, ∞ 4°C) followed by a 1% agarose gel run (130V 500mA 30-60 min). The qPCR with 10 µL 2x SYBR green, 1 µL each forward and reverse primer, 4 µL cDNA and respective volume H_2O (final volume 20 µL) was performed using StepOnePlus Real-Time PCR System. Gene-specific primers are listed in Table A 1. The housekeeping gene GAPDH served as the reference gene.

2.6 Viability staining

The mESCs were seeded as mentioned above and cultured on the respective samples (bacterial cellulose; DMA) with Hoechst 33342 in 1:10000 dilution (1 µg/mL), to visualize the nucleus, and with propidium iodide (PI) at a concentration of 100 nM to distinguish dead from viable cells. A second experiment revealed no significant difference in viability between mESC cultured with and without stains. Images were taken at the respective time points (2 h, 24 h, 48 h and 72 h) and cells counted to estimate viability and stemness.

2.7 Embryoid body formation

The DMA 1 mm was sterilized in ethanol, dried under the clean bench and coated with 2.2 wt% bovine gelatin in water at 37°C and 5% CO_2 for 1h, following drying for 30 min. For seeding the mESC cell suspension was applied on the micropattern at the required concentration in a volume of 1.5 mL, remaining on the micropattern for 30 sec before removing excess medium by tilting the DMA slide. Immediately after the DMA slide was inverted and placed on an especially designed and 3D printed table, enabling

culture of mESC Oct4-eGFP on the DMA in hanging droplets. The table was placed in a PBS filled petri dish and in order to prevent evaporation a PBS wetted humidifying pad was placed in the lid of the petri dish. As control mESC Oct4-eGFP were cultured under conventional conditions as mentioned above. The embryoid bodies (EBs) formed after 48 h incubation on the DMA in hanging droplets.

2.7.1 Immunofluorescence staining

EBs were formed as mentioned above, collected from the DMA and transferred to a fibronectin (10μg/mL) coated coverslip. The EBs were allowed to outgrow on the coverslips for 12 days (with regular medium changes), leading to spontaneous differentiation into all 3 germ layers (endo-, meso-, ectoderm). Following outgrowth an immunofluorescence staining for markers of endo-, meso- and ectoderm (FoxA2, Brachyury, β-III-Tubulin) was performed, by fixing the EBs with 3.7% paraformaldehyde in PBS for 15 min and permeabilising with 0.1% Triton-X 100 in PBS for 15 min. The respective EBs were incubated with the following primary antibodies each in 1:500 dilution in 1% BSA/PBS for 1 h: goat anti-FoxA2 (HNF 3β); goat anti-Brachyury; rabbit anti-β-III-Tubulin (TuJ1). Following the samples were washed and incubated with the respective, conjugated secondary antibodies, each in a 1:200 dilution in 1% BSA/PBS for 1 h in darkness: donkey anti-goat Cy3 and goat anti-rabbit Cy3. DAPI was added to all samples along with the secondary antibody in a dilution of 1:10000.

2.7.2 High-throughput screening

DMA slides (1 mm side length of spots) were prepared as mentioned above, sterilized in ethanol and dried under the clean bench. All 774 compounds from the ScreenWell® FDA approved drug library V2 (10 mM stock) were used for the primary screen in a dilution of 10 μM in 1% DMSO in DI water and printed in triplicates using the non-contact, liquid dispenser sciFLEXARRAYER S11. As vesicle control 1% DMSO in DI water was used. Empty spots (non-printed) on the compound slide served as internal control and completely empty DMA slide (no compounds printed on complete slide) as experimental control. The listed DMA slides were coated twice with 2.2 wt% bovine gelatin in water using the non-contact dispenser I-DOT One. The mESC Oct4-eGFP were seeded on the DMA as described above in a cell concentration of 0.2×10^6 cells/mL but by reducing the seeding time, before tilting the DMA to remove

excess medium, down to 30 sec. The cells were kept for 72 h in hanging droplets at 37°C and 5% CO_2 in order to form EBs. The primary HTS was conducted in a single repetition and with triplicates for each compound. The dose-response curve screen for the selected hit compounds was conducted with 5 different concentrations, ranging from 100 µM - 0.01 µM, each in quadruplicates.

2.8 Image acquisition and analysis

All images were taken using the microscope Keyence BZ9000 or Leica SPE confocal microscope. For the HTS the automated screening microscope Olympus IX81 was used. Exposure times were identical in all experiments and at the different channels and conditions. The size of the mESC colonies is considered as the indication of the growth rate; this was acquired using ImageJ (https://imagej.nih.gov/ij/). mESCs' stemness was assessed from the intrinsic Oct4-eGFP signal and evaluated as follows: the percentage of pluripotent mESC was obtained by counting GFP-positive (GFP+; complete fluorescence), GFP-negative (GFP-; no fluorescence) and mixed colonies (colony showing fluorescent and no fluorescent regions). For quantification purposes, the mean fluorescence signal intensity was obtained using ImageJ. In case of EBs and the HTS following analysis were made in collaboration with Markus Reischl (Institute for Applied Computer Sciences (IAI) KIT; Karlsruhe Germany): the mean fluorescence intensity, the roundness and size of the EBs as well as the area fraction of PI stained cells was measured using ImageJ. The algorithm applied for the automated identification and image processing was conducted using MATLAB R2015b. To find EBs, the Hoechst-channel was segmented the following way: 1) well-border were cut to avoid artifacts, 2) the 95th percentile of pixel-brightness was used to binarize the image, 3) noise was removed through opening (r=2), 4) holes were deleted by closing (r=2) and hole-filling, and 5) further opening (r=10) delivered only big objects contained in the image. All objects containing more than the preset threshold of 1200 pixels were kept for evaluation and characterized by the following features: area (µm2), solidity index, eccentricity index and roundness (mean of solidity and eccentricity). Within each found object the mean GFP value, the area percentage of PI and the median GFP in the whole image were additionally calculated. Objects were thereby considered valid, if the eccentricity feature was greater than 0 and the object was located centrally to avoid border artifacts. The fitted dose-response curves of the respective data were assessed

using the nonlinear curve fitting function in OriginPro (OriginLab Corporation) with the iteration algorithm Levenberg Marquardt (Jones, 2015).

2.9 Statistical analysis

All quantitative data was normalized to the respective control and presented as mean $\pm$ SD. For each experimental set at least 3 independent experiments were conducted and used for statistical analysis. All data was analyzed using two tailed student's t-test using OriginPro (OriginLab Corporation) and p-values < 0.05 were considered statistically significant

3 Results and Discussion

Embryonic stem cells (ESC) possess unique properties like the ability of self-renewal and the potential to differentiate into multiple cells of the organism, making them of high importance in tissue engineering, regenerative and transplantation medicine. *In vivo* these properties are influenced by a complex system of multiple cues, such as cell-cell interaction, cell-matrix interaction and soluble factors. In order to maintain the unique properties of stem cells, named stemness, various systems and materials are being developed that mimic this complexity. However the maintenance of stemness, despite precise regulation of these various cues, still remains difficult, further emitting the urge for new systems and materials that maintain the stem cells' undifferentiated state and enable investigation of embryonic stem cell development further elucidating the underlying mechanisms of differentiation.

In this work a transgenic mouse embryonic stem cell (mESC) line stably expressing eGFP (enhanced green fluorescent protein) fused to the pluripotency gene Oct4 (octamer-binding transcription factor 4) was used (Kirchhof *et al.*, 2000). Hence, this cell line enables direct read-out of the expression of Oct4 through the GFP level and characterization of mESCs' stemness. Conventional culture of mESCs includes multiple requirements in order to maintain their stemness. These requirements are 1) precoating of the culture flask using gelatin in order to provide attachment sites, 2) use of mitotically inactivated MEFs, known to increase cell attachment and secrete soluble factors maintaining stemness 3) medium supplementation with LIF inhibiting differentiation and 4) regular cell passaging (every 48 h) to prevent overgrowth, known to induce differentiation (Heo *et al.*, 2005). This demonstrates how laborious, time-consuming and costly mESCs culture is and despite precise control of the mentioned conditions maintenance of the undifferentiated state still remains challenging. Moreover the use of MEFs further carries the risk of contamination and the need for purification steps to isolates the mESC from the co-culture. In order to overcome these problems a lot of progress is being made in developing new MEF-free systems, facilitating mESC culture and promoting stemness. Many of the newly developed systems are thereby based on highly defined and controllable artificial materials, such as fibrous or polymeric materials, mimicking the embryonic stem cell niche and with this preventing spontaneous differentiation of mESCs.

3.1 Bacterial cellulose promotes long-term stemness of mESC

An example of a fibrous material that is widely used as substrate for cells in research is cellulose. Cellulose can be derived from various plants, fungi, and aerobic bacteria. Bacterial derived cellulose exhibits high purity, due to its lack of hemicellulose, lignin and pectin, further increasing its biocompatibility and applicability in clinical research. Bacterial cellulose (BC) in addition finds wide application in stem cells research, as for example as composite material directing differentiation into the osteogenic lineage (Favi *et al.*, 2016; Huang *et al.*, 2017; Ran *et al.*, 2017). Furthermore BC was shown to have morphological similarities to the ECM protein collagen (Geisel *et al.*, 2016) demonstrating its potential in partially mimicking *in vivo* microenvironment. A potential effect of BC on maintenance of mESC stemness due to its purity and morphological structure (fibrillarity, porosity and roughness) is hypothesized. In this work this potential of the bacterial cellulose for mESC culture was exploited reducing the need for precoated culture flasks as well as the need for MEFs, hence facilitating culture while maintaining the undifferentiated state of mESCs.

3.1.1 Fabrication of bacterial cellulose films

The bacterial cellulose (BC) was produced by culturing the bacterial strain *Komagataeibacter xylinus* in static culture, resulting in the formation of a cellulose layer at the liquid-air interface. The films were cleaned and dried following different drying procedures prior use, leading to different structural properties and mechanical characteristics, which were extensively studied in a previous work (Zeng *et al.*, 2014). The subsequent experiments presented here, if not stated differently, were conducted on room temperature dried and rewetted bacterial cellulose films (RT-BC wet).

In order to investigate the influence of the BC membrane on the maintenance of stem cells' stemness in a MEF-free culture system, a transgenic mouse embryonic stem cell line (mESC Oct4-eGFP) was used. The conventionally used *in vitro* systems for culturing mESC Oct4-eGFP (Figure 7A and B) require gelatin coating of the culture surface to provide attachment sites, as well as the use of mitotically inactivated MEFs, known to further enhance cell attachment and secrete soluble factors maintaining stemness. Furthermore, the cytokine LIF that is known to inhibit differentiation has to be added (Heo *et al.*, 2005). This procedure is laborious, time consuming and costly and, even with precise regulation of these requirements, maintenance of stemness

remains difficult. Importantly, using the BC membrane as culture material allowed us the direct cultivation of mESC Oct4-eGFP on the cellulose films without the need of gelatin precoating or the use of inactivated MEFs, significantly reducing costs and facilitating mESC culture (Figure 7A and B), whilst maintaining mESC stemness.

Artificial materials with unknown properties can influence cell viability and result in increased cytotoxicity. Hence, in order to assess the biocompatibility of the respective artificial material investigating the cell viability is highly important. The viability of the mESC Oct4-eGFP upon culture under the described conventional conditions and on the BC-RT wet films (Figure 7C) was measured by staining with propidium iodide (PI) to assess number of dead cells and Hoechst 33342 to assess total cell number. For better comparability between conventional culture and culture on BC, the obtained values of dead (PI positive, Hoechst 33342 positive) and viable cells (PI negative, Hoechst positive) were normalized to the total cell count of the respective samples. Upon culture on the BC-RT wet the percentage of dead cells measured at 2 h cultivation time was higher than upon conventional culture (Figure 7C). This could possibly be the effect of an increased stress level of the cells during the initial cultivation time due to the unusual surface properties of the BC and lack of previous cell conditioning to the surface. The percentages of live and dead cells over the time course of 24 h increased by 16% for the conventional culture conditions (2 h: 4%; 24 h: 20%), whereas using BC only leads to an increase by 6% (2 h: 22%; 24 h: 28%), further indicating the reduced viability to be based on an initially increased stress level. The growth rate from 2 h to 48 h was assessed by measuring the size of the mESC Oct4-eGFP colonies (Figure A 1A), showing an increased growth of mESCs colony size on BC in comparison to the conventional culture. Hence, despite an initial stress inducing cell death, maintenance of viable cells and increased proliferation over 24 h culture was achieved on BC films together with a strong reduction of culture requirements in comparison to the conventional mESC Oct4-eGFP culture. In addition the cultivation of mESCs on the free-standing BC membrane allowed facile cell transfer to a culture dish containing fresh medium further simplifying routine cell culture by reducing the number of steps needed during medium exchange in standard culture.
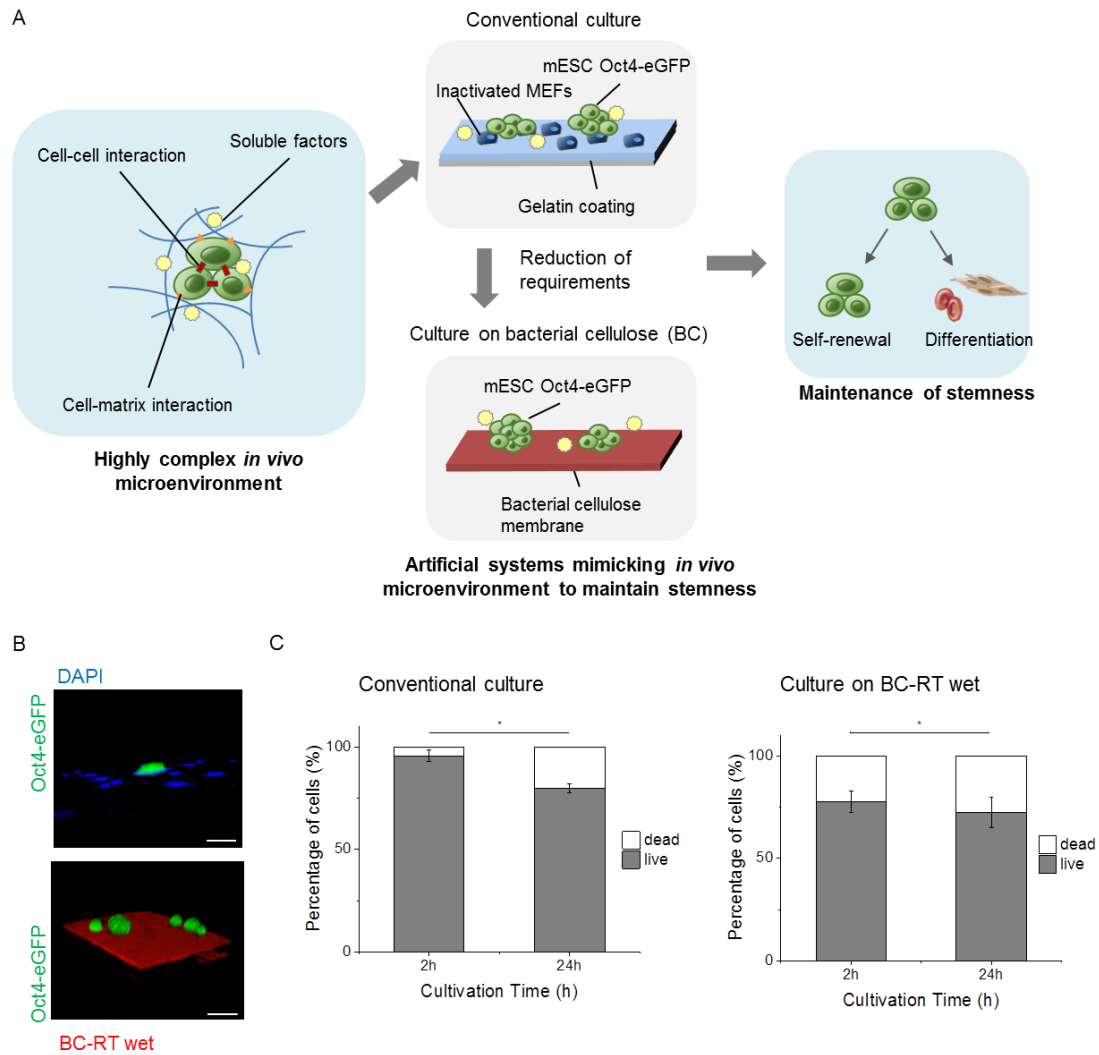
Figure 7. mESC Oct4-eGFP culture under conventional conditions and on bacterial cellulose. (A) Schematic representation demonstrating artificial culture systems (schematics in grey boxes) mimicking high complexity of the *in vivo* microenvironment of stem cells (left schematic, blue box) in order to enable maintenance of stemness. Conventional culture methods require gelatin coating, addition of inactivated MEFs and LIF to promote stemness (upper schematic, upper grey box). Culturing of mESC on bacterial cellulose possessing adjustable and variable structural properties (roughness, topography, porosity) (bottom schematic, bottom grey box) inhibits mESC´s differentiation and at the same time results in significant reduction of requirements compared to conventional culture (B) 3D reconstruction of confocal images showing conventional culture conditions (upper image) with inactivated MEFs (blue) and mESC Oct4-eGFP (green) as well as mESC Oct4-eGFP (green) cultured on BC-RT wet (red). (C) Viability of mESC Oct4-eGFP upon culture under conventional condition (left graph) and culture on BC-RT wet (right graph). Assessment of dead cells via PI staining. N=3. Statistical significance: t-test, * indicates p-value ≤0.05.
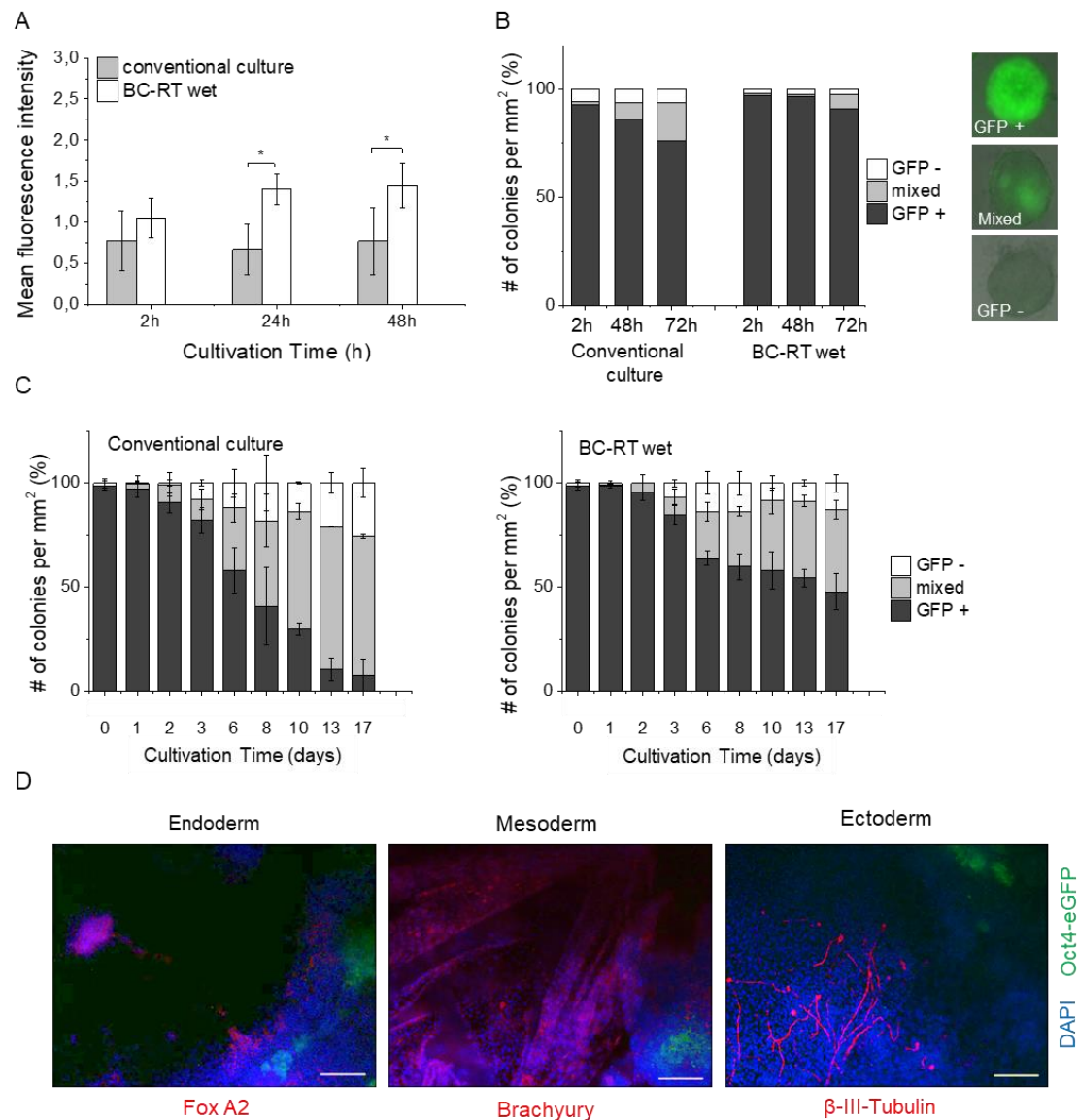
3.1.2 Assessment of mESC Oct4-eGFP stemness upon culture on bacterial cellulose

Previous studies showed close resemblance in the structural properties of BC films to the ECM protein collagen, indicating a possible influence on maintenance of stemness through the BC microstructure (Geisel *et al.*, 2016). Next, it was investigated how the microstructural properties of the BC films can influence stemness upon culture on the BC. For that, the roundness of mESC colonies was measured, known to be a morphological indicator of stemness, with reduced roundness indicating differentiation (Figure A 1B) (Rosowski *et al.*, 2015). The results demonstrate a decrease in roundness of mESC upon culture under conventional conditions, whereas culture on BC results in the maintenance of the roundness over the time course of 48 h. Furthermore, the expression of GFP was used as an indication for stemness due to its stable fusion to Oct4. To quantify the GFP expression the mean fluorescence intensity was measured as well as counted the number of completely undifferentiated colonies (GFP+), mixed colonies (GFP+ and GFP-) and fully differentiated colonies (GFP-) (Figure 8A and B). Figure 8A shows an increase of the mean fluorescence intensity of mESC Oct4-eGFP cultured on BC from 1 at 2 h to 1.5 at 24 h whereas under conventional culture conditions the mean fluorescence intensity decreases from 0.7 at 2 h to 0.6 at 24 h. This demonstrates a better maintenance of stemness and reduction of spontaneous differentiation most likely due to the specific surface properties of the cellulose films. The count of GFP+, mixed and GFP- colonies supports this observation, showing a reduction of GFP+ colonies by only ~8% upon culture on the BC and in contrast under conventional culture conditions by ~20% during 72 h cultivation time. These results indicate a reduction of spontaneous differentiation upon short time culture through the BC.

The long-term maintenance of the undifferentiated state of mESCs still remains challenging without precise regulation of the culture requirements using standard *in vitro* system. Thus, the effect of the BC films on differentiation and maintenance of stemness of mESC Oct4-eGFP under long-term culture conditions (17 days) was investigated. The mESC Oct4-eGFP were cultured under conventional culture conditions and on BC, both in 5 mL medium supplemented with LIF, without further passaging for 17 days. To ensure sufficient supply of nutrients during the time course of the experiment, medium was changed daily and LIF added freshly each time. The

number of colonies per mm^2 in both samples was counted and a strong increase in mixed and GFP- colonies was observed when mESC Oct4-eGFP were cultured under conventional conditions and a decrease in GFP+ colonies from 99% at day 0 to 8% at day 17. In contrast to that, culture on the BC significantly delayed spontaneous differentiation of mESC even under long-term culture, with a reduction in GFP+ colonies from 99% at day 0 to only 48% at day 17 (Figure 8C).

In order to prove the observed effect of BC on maintenance of stemness and the potential of the mESC Oct4-eGFP to differentiate into cell derivatives of all three germ layers, immunofluorescence staining for markers of the germ layers: endo-, meso- and ectoderm (Figure 8D and A 1) was performed. For this, mESC Oct4-eGFP were cultured under conventional conditions and on the BC film for 6 days before being detached and pipetted on the inner side of the lid of a petri dish. The petri dish lid was immediately inverted, in order to allow culture of mESCs in "hanging drops" and, hence, formation of mESC aggregates called embryoid bodies (EBs) that recapitulate the early embryonic development by differentiating into derivatives of all germ layers. After 48 h culture in "hanging drops", the EBs were collected and transferred to fibronectin coated cover slips for further 12 day culture resulting in attachment, outgrowth and differentiation of the EBs into cell derivatives of the respective germ layers. Following the outgrowth and differentiation of the EBs, immunofluorescence staining was performed for FoxA2, Brachyury, β-III-Tubulin that are markers for endo-, meso- and ectoderm, respectively. Representative images of immunofluorescence staining for the respective markers of each germ layer are shown in Figure 8D, proving the maintenance of the stemness of the respective mESCs after being cultured for 6 days on the BC.

Figure 8. Assessment of stemness of mESC Oct4-eGFP upon culture on BC-RT wet in comparison to conventional culture conditions. (A) Measurement of mean fluorescence intensity of mESC Oct4-eGFP under conventional culture conditions and under culture on BC-RT wet. Statistical significance: t-test, * indicates p-value ≤0.05. (B) Percentage of GFP+ , mixed and GFP – colonies per mm² at 2 h, 48 h and 72 h under conventional culture and on BC-RT wet. Right side: representative images of GFP+, mixed and GFP- colonies. (C) Percentage of GFP+, mixed and GFP- colonies under long term culture conditions (for 17 days). N=3, n > 50. (D) Immunofluorescence staining showing potential of mESC Oct4-eGFP to differentiate into 3 germ layers (endo-, meso-, and ectoderm) after being cultured on BC-RT wet. Cells were cultured on BC-RT wet for 6 days, detached and cultured for 48 h using "hanging drop" method to form embryoid bodies (EBs). EBs were transferred to fibronectin coated cover slips and cultured for 12 days. Subsequently immunofluorescence staining of endo-, meso- and ectoderm markers (FoxA2, Brachyury and β-III-Tubulin respectively) and cell nucleus (DAPI) was performed. Scale bar 100 μm.

Next, the underlying mechanism resulting in better maintenance and inhibition of differentiation upon culture on BC was investigated. In comparison to plant derived cellulose, BC exhibits higher purity and, does not contain lignin and hemicellulose. It is assumed that this difference could be responsible for the observed influence on stemness maintenance. To investigate this hypothesis mESC Oct4-eGFP cultured under conventional conditions, on BC RT-wet and on commercially available, plant-derived cellulose (filter paper FP, 180 μm thickness, surface roughness (Sa) 4.93 μm) were compared. Differences in the mean fluorescence intensity of mESC Oct4-eGFP colonies were observable between mESC grown on BC RT-wet and on FP. The BC RT-wet and the purchased FP differ not just in their origin and purity but also in their microstructural properties, as demonstrated by the measurements of thickness and surface roughness (Figure 9B). In particular BC is known as a form of nanocellulose since their cellulose fibrils present fiber diameter in the nanoscale (20 – 50 nm) in contrast to the micron scale diameter (20 – 50 μm) for the plant cellulose. Based on this the observed differences between FP and BC RT-wet can further arise from differences in thickness and topographical structure than solely from the origin of the cellulose.

As previous studies showed, mESC differentiation and stemness can be controlled over surface structure, roughness and porosity depending on enhanced cell attachment and actin cytoskeleton reorganization further suggesting an additional contribution of the physical properties on stemness (Das *et al.*, 2014; Murphy *et al.*, 2014; Zhou *et al.*, 2015b). To investigate the influence of the microstructural properties of the cellulose on stem cell differentiation various BC films were used that were dried using different drying procedures, which in turn changed the BC film thickness, porosity and surface roughness. Wet never dried BC (BC-W), freeze dried BC (BC-FD) and room temperature dried BC (BC-RT) were employed, whereas the latter was either used rewetted (BC-RT wet) or in dry state (BC-RT dry). The thickness and surface roughness of the films was measured using confocal microscopy and optical profilometry. Figure 9B clearly shows the effect the specific drying routes (BC-W, BC-FD, BC-RT dry) and rewetting (BC-RT wet) has on the thickness, ranging from 200 μm to 16 μm (Zeng *et al.*, 2014), and the surface roughness (Sa), ranging from 7.65 μm to 0.59 μm. First the cell attachment to the different cellulose derivatives after 24 h was examined. Therefore, mESC Oct4-eGFP were seeded in the same cell concentration on the various BC films, imaged using fluorescence microscopy and evaluated by counting the number of attached cells and normalizing these values to the initial cell concentration. The best cell

attachment was achieved with 32% on room temperature dried BC independent of rewetting (Figure 9C; BC-RT wet and BC-RT dry; both 32%) and the lowest cell attachment with 7% was achieved on the freeze dried BC (BC-FD), indicating surface roughness to be an important factor in cell attachment as thickness of BC-RT wet is only slightly differing from thickness of BC-FD.

Next the different cellulose derivatives were checked for their ability in promoting and maintaining stemness, by measuring the mean fluorescence intensity of mESC Oct4-eGFP cultured on the respective cellulose samples for 48 h. In order to maintain equal and sufficient nutrient supply between the respective BC films, 5 mL medium with LIF was added to all samples after seeding. The highest mean fluorescence intensity was measured on BC-RT wet, whereas its completely dry state (BC-RT dry) showed a reduced intensity. A possible cause for these differences could be due to variances in the absorption capacity of liquids by the rewetted and dry BC films, with higher capacity in case of the dry BC film. This in turn can result in a faster rate of absorption of the cell suspension and with this to possible higher forces acting on the mESC Oct4-eGFP during absorption by the BC film, inducing differentiation. The reduced mean fluorescence intensity measured in case of the also dry BC-FD sample is comparable to the values measured for BC-RT dry and strongly supports the hypothesis of higher absorption capacity of cell suspension by dry BC films and with it higher forces acting on the cells inducing differentiation. Differences in the surface roughness of the BC films can also influence the observed differences in maintenance of stemness (BC-RT wet: 1.29 µm; BC-FD: 7.66 µm).

Further, the ability of the BC to act as storage for nutrients and soluble factors such as the ECM protein collagen (Geisel *et al.*, 2016) was tested. This was done by preincubating the BC-RT wet films with culture medium obtained from 24 h mESC culture (BC-RT wet: Medium) or with LIF alone (BC-RT wet: LIF) for 5 min prior cell seeding (Figure A 2A). Surprisingly, both preconditioned samples (BC-RT wet: Medium; BC-RT wet: LIF) showed lower mean fluorescence intensity than the non-preconditioned sample (BC-RT wet) suggesting increased absorption of metabolites or soluble factors that induce differentiation. Furthermore differences in cell attachment based on biochemical modification of the BC surface due to the preconditioning, resulting in differentiation could be possible. This enhanced cell attachment in turn can lead to changes in the cytoskeleton of mESC, which is known to

be an important regulator of cell differentiation through activation of subsequent signaling pathways and transcription factors (Das *et al.*, 2014; Murphy *et al.*, 2014; Zhou *et al.*, 2015b).
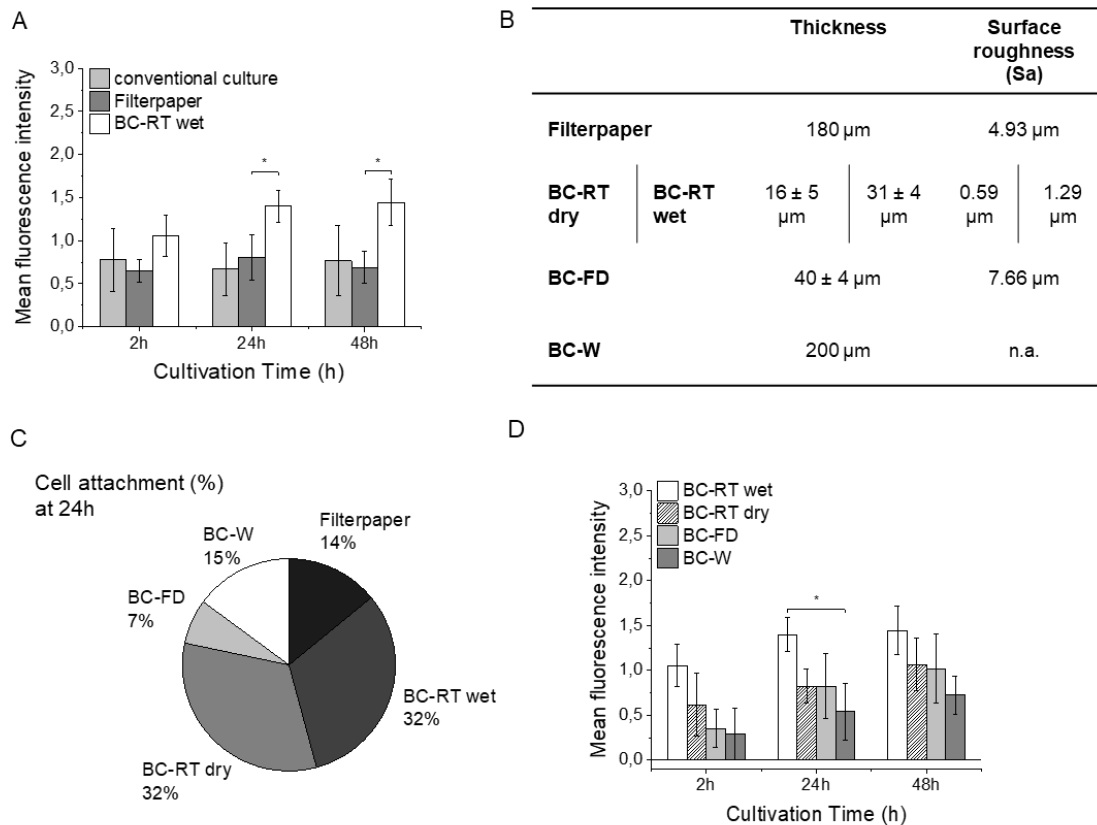
Figure 9. Assessment of stemness of mESC Oct4-eGFP upon culture on various cellulose samples. (A) Mean fluorescence intensity of mESC Oct4-eGFP cultured on BC-RT wet in comparison to culture on filter paper: Whatman® qualitative filter paper Grade 1. Cultivation time was 2 h – 48 h. (B) Cell attachment at 24 h of culture on differently bacterial cellulose samples that were dried using various methods. BC-W: never dried bacterial cellulose. BC-RT: room temperature dried bacterial cellulose. Deployed for experiments in dry state (BC-RT dry) and wetted state (BC-RT wet; wetted with di-water). BC-FD: freeze dried bacterial cellulose. (C) Mean fluorescence intensity of mESC Oct4-eGFP upon culture on differently dried bacterial cellulose samples. Cultivation time was 2 h – 48 h. N=3. Statistical significance: t-test, * indicates p-value ≤0.05.

The previous results demonstrate the strongest effect on mESC Oct4-eGFP stemness resulting from culture on BC-RT wet films, indicating influence through surface properties and absorption capacity of the cell suspension through the material. In order to show the influence of the surface properties on stemness the surface structure was masked by applying a gelatin coating on the BC-RT wet film prior cell seeding (Figure

A 2B). The gelatin masking resulted in a significant reduction of the mean fluorescence intensity in comparison to uncoated BC-RT wet, supporting the previous results regarding the influence of the surface topography (Figure 9A and B).

Previous studies showed an effect of different surface structures, such as a porous fibrillary structure, on cell attachment through infiltration into porous material and degradation of the surrounding matrix by the cells, resulting in regulation of differentiation (Kang *et al.*, 2017; Shariati *et al.*, 2016). By imaging using a confocal microscope, however, no infiltration of mESC into the BC-RT wet films was observable as expected by the reduced porosity of the surface layer of the films dried at room temperature. In order to further investigate such an infiltration and degradation of the cellulose by the mESC Oct4-eGFP, the thickness of the cellulose films were measured before (BC-RT wet: mESC) and after (BC-RT wet: mESC +Trypsin) mESC cell detachment (Figure A 2C). As controls, an empty BC film incubated under the same conditions (BC-RT wet: control; no cells; 5 mL + LIF; 48 h) showing a thickness of ~31 µm was used. After detachment of the mESC Oct4-eGFP using trypsin partial dissolution of the BC film was observed, indicated by a reduced thickness to 22 µm (Figure A 2C; BC-RT wet mESC +Trypsin). Dissolving of the BC structure through enzymatic cleavage can be excluded, since treatment of BC-RT wet with trypsin alone showed no significant reduction in thickness (Figure A 2C; BC-RT wet +Trypsin). It is assumed that the observed partial dissolution of the BC film results from cell attachment by a partial ingrowth of mESC Oct4-eGFP into the cellulose membrane and when detaching the cells, the cellulose structure gets loosened up, leading to partial detachment of cellulose fibers and with this reduction in thickness. However, in order to precisely identify the underlying mechanism of enhanced cell attachment and maintenance of stemness further investigations are necessary (Kumar *et al.*, 2015).

The results demonstrate the potential of BC membrane as porous material to promote stemness of mESCs over short-term and long-term culture conditions. These observed effects on maintenance of stemness can be attributed to result from enhanced cell attachment of mESCs to the BC based on the surface topography and structural properties of the BC films (surface roughness, thickness, absorbing capacity).

3.2 Droplet Microarray based on patterned superhydrophobic surfaces prevents stem cell differentiation and enables high-throughput stem cell screening[1]

In the next part of the project an artificial substrate was employed that is, other than the naturally derived bacterial cellulose demonstrated in the previous part, highly controllable in its chemical composition and surface topography enabling culture and maintenance of undifferentiated stem cells. Therefore a highly defined nanoporous HEMA-EDMA polymer was used, exhibiting a dual-functionality through its surface roughness, namely the ability to maintain the undifferentiated state of mESC (Jaggy *et al.*, 2015) and to generate through modification a miniaturized platform of multiple microdroplets based on a superhydrophobic-hydrophilic micropattern (Droplet Microarray).

3.2.1 Fabrication of Droplet Microarray (DMA) and formation of stem cell arrays

To generate the Droplet Microarray (DMA), glass slides (7.5 cm x 2.5 cm) were coated with a 3.6 µm-thick, nanoporous HEMA-EDMA polymer layer. The surface roughness (Sa) for the nanoporous HEMA-EDMA polymer used in this work was 68 ± 30 nm with a 50% porosity and pores of 80 - 250 nm in diameter based on SEM (Feng *et al.*, 2014; Jaggy *et al.*, 2015). Modification of the surface via the thiol-yne click reaction (Feng *et al.*, 2014) resulted in surface areas with hydrophilic (static water contact angle (WCA ~8°)) and superhydrophobic (advancing WCA ~161°, receding WCA ~148°, static WCA ~153° and sliding angle ~7.5°) properties (Figure 10). Patterns of hydrophilic square spots with sides 3 and 1 mm long and separated by superhydrophobic borders 1 and 0.5 mm wide were created (Feng *et al.*, 2014; Popova *et al.*, 2016; Ueda *et al.*, 2012).

---

[1] **Tronser, T., Popova, A. A., Jaggy, M., Bastmeyer, M. & Levkin, P. A. (2017)**. Droplet Microarray Based on Patterned Superhydrophobic Surfaces Prevents Stem Cell Differentiation and Enables High-Throughput Stem Cell Screening. *Adv Healthc Mater*.

Due to the extreme difference in dewettability of the wettable hydrophilic spots and water repellent superhydrophobic barriers, multiple, separated microdroplets (1 mm: 588 spots/slide; 3 mm: 108 spots/slide) form spontaneously upon contact with aqueous solutions (Figure 10) through the effect of discontinuous dewetting. Such spontaneous pipetting-free formation of droplets was used to create an array of separated droplets containing mESC (Figure 10).
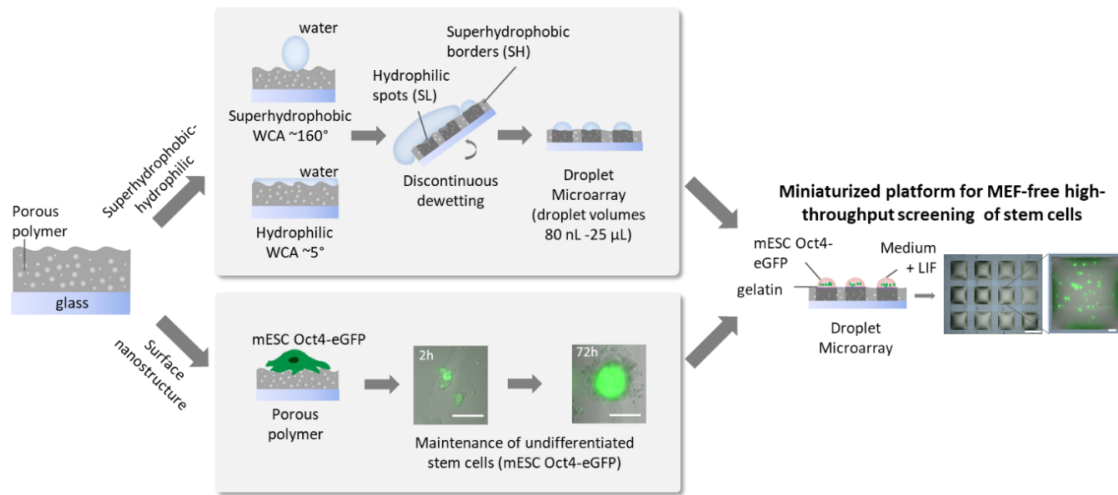
Figure 10. Schematic representation illustrating the multifunctionality of the superhydrophobic-hydrophilic nanoporous polymer. Surface roughness and modification enable generation of superhydrophobic (WCA ~160°) and hydrophilic (WCA ~5°) areas. Due to the extreme difference in water repellency of superhydrophobic borders and hydrophilic spots, droplets of controllable volumes (80 nL - 25 µL) are spontaneously formed when a droplet of cell suspension is rolled on the surface. Thereby the average initial cell number per spot is for 1 mm spots (1 mm^2 spot area, 80 nL) ~20 cells/mm^2 (~0.001 mm^2 average colony size at 48 h) and for 3 mm spot (9 mm^2 spot area, 25 µL) ~16 cells/mm^2 (~0.003 mm^2 average colony size at 48 h) On the other hand, the porous polymer's surface roughness (68 ± 30 nm) also promotes the maintenance of stemness of mouse embryonic stem cells (mESC). A transgenic stem cell line with GFP stably fused to Oct4 was used in this study (mESC Oct4-eGFP).
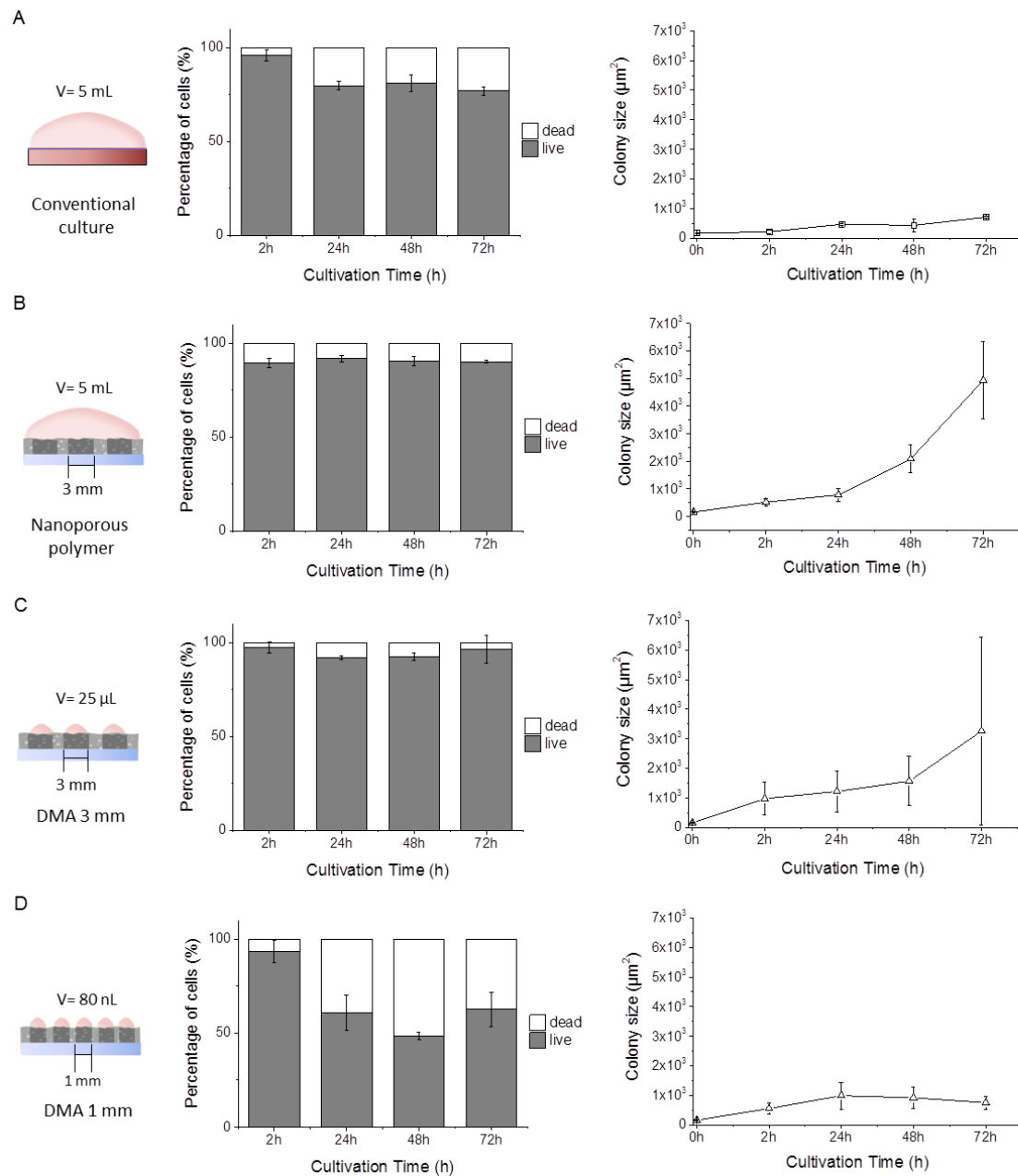
3.2.2 Viability and growth of mESC on the DMA

In order to evaluate the ability of the DMA to maintain pluripotency and self-renewal of mESCs cultured inside droplets the transgenic mouse embryonic stem cell line (mESC Oct4-eGFP), stably expressing eGFP fused to the pluripotency gene Oct4 (Kirchhof *et al.*, 2000) was chosen. This cell line enables immediate read-out and characterization of stemness by measuring the mean fluorescence intensity correlating with expression levels of the Oct4-eGFP reporter gene as well as by counting cells and cell colonies. Conventional culture conditions for mESCs included culturing in flasks precoated with gelatin in the presence of mitotically inactivated MEFs in culturing medium supplemented with LIF. Under these conditions, the spontaneous differentiation of mESC was inhibited for about 2 days before the cells had to be passaged. The absence of only one of the aforementioned requirements, such as MEFs, can trigger the spontaneous differentiation of mESCs (Heo *et al.*, 2005).

Volume of the droplets formed on DMA slides can be varied between 80 nL and 25 μL, which is significantly smaller than in conventional Petri dishes and might influence cell viability. The viability of mESC Oct4-eGFP on the DMA was analyzed and compared that to that of mESCs cultured under conventional conditions (Figure 11A-D). mESC Oct4-eGFP were stained with propidium iodide (PI) and Hoechst 33342 to quantify the percentage of dead (PI-positive and Hoechst-positive) and viable (PI-negative and Hoechst-positive) cells. The greatest viability was observed when mESCs were cultured in 5 mL medium on the patterned, nanoporous polymer surfaces (Figure 11B; 25 nL/cell), and on the DMA with 3 mm spot size and 25 μL volume per droplet (Figure 11C; 160 nL/cell). In comparison with conventional culture conditions (5 mL volume; 25 nL/cell; Figure 11A), the mESCs cultured on the DMA with spots measuring 1 mm (80 nL volume; Figure 11D) exhibited decreased viability after 48 h of culturing. Whereas regular medium exchange in 1 mm droplets on the DMA resulted in a lower percentage of dead cells and improved viability after 48 h of culturing (Figure A 3A). These results demonstrate that the reduced cell viability in 1 mm (80 nL volume; 4 nL/cell) droplets (Figure 11D) resulted from a limited amount of nutrients appropriate for extended culture periods ($\geq$ 48 h) in smaller volumes.

Next the mESC cell growth was examined at 2 h, 24 h, 48 h and 72 h under the aforementioned conditions without cell passaging to assess the effect of surface roughness and volume size of the droplets on proliferation and cell growth (Figure 11

and Figure A 3B). The mESC colony size was measured and used as an indicator for colony growth, since the assessment of cell growth and proliferation by counting individual cells in colonies of particular sizes proved to be difficult. A higher growth rate was observed when the mESCs were cultured on the fully immersed, patterned, nanoporous polymer surface or on the DMA (1 mm spot size, 80 nL volume, average initial cell number of 20 per mm^2; 3 mm spot size, 25 µL volume, average initial cell number of 16 per mm^2) (Figure 11B-D) than mESCs grown under conventional culture conditions involving MEFs and large medium volume (Figure 11A). The results demonstrate increased growth and comparable viability of mESCs cultured on the immersed, nanoporous polymer in 5 mL volume and even on the DMA with 3 mm and 1 mm spot size and smaller volumes (80 nL - 25 µL), when compared with the conventional culture method. The positive effect on mESCs´ viability, resulting from the polymer surface roughness (Figure 11A-B), enables culture of mESC in droplets with volumes of 80 nL - 25 µL (1 mm – 3 mm spot size). Though longer culture periods ($\geq$ 48 h) in small volumes such as 80 nL further require regular medium change to sustain a sufficient supply of nutrients that maintains mESC viability comparable to that of conventional culture (Figure 11A and Figure A 3 A). Furthermore the surface roughness of the polymer in combination with the culture volume enhances proliferation and growth of mESCs (Figure 11A-D).

Figure 11. Viability and growth rate of mESC Oct4-eGFP over time under different conditions.
(A) mESC grown under conventional culture conditions (+MEFs, +gelatin, +LIF; 5 mL total volume).
(B) mESC grown on the nanoporous polymer surface (-MEFs, +gelatin, +LIF; 5 mL total volume).
mESCs grown on DMA in individual droplets with (C) 3 mm spot size (-MEFs, +gelatin, +LIF; 25 μL total volume) and (D) 1 mm spot size (-MEFs, +gelatin, +LIF; ~80 nL volume). To test viability, mESCs were stained with propidium iodide (PI; dead cells) and Hoechst 33342 (cell nucleus), and the percentage of dead (PI+, Hoechst+) and viable (PI-, Hoechst+) cells was assessed. The growth rate was quantified by measuring colony size. N=3; n >150
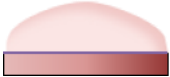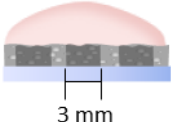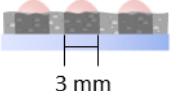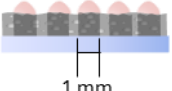
3.2.3 Quantifying mESC stemness on the Droplet Microarray via the Oct4-eGFP reporter gene

The maintenance of stemness and mESC differentiation depend on several factors such as a precisely regulated microenvironment and controlled medium composition. To assess the importance of creating the ideal microenvironment for the individual factors used in conventional culture, the influence of each individual factor, namely gelatin coating, MEFs, and LIF supplementation on stemness of mESC cultured in polystyrene, cell culture Petri dishes was analyzed. For this purpose one of these factors was removed at a time and compared the mean fluorescence intensity to control conditions with all the factors present (Figure A 4A). The results revealed a significant decrease by three times in the Oct4-eGFP mean fluorescence intensity in the absence of medium supplementation with LIF, indicating that LIF can be considered the main factor influencing the maintenance of mESC stemness. Furthermore, the results demonstrate that coating the Petri dish surface with gelatin is an important factor for maintaining stemness, resulting in a 2.5-fold decrease of the Oct4-eGFP mean fluorescence intensity. In contrast, it was noted that coating the DMA surface with gelatin yielded no visible effect on the mESC´s fluorescence intensity (Figure A 4B). To ensure the DMA's comparability to the conventional culture, all following experiments were conducted by supplementing the medium with LIF and coating the DMA with gelatin.

Next the effect of the nanoporous polymer, in relation to different culturing volumes ranging from 80 nL to 5 mL, on the maintenance of stemness and differentiation of mESCs was investigated by comparing the mean fluorescence intensity and percentage distribution of GFP+, mixed and GFP- colonies (Figure 12A and Table 8). mESCs were cultured under conventional conditions in 5 mL culturing volume, on the immersed nanoporous polymer (5 mL culturing volume) and in droplets on the DMA with hydrophilic spots of various sizes (1 mm - 3 mm) and volumes (80 nL-25 µL) (Table 8). Culturing mESCs on the DMA with spots measuring 1 mm revealed a significant inhibition of spontaneous differentiation for up to 72 h and better maintenance of Oct4-eGFP expression compared to the conventional culture (Figure 12A). A further increase in the mean fluorescence intensity was apparent in conjunction with increasing spot size and volume, as evident for DMA with spots measuring 3 mm with 25 µL volume (Figure 12A) as well as for the completely immersed, nanoporous polymer with

5 mL culturing volume. In contrast no difference was observed in the GFP signal mean fluorescence intensity of mESCs cultured on the DMA with smaller spots measuring 500 µm and 350 µm (Figure A 4C) when compared to that of mESCs in conventional culture conditions. These findings demonstrate the positive influence of the culturing volume on the maintenance of stemness, with volumes higher than 80 nL leading to an increased Oct4 level as indicated by the Oct4-eGFP reporter gene. The mean fluorescence intensity of mESCs cultured on nanoporous polymer in 5 mL volume was four-fold higher than that of mESCs in conventional culture of 5 mL volume, indicating a positive effect of the nanoporous polymer itself on the Oct4 level and on maintaining mESC stemness regardless of the volume (Figure 12A). The tendency in maintaining stemness under different culturing conditions as estimated by mean fluorescence intensity concurs closely with that assessed by comparing the percentage distribution of GFP+, mixed and GFP- colonies per mm^2 (Figure 12A, right side) with 21%, 73%, 43% and 37% of GFP+ colonies remaining after 72 h under conventional culture conditions (5 mL), on the nanoporous polymer (5 mL), and on the DMA with spot sizes of 3 mm (25 µL) and 1 mm (80 nL). However, a slight decrease in percentage of GFP+ and mixed colonies over time (2 h - 72 h) can be observed within the individual, tested conditions. A total decrease from 2 h to 72 h of ~35%, ~5%, ~10%, ~25% under conventional culture conditions (5 mL), on the nanoporous polymer (5 mL), and on the DMA with 3 mm (25 µL) and 1 mm (80 nL) spot size can be observed. As the experiment, shown in Figure 12A, was conducted without any medium change and passaging of the cells throughout the incubation time of 72 h, an increasing lack of nutrients and LIF over time can be assumed, possibly resulting in a decreased viability and an increased induction of spontaneous differentiation over time.

Table 8. Direct comparison between conventional culture conditions, nanoporous polymer and the DMA showing feasible miniaturization of mESC culture using the DMA while promoting stemness.

	Conventional culture	Nanoporous polymer	DMA on nanoporous polymer	
			3 mm	1 mm
	$V = 5$ mL	$V = 5$ mL	$V = 25$ µL	$V = 80$ nL
			3 mm	1 mm
Culture area	55 cm^2	55 cm^2	9 mm^2	1 mm^2
Volume	5×10^6 nL	5×10^6 nL	25×10^3 nL	80 nL
Initial cell number per mm^2	36	36	16	20
Volume per cell	25 nL/cell	25 nL/cell	160 nL/cell	4 nL/cell
Density of experiments per cm^2	1	1	9	49
MEFs (mouse embryonic fibroblast)	Yes	-	-	-
Number of Oct4-eGFP positive colonies / mm^2 (at 72 h)	4 (21%)	5 (73%)	3 (43%)	2 (37%)
Number of Oct4-eGFP negative colonies/ mm^2 (at 72 h)	12 (63%)	1 (15%)	2 (30%)	3 (44%)

To confirm the observed positive effect of nanoporous polymer and different culturing volumes on prolonging the maintenance of mESC stemness using different read-outs, the mESC stemness was quantified via flow cytometry (Figure 12B) and qPCR (Figure A 5). For the flow cytometric analysis, the mESC Oct4-eGFP were cultured under different conditions for up to 72 h before being detached and stained with propidium iodide to distinguish between viable (PI-) and dead cells (PI+). A threshold was set before measuring in order to assess the number of true GFP+ cells without including

false positive signals generated by debris, for example. The results in Figure 12B illustrate the number of PI- and GFP+ cells exceeding the preset threshold and normalized to the control sample. The flow cytometric results correlate well with the results obtained using microscopic read-out, and indicate the inhibition of spontaneous differentiation of mESCs when cultured on the nanoporous polymer (5 mL volume) and in the individual droplets (3 mm 25 µL; 1 mm 80 nL) on the DMA (Figure 12B). The assessment of mESC stemness via direct quantification of the Oct4 expression level using qPCR (Figure A 5) also exhibited the nanoporous polymer's positive effect, resulting from the surface roughness, on maintaining stemness in relation to the culture volume and was in good agreement with results obtained using microscopic read-out.

Taken together, these results further demonstrate the dual-functionality of the polymers surface roughness that enables the generation of an array with multiple droplets of various sizes and volumes (DMA 3 mm and 1 mm) allowing culture of mESC, while at the same time maintaining stemness and inhibiting spontaneous differentiation for up to 72 h cultivation time.
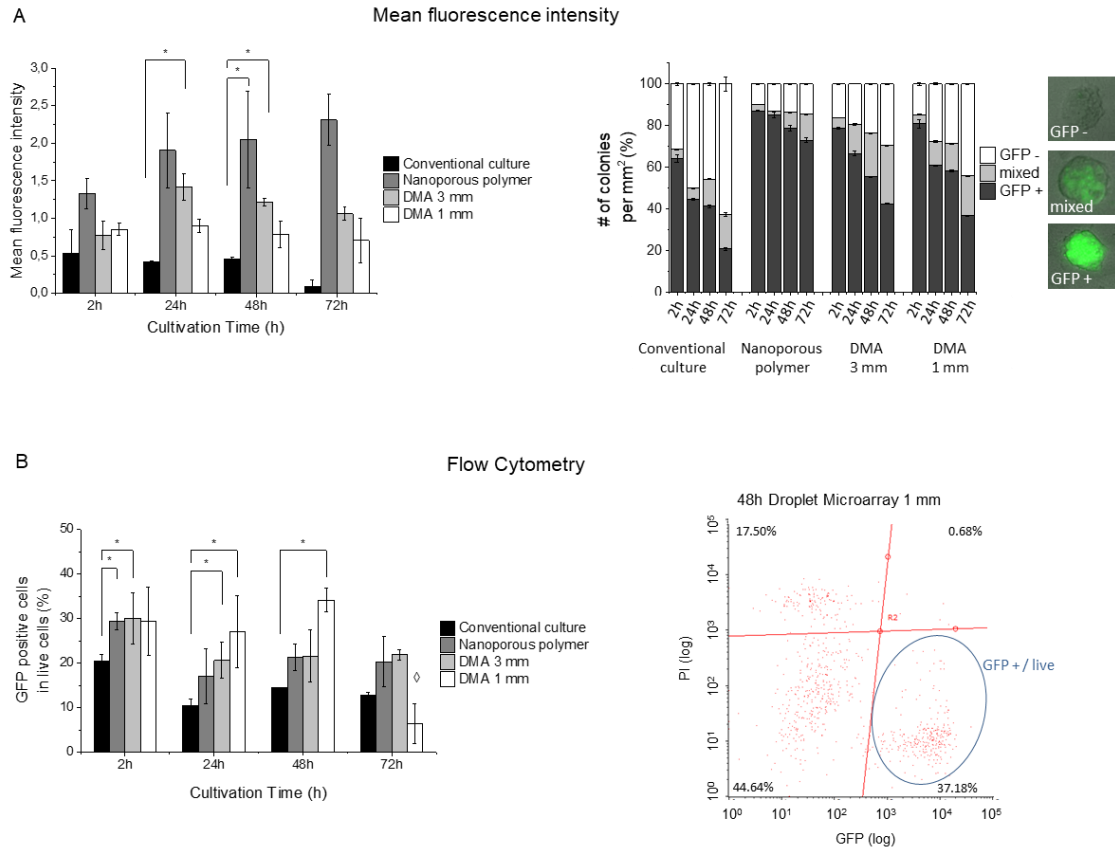
Figure 12 Quantifying mESC Oct4-eGFP stemness. (A) Measurement of Oct4-eGFP mean fluorescence intensity obtained *via* image analysis and number of GFP+, mixed, and GFP- colonies per mm². Representative images of colonies defined as GFP+, mixed and GFP-. N=3; n >100 (B) Flow cytometric analysis showing count of GFP positive cells with fluorescence intensities exceeding preset threshold. ◊ decreased viability of mESCs. Dot plot showing results of DMA 1 mm spot size and 48 h cultivation time. Gated population depicting GFP+ and live (PI-) cell count. N=3; n= 5000 counted cells; statistical significance: t-test, *indicates p-value ≤0.05.

In order to show that the mESCs, cultured under conventional conditions and on the DMA for 72 h, retain their ability to differentiate into cells of the three germ layers endo-, meso-, and ectoderm (pluripotency), embryoid bodies (EBs, agglomerates of stem cells) were formed. For this the "hanging drop" method was used. Therefore, mESC cultured under conventional conditions (5 mL) and on the DMA 3 mm spots (25 µL) were detached and cultured in absence of LIF in "hanging drops". This resulted in the formation of EBs and in a disordered differentiation into cells of the three germ layers. The EBs were stained for particular markers of endo-, meso-, and ectoderm (FoxA2, Brachyury, β-III-Tubulin). Representative images of the immunofluorescence staining for markers of all three germ layers are presented in Figure 13 showing

differentiation into cells from endo-, meso-, and ectoderm upon conventional culture and culture on the DMA, proving the pluripotential of the respective mESC.

Next the enhancing effect of the polymers surface on the maintenance of stemness for cultivation periods longer than 72 h (up to 20 days), which remains, without precise regulation of culture conditions and regular passaging (every 2nd day), challenging using standard *in vitro* culture was examined.
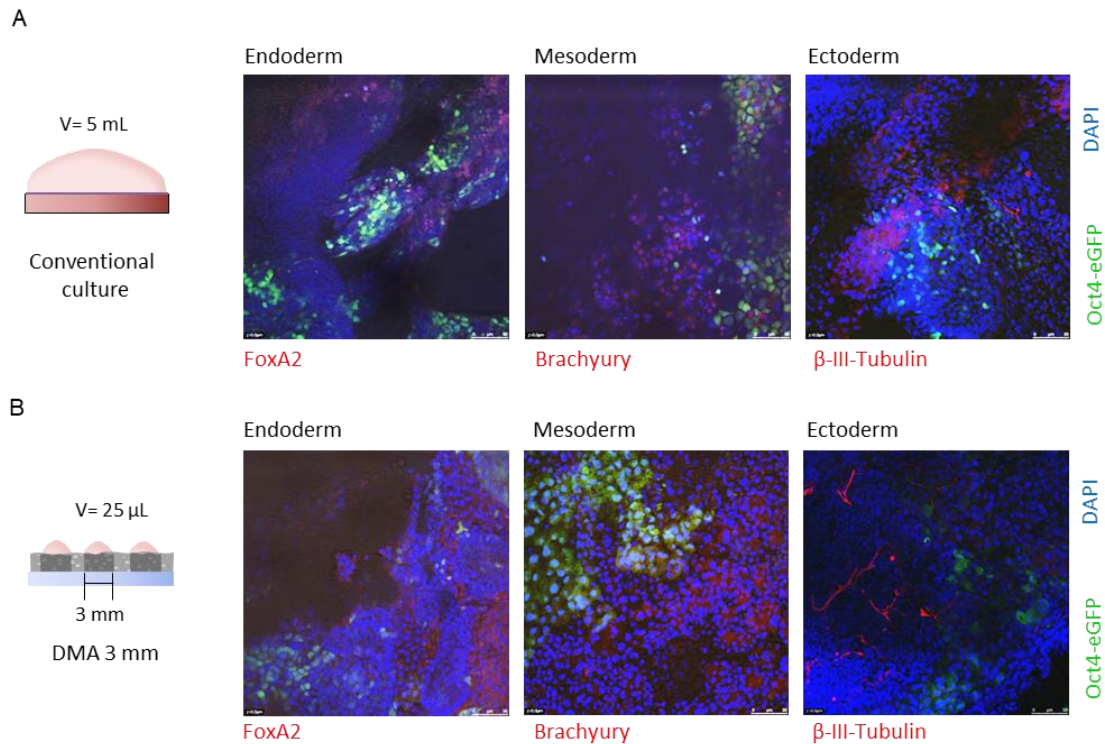
Figure 13 Immunofluorescence staining showing potential of mESC Oct4-eGFP to differentiate into three germ layers (endoderm, mesoderm, ectoderm). mESC Oct4-eGFP were grown under (A) conventional culture conditions (5 mL volume) and (B) on the DMA with 3 mm spot size (25 μL volume) for 72 h. Cells were detached and cultured for 48 h using the "hanging drop" method to generate embryoid bodies (EBs). EBs of respective samples were transferred to Fibronectin coated cover slips and cultured for 12 days. Subsequently immunofluorescence staining of endo-, meso-, and ectoderm markers (FoxA2, Brachyury, β-III-Tubulin) and DAPI (cell nucleus) on the respective cover slips was performed.

Maintaining stemness *in vitro* is challenging and requires precise and closely regulated environmental and culturing conditions. As shown in Figure 12A, it was possible to reduce spontaneous differentiation by 19% − 48% upon culture of mESC on the DMA (1 mm or 3 mm) and the nanoporous polymer without passaging for up to 72 h. To investigate the effect of the nanoporous polymer on maintaining stemness for long-term culture, mESC were cultured under conventional culture conditions

(+MEF, +gelatin coating, +LIF), in absence of MEFs (-MEFs, +gelatin coating, +LIF) and on the nanoporous polymer surface (-MEFs, +gelatin coating, +LIF), all in final volume of 5 mL and without passaging the cells (Figure A 6). The culture medium was changed every 2nd day to maintain sufficient nutrient supply and to sustain the mESCs' viability. After 3 days of cultivation, mESCs grown under conventional culture conditions and in the absence of MEFs exhibited increased differentiation, as indicated by the elevated numbers of GFP- of ~14% and mixed colonies of ~9% (Figure A 6; Conventional culture and Ctrl -MEFs). After 20 days of culture, mESC grown on the nanoporous polymer surface displayed a ~25% decrease in the percentage of GFP+ colonies compared to a ~96% decrease in the conventional culture revealing delayed spontaneous mESC differentiation compared to the conventional culture conditions (Figure A 6; Nanoporous polymer). As the initial cell density and LIF concentration were kept the same and as the culture medium in the long-term culture samples (Figure A 6) was changed regularly to maintain adequate nutrient supply, the inhibiting effect on maintenance of stemness and mESC differentiation must be an impact from the polymer's surface roughness.

It was recently shown, that the HEMA-EDMA surface roughness of 68 ± 30 nm and higher (nano- and micro-nanorough) resulted in a reduced integrin clustering and formation of actin-rich protrusions-like extensions (Jaggy *et al.*, 2015). Based on this and recent findings describing the influence and importance of cell surface interaction (cell anchorage; integrin signaling) on stem cell development and differentiation it was hypothesized, that a reduced integrin signaling in combination with actin-rich protrusion are involved in the maintenance of stemness and could also be the underlying mechanism resulting in the differences in stem cell differentiation observed on the nanoporous DMA (roughness 68 ± 30 nm) (Brafman *et al.*, 2013; Hayashi *et al.*, 2007; Jaggy *et al.*, 2015).

In this part of the project the potential of the DMA based on the nanoporous HEMA-EDMA polymer to maintain mESC stemness in micro to nanodroplets (25 µL to 80 nL volume) due to the polymer surface roughness was shown. The prolonged maintenance as well as the culture in multiple, defined and separated microdroplets on the DMA, demonstrates its potential application as miniaturized platform enabling high-throughput screening of undifferentiated mESCs.

3.3 Droplet Microarray: miniaturized platform for rapid formation and high-throughput screening of embryoid bodies

In the previous part the potential applicability of the DMA for high-throughput screening (HTS) of mESC while promoting their undifferentiated state was demonstrated. The presented methodology allows HTS of mESC in 2D culture. However the development and the performance of HTS on 3D model system, due to their high resemblance of the *in vivo*-like state, is gaining more and more importance in drug discovery, pharmaceutical and clinical research. HTS on 3D model systems, hence, leads to more precise and clinically relevant results. Stem cell research is thereby focusing on the generation and use of organoids (3D cell aggregates showing features of the represented organ) and embryoid bodies (EB, formed in suspension culture of stem cells). EBs are embryonic stem cell aggregates that exhibit similarities to the embryo and recapitulate the early embryonic development differentiating into cell derivatives of all three germ layers (endo-, meso-, and ectoderm). Therefore the use of EBs in HTS can help to identify compounds with developmental toxicity, resulting in an increased drug safety and possibly reduced use of *in vivo* testing at early stages of drug discovery. Main methods applied for the generation of EBs in drug screening are currently the use of low adherence plates or "hanging drop" method, both requiring multiple pipetting steps and further emitting the need for pipetting robotics to conduct HTS.

In the next part the DMA was applied in order to generate an array of multiple microdroplets in a facile, one-step seeding method containing homogeneous EBs. Thereby the individual EBs in the confined microdroplets can be cultured and treated separately, enabling miniaturized screening in low volumes of compound effect on embryonic development and embryotoxicity in a high-throughput manner.

3.3.1 Use of the DMA for generation of an embryoid body (EB) array

The DMA was produced as follows: briefly, a microscopic glass slide (7.5 cm x 2.5 cm) was coated with a 3.6 µm-thin nanoporous poly(2-hydroxyethyl methacrylate-*co*-ethylene dimethacrylate) (HEMA-EDMA) layer (Tronser *et al.*, 2017). Surface modification of the polymer layer, performed using the photo-induced thiol-yne click chemistry, resulted in formation of hydrophilic spots (static water contact angle <10°), separated by superhydrophobic borders (advancing, static and receding water contact angles ~161°, ~153° and ~148°, respectively) (Feng *et al.*, 2014). The extreme difference in the wettability of the hydrophilic spots and the superhydrophobic borders enables the effect of discontinuous dewetting and formation of high-density arrays of microdroplets by simple immersing the superhydrophobic-hydrophilic array into a cell suspension or by rolling a bigger droplet over the array (Feng *et al.*, 2014; Popova *et al.*, 2015; Popova *et al.*, 2016; Popova *et al.*, 2017; Tronser *et al.*, 2017; Ueda *et al.*, 2012; Ueda *et al.*, 2016). In this work the "standing droplet" method was used, which is based on placing a droplet of cell suspension onto the superhydrophobic-hydrophilic array for 30 seconds, followed by tilting the slide to remove excess medium and to form a Droplet Microarray containing mESCs (Figure 14A). In this part of the project spots of 1 mm side length separated by 0.5 mm superhydrophobic borders were used, generating a microarray consisting of 588 microreservoirs, (Figure 14B) enabling culture and screening of stem cells in individual, separated nanoliter droplets (average droplet volume 80 nL) (Popova *et al.*, 2015; Popova *et al.*, 2016; Tronser *et al.*, 2017; Ueda *et al.*, 2012).

For the generation of an embryoid body array, a transgenic mouse embryonic stem cell line, stably expressing eGFP fused to the pluripotency gene Oct4 was chosen (mESC Oct4-eGFP). This cell line enables direct microscopical read-out of stemness through the Oct4-eGFP construct, which makes it convenient for high-throughput screening applications (Kirchhof *et al.*, 2000). Thus, mESC Oct4-eGFP were seeded onto a DMA slide in a single-step, creating a microdroplet array containing cells. The DMA was immediately turned over, allowing culture of mESC in hanging microdroplets for 72 h (Figure 14A), whereas the first formed 3D mESC aggregates were already observed after 48 h cultivation (Figure 14C). This is in close concordance with conventional methods used to form EBs, such as the "hanging drop" method during which dense ESC aggregates are formed after 48 -72 h (Buesen *et al.*, 2004).

Embryoid bodies recapitulate the early embryonic development and have the potential to differentiate into cell derivatives of all three germ layers. In order to proof that the observed mESC aggregates are in fact embryoid bodies and have the potential to differentiate into the respective cell derivatives, immunofluorescence staining for specific markers of the three germ layers was performed. Therefore, mESC Oct4-eGFP were cultured on the inverted DMA in hanging droplets for 48 h in order to form potential EBs. These potential EBs were then collected and cultured for further 12 days on fibronectin coated cover slips, enabling outgrowth and differentiation into cells of the three germ layers. The markers used for immunofluorescence staining were FoxA2, Brachyury and β-III-tubulin for endo-, meso-, and ectoderm, respectively and the presence of the respective markers in the tested samples (Figure 14D) was shown, proving the mESC aggregates that formed on the DMA to be EBs with the potential to differentiate into all three germ layers.
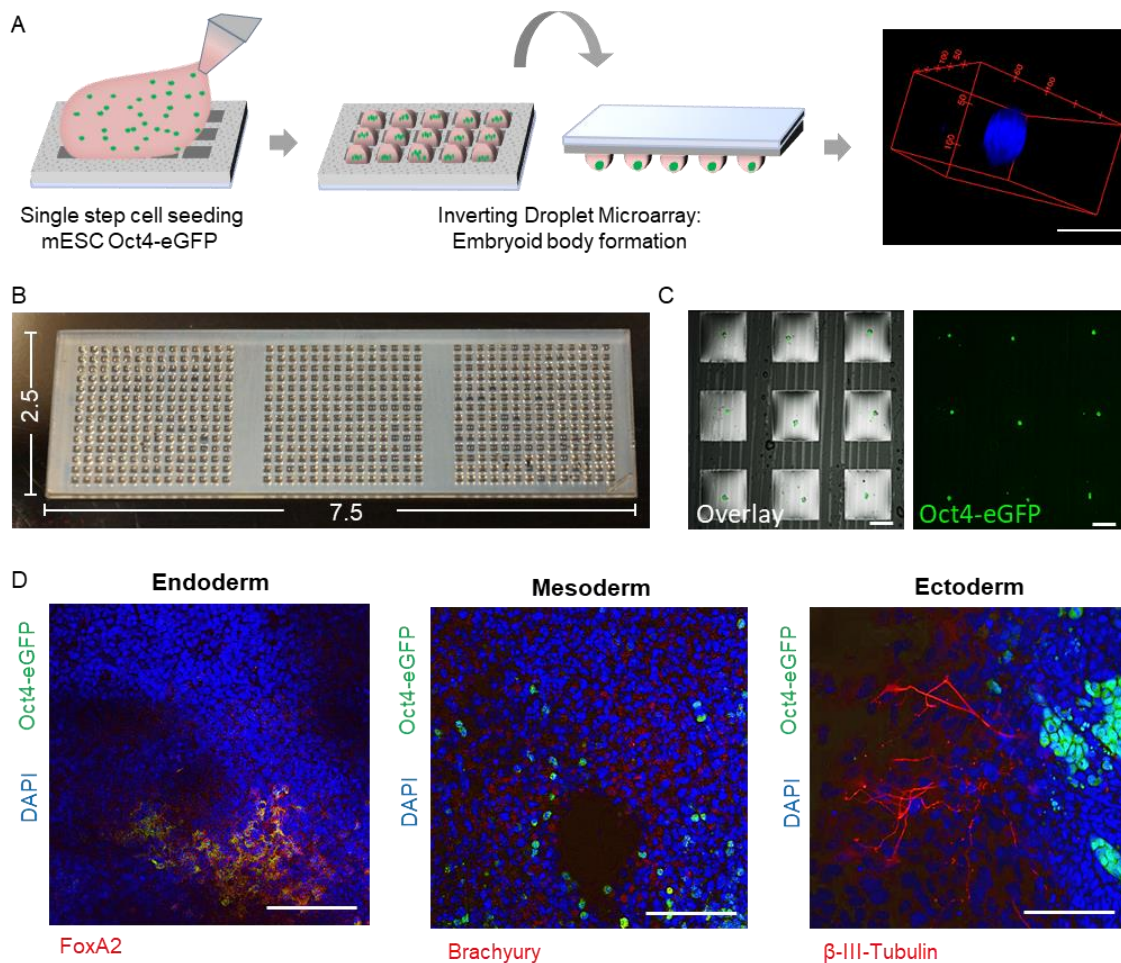
Figure 14. Droplet Microarray as platform for embryoid body formation. (A) Schematic representation of the experimental set-up for the formation of microarrays of single embryoid bodies (EB) and confocal microscopy-based 3D reconstruction of a single EB. Scale bar 100 µm (B) Representative image of DMA with 588 microdroplets. (C) Fluorescence microscopy image showing single EBs formed on DMA (1 mm side length of spots) in individual microdroplets after 48 h incubation. Left: overlay of green channel and brightfield; right: green channel (Oct4-eGFP). Scale bar 500 µm. (D) Proof of potential of the EBs formed on the DMA to differentiate into cell derivatives of all germ layers. After 48 h EBs formed on the inverted DMA, were collected and transferred to fibronectin coated coverslips. Following, EBs were cultured on coverslips for 12 days with regular medium changes, allowing outgrowth of EBs and spontaneous differentiation into all 3 germ layers (endo-, meso-, and ectoderm). To proof differentiation into all 3 germ layers immunofluorescence staining for markers of endo-, meso-, and ectoderm (FoxA2, Brachyury, β-III-Tubulin) was performed on respective samples. Immunofluorescence images showing differentiated cells expressing marker of respective germ layer (red channel), cell nucleus (DAPI staining, blue channel) and undifferentiated cells (Oct4-eGFP, green channel). Scale bar 100 µm. N=3, n > 150

In HTS it is important to achieve high homogeneity of the EB sizes in order to sustain high comparability and reproducibility of the obtained results. One of the problems of EB formation in higher-throughput is the difficulty to keep their size and roundness equal. Thus, the formed EBs were analyzed and characterized for their homogeneity, size and roundness. For the quantification, the DMA was turned over again, the EBs were imaged using an inverted fluorescence microscope and the respective parameters were measured using ImageJ. A strong correlation between initial cell density and size of the EBs (area and diameter) (Figure 15A) was observed. The initial cell concentration of 0.16×10^6 cells/mL, which is approximately ~13 mESC per spot, resulted in formation of EBs with an average diameter of 34 ± 4.5 μm (Figure 15A). In contrast an increase of the initial cell number by only 3 cells per spot, from ~13 to ~16 cells (from 0.16×10^6 cells/mL to 0.2×10^6 cells/mL, respectively), resulted in an increase of the average diameter by ~15 μm (from 34 ± 4.5 μm to 49 ± 0.02 μm). A further increase in the EB size was observed with increase of the initial cell density to 0.3×10^6 cells/mL. On the contrary, the initial cell density showed only slight effect on the roundness of the EBs. The roundness thereby is defined by how close the EB morphology approaches that of a mathematically perfect circle (roundness of 1). The EBs showed a roundness of 0.83 ± 0.1, 0.84 ± 0.02 and 0.74 ± 0.06 in case of 0.16×10^6 cells/mL, 0.2×10^6 cells/mL and 0.3×10^6 cells/mL, respectively. Good homogeneity in size (49 ± 0.02 μm) and roundness (0.84 ± 0.02), demonstrated by low variances between individual EBs, was achieved in case of 0.2×10^6 cells/mL initial cell seeding concentration (Figure 15A) and thus employed for all following experiments.

Using the described method homogeneous distribution of formed EBs on the DMA was achieved, with an average of 63% of single EBs formed per spot, 11% of two EBs, 4% with more than two EBs and 21% of empty spots (Figure 15B). The high percentage of droplets containing single EBs enables drug screening and developmental investigation of individual EBs and is in close concordance with the percentage of formed EBs using conventional methods, like the "hanging drop" method (Kurosawa *et al.*, 2003).

Further the viability of the EBs upon culture in hanging droplets for up to 72 h was assessed, by measuring the area fraction of viable and dead cells in regard to the total EB area. mESCs Oct4-eGFP were seeded and cultured for 72 h in presence of propidium iodide (PI), to estimate the number of dead cells (PI positive, Hoechst positive), and in presence of Hoechst 33342, to assess the number of viable

cells (PI negative, Hoechst positive). The culture in hanging droplets on the DMA showed 90-95% viability of EBs during the first 48 h and 85% after 72 h of culture (Figure 15C).
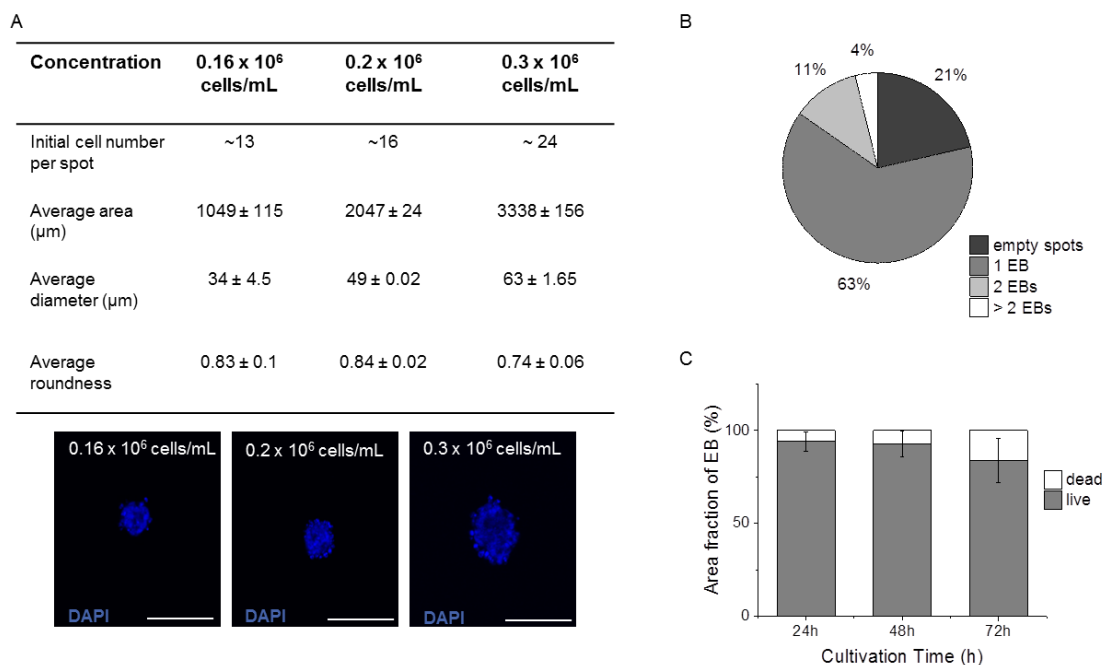
Figure 15. Characterization of formed EBs. (A) Table with average area, diameter and roundness of EBs in regard of the initial cell seeding concentration. N=3, n > 200. Representative fluorescence images of EBs with different initial cell seeding concentrations after 72 h incubation. DAPI staining of cell nucleus. Scale bar 100 μm. (B) Distribution of EBs on DMA. Percentage of droplets with 1 EB, 2 EBs, > 2 EBs and empty spots. Initial cell seeding concentration used was 0.2×10^6 cells/mL. (C) Estimation of viability by measuring area fraction of dead and viable cells of respective EBs. Propidium iodide (PI; 100 nM) and Hoechst 33342 (1:100000) were used to stain dead cells (PI positive, Hoechst positive) and viable cells (PI negative, Hoechst positive). Images were taken at 24 h, 48 h and 72 h. N=3, n >100.

3.3.2 Establishment of the DMA as platform for high-throughput screening

The results demonstrate the feasibility of using the DMA for facile, one-step formation of arrays of multiple, homogeneous EBs while maintaining good viability within 72 h cultivation time. To evaluate the DMA as a HTS platform for EBs, preliminary investigations had to be conducted, such as the investigation for possible cross-contamination between compounds that were previously printed onto the individual spots of the DMA. This cross-contamination can occur during the seeding

process due to the use of the "standing droplet" method, during which all individual spots are covered by a big droplet of cell suspension for 30 sec. In order to prevent the compounds from dissolving during this 30 sec seeding procedure, the hydrophilic spots containing the respective preprinted compounds were coated with 2.2 wt% gelatin in water using a non-contact printer. Figure 16 shows the results of the cross-contamination pretest using doxorubicin in a concentration of 10 µM that was printed in a checker board pattern on the DMA, followed by coating with 2.2 wt% gelatin in water. In a first step, seeding was mimicked by applying a standing droplet of PBS covering all spots of the DMA. The brightness of each spot in line was measured before and after applying PBS (Figure 16A) and the results demonstrate a reduction of cross-contamination between the spots containing doxorubicin (red fluorescence; Line 1) and the neighboring, individual empty spots (no fluorescence; Line 2) to the greatest possible extent. Further, mESCs Oct4-eGFP were seeded on a DMA slide with doxorubicin preprinted, cultured for 24 h and followed by quantification of the drug´s effect on viability and stemness in 2D culture. The percentage of dead cells was higher in spots containing doxorubicin (Slide 1: compound slide) than on the empty control slide (Slide 2: empty slide, Figure 16B) indicating its cytotoxic effect. Furthermore a strong decrease in the percentage of GFP+ cells can be observed on the doxorubicin spots (Slide 1) compared to the control slide (Slide 2), rather due to the cytotoxic effect of doxorubicin resulting in a general decrease of the total cell number than due to an induction of differentiation (Figure 16C). The percentage of viable cells as well as the percentage of GFP+ cells in the empty spots on the compound slide (Slide 1), that are in close proximity to the doxorubicin spots, show a slight decrease compared to the compound-free control slide (Slide 2), indicating a minimal cross-contamination during the seeding procedure in case of water soluble compounds such as doxorubicin. However the observed differences between the empty spots and the doxorubicin containing spots (Slide 1: compound slide) demonstrate an acceptable reduction of cross-contamination to the greatest possible extent through the gelatin coating using this experimental set-up. Various options to further decrease or completely prevent cross-contamination, as for example the decrease of the seeding time from 30 sec down to 10 sec as well as employing a non-contact cell printer for direct seeding of the cells into the respective droplets, are possible and will be investigated in future.
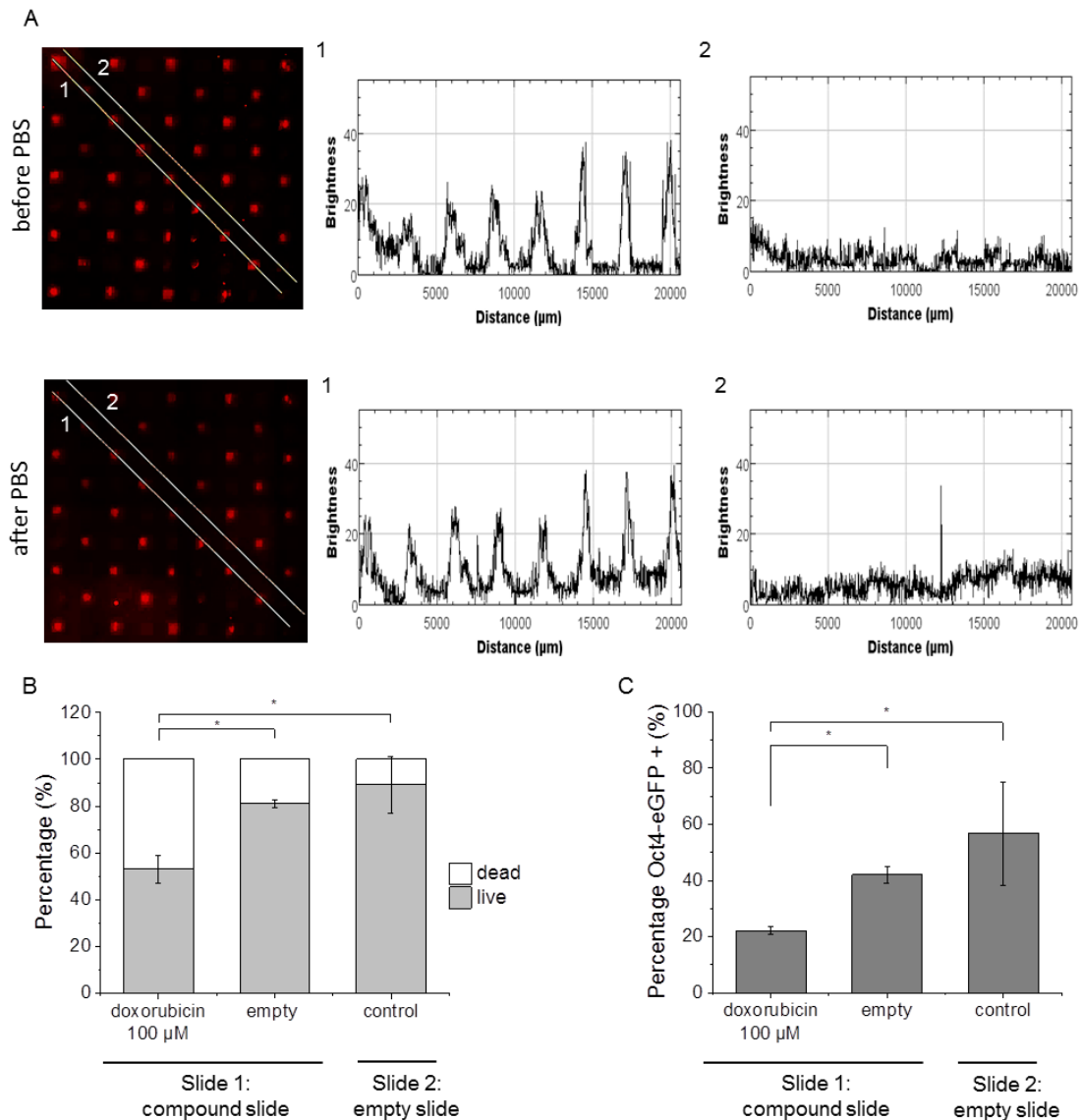
Figure 16. Pretest for cross-contamination between individual spots on DMA slide during seeding. (A) Fluorescence image of DMA slide with printed doxorubicin (red fluorescence; 10 µM) and empty spots (no fluorescence) in checker board format before (upper image) and after (bottom image) applying PBS in "standing droplet" covering all spots. Brightness measurement of doxorubicin spots (line 1) and empty spots (line 2). (B) 2D culture of mESC Oct4-eGFP on slides preprinted with doxorubicin. Percentage of dead (PI positive; hollow bars) and viable cells (PI negative; grey bars) on spots containing doxorubicin (10 µM) and empty spots after 24 h incubation. Slide 1: compound slide with doxorubicin (10 µM) printed in checker board format on the DMA. As control serves slide 2: empty slide without compound (compound-free slide). (C) Percentage of GFP+ mESC Oct4-eGFP on doxorubicin and empty spots on the compound slide after 24 h incubation. Slide 1: compound slide with doxorubicin (10 µM) printed in checker board format on the DMA. As control serves slide 2: empty slide without compound (compound-free slide). N=3, n > 100; statistical significance: t-test, *indicates p-value ≤0.05.

3.3.3 High-throughput screening of FDA approved compound library

The previous results demonstrate the feasibility of using the DMA platform preprinted with a library of compounds for HTS of EBs. This new methodology shows promising potential in facilitating and advancing drug screening using stem cells. Currently drug screenings are mainly done using 2D stem cell culture systems, in which major differences in stem cell behavior can be observed due to dissimilarities to the *in vivo* microenvironment of stem cells (Gaharwar *et al.*, 2016; Walker *et al.*, 2009). Hence, huge efforts are made to establish 3D stem cell culture systems that resemble a more natural microenvironment and enable replacement of conventional 2D screening systems. In case of embryonic stem cells such a 3D, *in vitro* system is the use of EBs. Thereby conventional methods, such as low adherence microtiter plates and the "hanging drop" method, used for screening of EBs have several limitations. First of all high amount of valuable stem cells and costly reagents are needed. This and the limited availability, and restricted expandability of stem cells make it impossible to perform HTS of EBs using the conventional methods. Furthermore these methods require several pipetting steps in order to perform screenings of EBs, emitting the urge for pipetting robotics. The DMA, however, allows a reduction of cells and reagents by 1000 fold (from microliter to nanoliter range) enabling HTS of EBs in miniaturized and defined volumes. In addition using the preprinted DMA allows fast formation and screening of multiple EBs in a single pipetting step, facilitating HTS and restricting the need for pipetting robotics. In order to exploit these benefits given by the use of the DMA as miniaturized screening platform, a HTS of 774 FDA-approved compounds using EBs to identify compounds with effect on embryonic development was performed. Therefore FDA-approved compounds were preprinted on the DMA in the respective hydrophilic spots and coated with 2.2 wt% gelatin in water, using a non-contact printer. For better comprehensibility the preprinted DMA will subsequently be referred as library-DMAs. Following preprinting, mESC Oct4-eGFP were seeded on the library-DMA and immediately inverted to allow cultivation in hanging droplets and formation of EBs in presence of the respective compounds for 72 h. Thereby a uniform dissolving rate within the various compounds is assumed, although differences due to variable solubility of the compounds, can be possible. Pretests using the compounds 13-cis-retinoic acid and 5-fluorouracil, each preprinted on the DMA in a concentration of 10 μM, showed a decrease in mean fluorescence intensity of the EBs compared to the

internal control (empty spots), indicating differentiation induced by the respective compounds present (Figure 17B). Further in case of 13-cis-retinoic acid a decrease of the EB size can be observed compared to the control, as shown in a previous study (Nierode *et al.*, 2016). The observed effects of the compounds on the EB development within the first 72 h demonstrate the applicability of the library-DMA for screening of EBs. Next a primary screen with 774 compounds of the FDA-approved drug library printed on the DMA was conducted, with each compound in 10 µM concentration and in triplicates, resulting in a screen of 2700 samples in total using only 9 single-pipetting steps. In contrast to that, common EB drug screening methods, like the use of low adherence plates, would require a 300 fold higher number of pipetting steps in order to perform a screen of 2700 samples in one run, further emitting the urge for pipetting robotics. After 72 h incubation time of mESC Oct4-eGFP cultured on the respective library-DMA in hanging droplets, the EB size, EB roundness, toxicity of the compounds and effect on differentiation were assessed (Table A 2). Further compounds that repeatedly inhibited EB formation were considered negative hits, whereas compounds that led to EB formation in all triplicates were considered positive hits (Figure 17C). Out of the 774 tested compounds, 84 compounds repeatedly showed inhibition of EB formation (negative hits) and 50 compounds (10 compounds increasing EB size; 22 compounds reducing EB size; 7 compounds showing toxicity) led to EB formation in all replicates (positive hits). The observed variances in positive and negative EB formation between the replicates of the remaining 640 compounds could be due to marginal differences in EB size between the replicates, with sizes above and below the preset size threshold, thereby causing the observed variances, as samples below the threshold would be excluded by the detection algorithm and hence, considered as negative hit. Further reasons for the observed variances between the replicates could be differences in initial cell number based on the "standing droplet" seeding method and possible differences in diffusion rate of the compounds through the gelatin coating. Especially the latter could be overcome by employing a non-contact cell printer for cell seeding, which could result in a more precise regulation of initial cell number per spot and furthermore, through direct printing of the cells into the compound containing spots, enable cross-contamination-free screening without the need for further gelatin coating.
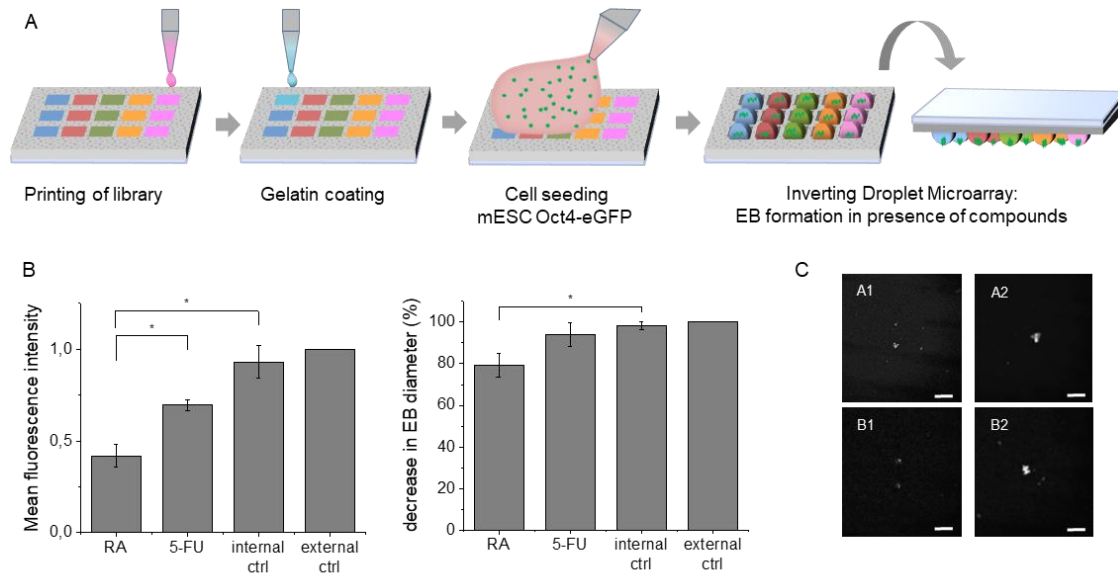
Figure 17. Screening of 774 FD-approved compounds with EBs. Schematic showing workflow of high-throughput screen of compounds using EBs on DMA. Compounds are preprinted into individual hydrophilic spots using a non-contact, liquid dispenser, followed by gelatin coating to reduce leakage of the compounds during the seeding procedure. mESC Oct4-eGFP were seeded with 0.2 x 10^6 cells/mL on the DMA in presence of Hoechst 33342 (1:100000) and PI (100 nM). The DMA was immediately inverted allowing culture of mESC Oct4-eGFP in hanging droplets and formation of EBs in presence of respective compounds for 72 h. (B) Investigation of possible cross-contamination due to seeding procedure on preprinted compound DMA slide. Compounds used for cross-contamination test: 13-cis-retinoic acid (RA; 10 μM); 5-fluorouracil (5-FU, 10 μM). Internal controls are spots without compounds (empty spots) in close proximity to spots with preprinted compounds. Results are normalized to experimental control slide (external control): DMA slide with no compounds printed. Measurement of mean fluorescence intensity of the EBs on the respective spots (RA: RA printed spots, 5-FU: 5-FU printed spots, internal ctrl: empty control spots next to compound spots, external ctrl: compound-free DMA slide) and EB diameter. N=3; n >100. (C) Representative images of Hoechst stain of neighboring spots during the HTS of 774 FDA-approved compounds. Replicates in spots A1 and B1 are showing mESC Oct4-eGFP cultured in presence of 10 μM metyrapone, resulting in no EB formation (negative hit). Replicates in spots A2 and B2 show mESC Oct4-eGFP cultured in presence of 10μM mexiletine HCl, resulting in EB formation with effect on EB diameter (positive hit). Scale bar 100 μm; statistical significance: t-test, *indicates p-value ≤0.05.

3.3.4 Validation of primary high-throughput screen: dose-response-curve

12 compounds, out of the 134 hits, were selected that showed significant effect on at least one of the measured parameters and used those further in a secondary screen (dose-response-curve screen) in order to confirm the observed effects (Figure 18A). The secondary screen showed reproducible dose dependent effects of the respective compounds, in close concordance with the previous observations of the primary screen (Figure A 7- Figure A 10). Compounds inhibiting EB formation during the primary screen (busulfan, digoxin, mycophenolate mofetil) also showed dose-dependent effects on EB formation in the secondary screen, with formation of normally sized EBs (~70 µm) at lowest concentration (0.1µM), increasing reduction in EB size with mediate concentrations (1-10 µM) and no EB formation with highest concentration (30 µM), respectively (Figure 18A and Figure A 7). In case of busulfan previous studies observed similar effects, proving strong embryotoxicity of this compound through induction of DNA damage by alkylation (Table 9) (Mehta *et al.*, 2008; Murdter *et al.*, 2001; Wobus & Loser, 2011). Strong dose dependent effects in EB size were observed for propafenone HCl and mycophenolate mofetil. With increase of the dose from 1 µM to 30 µM, propafenone HCl and mycophenolate mofetil showed an increase in EB size by ~20% and a decrease in EB size by ~60%, respectively (Figure 18B). Treatment with propafenone HCl resulted besides in increased EB size also in a slight increase in toxicity with high doses. This correlates qualitatively with previous studies, in which propafenone HCl has been declared as moderate embryotoxic compound (Table 9) (Paquette *et al.*, 2008). Regarding the other parameters that were measured, close correlation between EB size and stemness can be observed. Higher dose resulted in increased EB size and stemness for propafenone HCl, and accordingly in reduced EB size and stemness for mycophenolate mofetil (Figure 18B and Figure A 10) that is known to promote osteoblast differentiation (Table 9) (Darcy *et al.*, 2012). These results indicate an effect of the respective compounds not only on proliferation but also on differentiation. In contrast, meclizine dihydrochloride showed only slight effect on EB size, roundness or viability but a significant reduction in the mean fluorescence intensity of EBs, indicating the main effect to be on induction of differentiation (Figure 18B). Other compounds strongly affecting stemness and differentiation, measured by the GFP intensity were mesna and digoxin (Figure A 10). Thereby a possible explanation for the

induced differentiation in case of digoxin can be its function as $Na^+ K^+$ ATPase inhibitor (Lin *et al.*, 2017). This subsequently leads to an increased level of intracellular calcium, which may promote activation of contractile proteins such as actin, further resulting in changes of the cytoskeleton that have been shown to strongly influence stem cell behavior and induce differentiation in previous studies (Table 9) (Clausen, 2002; Das *et al.*, 2014). Also lansoprazole showed decreased GFP intensity indicating induced differentiation, which correlates with previous research proving its effect on osteoblastic differentiation (Table 9) (Costa-Rodrigues *et al.*, 2013; Mishima *et al.*, 2015).
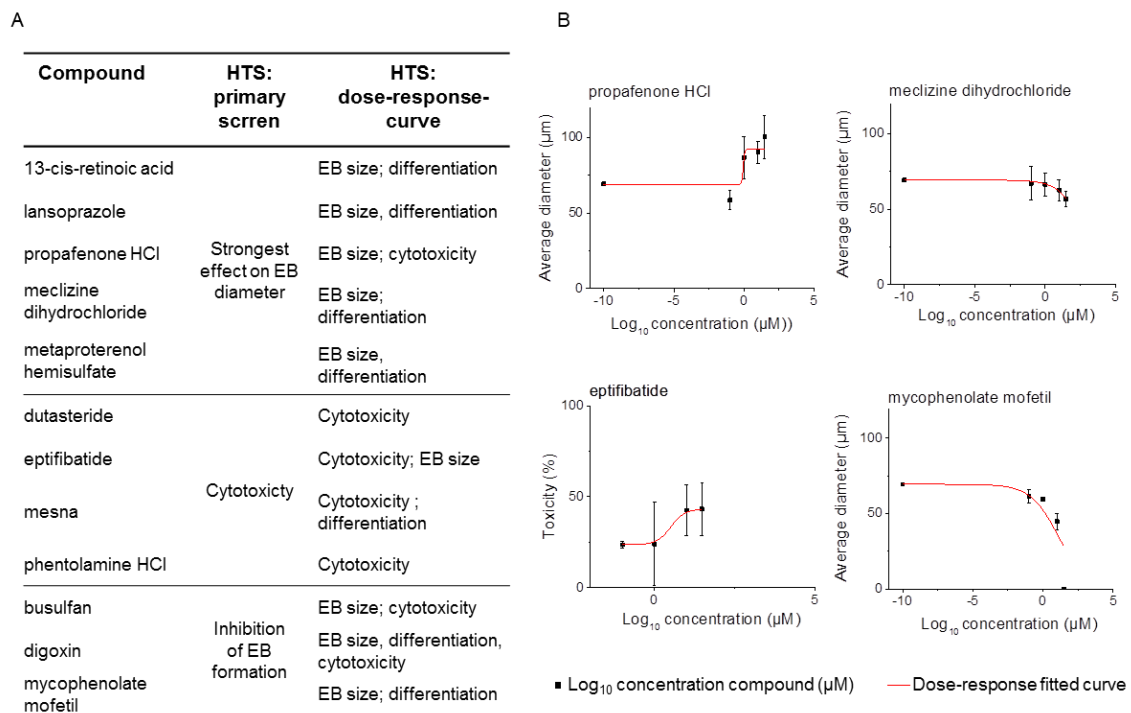
Figure 18. Screening of 12 hit compounds identified during HTS: primary screen. (A) Table showing 12 hit compounds chosen from primary screen for consecutive run of dose-response-curve test with effect observed during primary and dose-response-curve screen. Compounds were chosen on their effect on EB formation, EB diameter, and cytotoxicity. (B) Fitted dose-response-curves for 4 (propafenone HCl, mycophenolate mofetil, eptifibatide, meclizine dihydrochloride) out of 12 hit compounds showing effect on EB size, toxicity and differentiation. Concentrations used were 0.1 μM, 1 μM, 10 μM and 30 μM, with each concentration in 4 replicates. Internal controls were empty spots and vector controls containing DMSO in respective concentration (1%). As experimental control served an empty DMA slide. Incubation time of mESC Oct4-eGFP in hanging droplets with compounds was 72 h. N=3.

A strong effect on toxicity was observed upon treatment with eptifibatide, resulting in an increase by ~20% from 1 µM to 30 µM (Figure 18B). However only slight dose dependent effect of eptifibatide was observed on EB size, and no dose dependent effect on roundness and stemness, indicating a sole cytotoxic effect of the compound. In regard of the toxic effect of some of the residual compounds high standard deviations due to strong variances between the respective replicates was shown (Figure A 9). This can be due to the way of imaging and the 3 dimensionality of the EBs. In order to ensure data assessment of all compounds in a timely manner, the imaging of EBs had to be reduced to single plane, which can result in imaging of planes in varying z-positions between the individual replicates and in turn to different percentages of viable and dead cells depending on the position within the EB. Another possible factor influencing the measurement of viable and dead cells could be, that during imaging of a 3D object the fluorescent signal emitted by stained cells lying underneath the current plane could also be detected and measured during imaging. However, the overall presented results demonstrate qualitative correlation of the obtained data with previous screenings conducted using conventional methods such as the "hanging drop" method. For quantitative comparison between HTS on EBs using the Droplet Microarray and conventional methods, further experiments have to be performed. All in all the presented data prove the applicability of the library-DMA for HTS of EBs, enabling investigation of compound dependent effects on embryonic development and embryotoxicity.

Table 9. Summary of the effect of selected FDA-approved compounds based on studies using embryonic stem cells (2D) or embryoid bodies (3D).

Compound		Reference
13-cis-retinoic acid	Neuronal and adipogenic differentiation; reduced EB size (tested range 0.1 – 100 µM)	(Dani *et al.*, 1997; Hong *et al.*, 2015; Warkus *et al.*, 2016)
lansoprazole	Osteoblastic differentiation (tested range 5 – 1000 µM)	(Costa-Rodrigues *et al.*, 2013; Mishima *et al.*, 2015)
propafenone HCl	Moderate embryotoxic (tested range 10 1000 µg/mL)	(Paquette *et al.*, 2008)
busulfan	Strong embryotoxic (tested range: 0.001 – 10 µg/mL)	(Mehta *et al.*, 2008; Murdter *et al.*, 2001)
digoxin	Cytotoxic in ESCs (used 2.5 µM)	(Lin *et al.*, 2017)
mycophenolate mofetil	Osteoblastic differentiation (tested range 1 – 25 µM)	(Darcy *et al.*, 2012)

4 Conclusion and Outlook

In this PhD work two artificial substrates, bacterial cellulose and a chemically defined porous poly(2-hydroxyethyl methacrylate-*co*-ethylene dimethacrylate) (HEMA-EDMA), were exploited for culturing mouse embryonic stem cells (mESC), showing the potential to promote mESC stemness over short-term and long-term culture conditions through their micro- and nanostructured as well as porous surface. In order to investigate this, a transgenic mouse embryonic stem cell line, stably expressing GFP fused to the pluripotency gene Oct 4 (mESC Oct4-eGFP), was used. These stem cells allow for the direct read-out of the differentiation state of the mESC using fluorescence microscopy. For both materials, the results indicated significant facilitation of mESC culture and, in the case of the HEMA-DMA substrate, the ability to perform high-throughput screening of stem cells was demonstrated.

In the first part, the potential of the bacterial cellulose derived from *Komagataeibacter xylinus* to maintain the undifferentiated state of mESC was investigated. Bacterial cellulose is widely used in tissue engineering, transplantation and regenerative medicine as scaffold material for cell transfer or directed differentiation. In particular, the latter finds high importance in the field of stem cell research, as controlled differentiation and maintenance of stemness *in vitro* still remains challenging and precise regulation of multiple parameters is required in order to maintain their undifferentiated state. In case of mESC culture, these requirements include precoating of the culture vessel to provide sufficient cell attachment, regular cell passaging to prevent overgrowth that induces differentiation, medium supplementation with leukemia inhibitory factor known to inhibit differentiation and the use of mitotically inactivated mouse embryonic fibroblasts (MEFs) that provide cell attachment sites and secrete soluble factor promoting stemness. This demonstrates how laborious, time consuming and costly mESC culture is using conventional culture methods. By using bacterial cellulose it was possible, to culture mESC without gelatin coating and mitotically inactivated MEFs for up to 72 h, maintaining the mESCs' undifferentiated state and significantly facilitating culture conditions in comparison to conventional culture. Furthermore, the application of bacterial cellulose showed improved maintenance of stemness with delay of spontaneous differentiation during long-term culture (17 days) of mESC. The observed influence can be attributed to an enhanced cell attachment to the substrate based on the biochemical and structural properties,

believing surface roughness, thickness and liquid absorbing capacity of the bacterial cellulose to be important contributors to the maintenance of stemness. However, further experiments have to be conducted to elucidate the precise underlying mechanism resulting in enhanced cell attachment and maintenance of stemness. The application of bacterial cellulose in stem cell culture significantly reduces costs and facilitates mESC culture compared to conventional methods. Future combination of photopatterning methodologies or preparation of bacterial cellulose composites could allow investigation of stem cells upon different geometries and composite materials, while maintaining the undifferentiated state of mESCs by its surface topography. Thereby, the application of bacterial cellulose as a flexible membrane material of high purity, biocompatibility and the possibility for scalable manufacturing possesses the potential to advance stem cell research.

As mentioned before, culturing and maintaining stemness *in vitro* are still challenging and require precisely controlled conditions (Jeon *et al.*, 2012; Llames *et al.*, 2015). Hence, a lot of research is done in order to elucidate the underlying mechanisms of differentiation and screening for further factors promoting stemness. High-throughput screening of compounds maintaining stemness as well as investigation of the underlying mechanisms of differentiation are usually conducted in microtiter plates (96-, 384-, 1536-well plates), which entail high consumption of reagents and valuable cells (Ankam *et al.*, 2013; Fernandes *et al.*, 2009). The restricted availability of stem cells makes high-throughput screening of stem cells using conventional microtiter plates challenging and creates the urge for miniaturization required to reduce the amount of cells needed for an experiment (Du *et al.*, 2016; Mayr & Fuerst, 2008; Nirmalanandhan & Sittampalam, 2009). In the second part of this work, the highly chemically defined nanorough and porous HEMA-EDMA substrate was applied. This polymer exhibits a dual-functionality, namely the potential to inhibit mESC differentiation through its surface topography (Jaggy *et al.*, 2015) and the ability to generate arrays of microdroplets (Droplet Microarray) *via* the effect of discontinuous dewetting. The latter is a result of the ability to create patterns of hydrophilic and superhydrophobic areas that exhibit extreme and opposite degrees of wettability and dewettability. It was possible to culture and maintain pluripotent mESCs in the absence of mitotically-inactivated MEFs inside of nano-to-microliter sized droplets of the Droplet Microarray, providing a MEF-free array system for screening and investigation of mESCs. The Droplet Microarray enables culture of mESC in individual droplets of 80 nL volume resulting in

a 20 x volume reduction compared to 1536-well plates (~ 1500 nL) and at least 125 x reduction compared with 384-well plates, which is the most commonly used plate format. However, longer cultivation periods (> 72 h) in a volume of 80 nL as well as a further volume reduction (e.g. by us of 500 µm spots with ~ 9 ± 2 nL) can result in decreased viability based on increased lack of nutrient over time and a reduced volume per cell ratio, respectively. Investigation of mESC development, differentiation, and maintenance of stemness using the Droplet Microarray showed the dependence of stem cell behavior on droplet volume in nano- and microliter scale. An increased cell growth rate of mESC cultured on the platform and the inhibition of spontaneous differentiation of mESCs cultured on the Droplet Microarray, as indicated by the Oct4-eGFP expression level, was observed. The difference in the behavior of mESCs is attributed on the porous polymer´s nanorough surface (Jaggy *et al.*, 2015). The results demonstrate that the Droplet Microarray possesses the potential for the screening of mESCs under conditions of prolonged inhibition of stem cells' spontaneous differentiation. Hence, the Droplet Microarray can be a useful platform for applications in the field of stem cell research and high-throughput screening of stem cells with chemical libraries, identifying compounds with effect on stemness that can further improve stem cell culture and enable stem cell expansion. Furthermore, through the improved maintenance of stemness based on the polymer's nanorough surface and the ability for screening and separate treatment of the mESCs in the individual droplets with a multitude of compounds, the Droplet Microarray can be a useful platform in biomedical research as well as in the field of regenerative medicine and tissue engineering.

Screening systems resembling a more natural environment are gaining more and more importance as they enable generation of robust and biomedical more relevant results during the process of drug discovery (Liu *et al.*, 2016; Manganelli *et al.*, 2014). Main approaches in developing such systems are executed using various materials that enable a more precise modulation of the mechanical and physical properties of the microenvironment such as hydrogels or other polymeric materials (Giobbe *et al.*, 2012). Besides the mechano-physical properties, cell-cell interaction has been shown to be another important factor influencing cell development and behavior. Hence, a lot of research is devoted to the development of 3D cell models, in which cells are in direct contact interacting with each other or other cell types, such as in spheroids or in organoids (Becavin *et al.*, 2016; Liu *et al.*, 2016; Nierode *et al.*, 2016). In case of

embryonic stem cells, embryoid bodies (EBs) represent such a 3D model with close resemblance to the *in vivo* state as EBs recapitulate the early embryonic development and are able to differentiate into multiple cell derivatives of the three germ layers, endo-, meso- and ectoderm (Pettinato *et al.*, 2015). The use of EBs in drug screenings is of high importance because of the possibility to identify and exclude compounds showing developmental toxicity in an early stage of drug discovery, further increasing drug safety and reducing the use of *in vivo* testing for drug discovery. However, current methods used for screening of EBs, such as low adherence plate and "hanging drop" method, have several drawbacks, reducing their applicability in drug screening. In order to perform high-throughput screening of EBs conventional methods require multiple pipetting steps as well as high amount of expensive compounds and valuable cells (Kurosawa, 2007). The limited availability and restricted expandability of stem cells further complicates high-throughput screening of EBs using the previously mentioned conventional methods. In the third part of this PhD work, the Droplet Microarray platform was exploited for its potential in conducting high-throughput screening of cells in defined, nanoliter sized droplets, significantly reducing the amount of cells and reagents needed, and its possibility in forming multiple and homogeneous EBs through single step pipetting. The latter can be achieved by applying a mESC cell suspension on the superhydrophobic-hydrophilic micropattern of the Droplet Microarray resulting in immediate formation of multiple, separated microdroplets containing cells, followed by inverted culture of the mESCs in hanging microdroplets on the Droplet Microarray leading to formation of a dense array for high-throughput screening containing multiple single EBs (~63% of single EBs per array). This embryoid bodies array was applied in a high-throughput screen of 774 compounds of the FDA-approved drug library as well as a subsequent secondary screen (dose-response-curve screen) identifying compounds with effect on embryonic development (e.g. propafenone HCl, mycophenolate mofetil) and embryotoxicity (e.g. eptifibatide). Thereby a uniform dissolving rate of the respective compounds was assumed. However, variable dissolving rates that can result from differences in solubility of the compounds cannot fully be excluded. Furthermore differences in the dissolving rate can be based on variable diffusion of the compounds through the gelatin coating, which was primarily used to reduce cross-contamination during the seeding procedure. For quantitative assessment of the dissolving rate within the various compounds further experiments have to be conducted. The in the third part of the PhD work presented results demonstrate that the Droplet Microarray is a useful

platform facilitating and accelerating investigations of embryonic development and embryotoxicity using embryoid bodies, which can help to advance biomedical relevant drug screenings, increase drug safety and reduce the use of premature *in vivo* testing during early stages of drug discovery.

In conclusion it can be said that despite the progress and the presented achievements in the field of biofunctional materials for high-throughput screening of stem cells a lot of challenges still have to be overcome to further facilitate and accelerate progress in drug discovery, tissue engineering and regenerative medicine. In future, I am planning to utilize the Droplet Microarray with its defined physico-chemical properties and its superhydrophobic-hydrophilic micropattern as miniaturized platform for ultra-high-throughput screening on more complex cellular systems, such as organoids. Thus, through the use of more complex cellular systems an even stronger resemblance of the *in vivo* microenvironment can be achieved, resulting in more biomedical relevant drug screenings. Further I am planning to combine the inherent miniaturization and possibility for high-throughput screenings of the Droplet Microarray with the use of a non-contact cell printer, eliminating the risk of cross-contamination and enabling accurate deposition of variable cell types into the hydrophilic spots with high regulation of cell number and cell culture volume. In addition, this allows investigation and high-throughput drug screening within defined, complex co-culture systems, possessing the potential of precise modulation and resemblance of the *in vivo* microenvironment. To summarize the combination of novel, highly chemically defined, biofunctional materials with the ability for miniaturized high-throughput screening are promising systems that can accelerate drug discovery and advance research progress in stem cell research, biomedicine, tissue engineering and regenerative medicine.

5 Appendix

5.1 Bacterial cellulose promotes long-term stemness of mESC
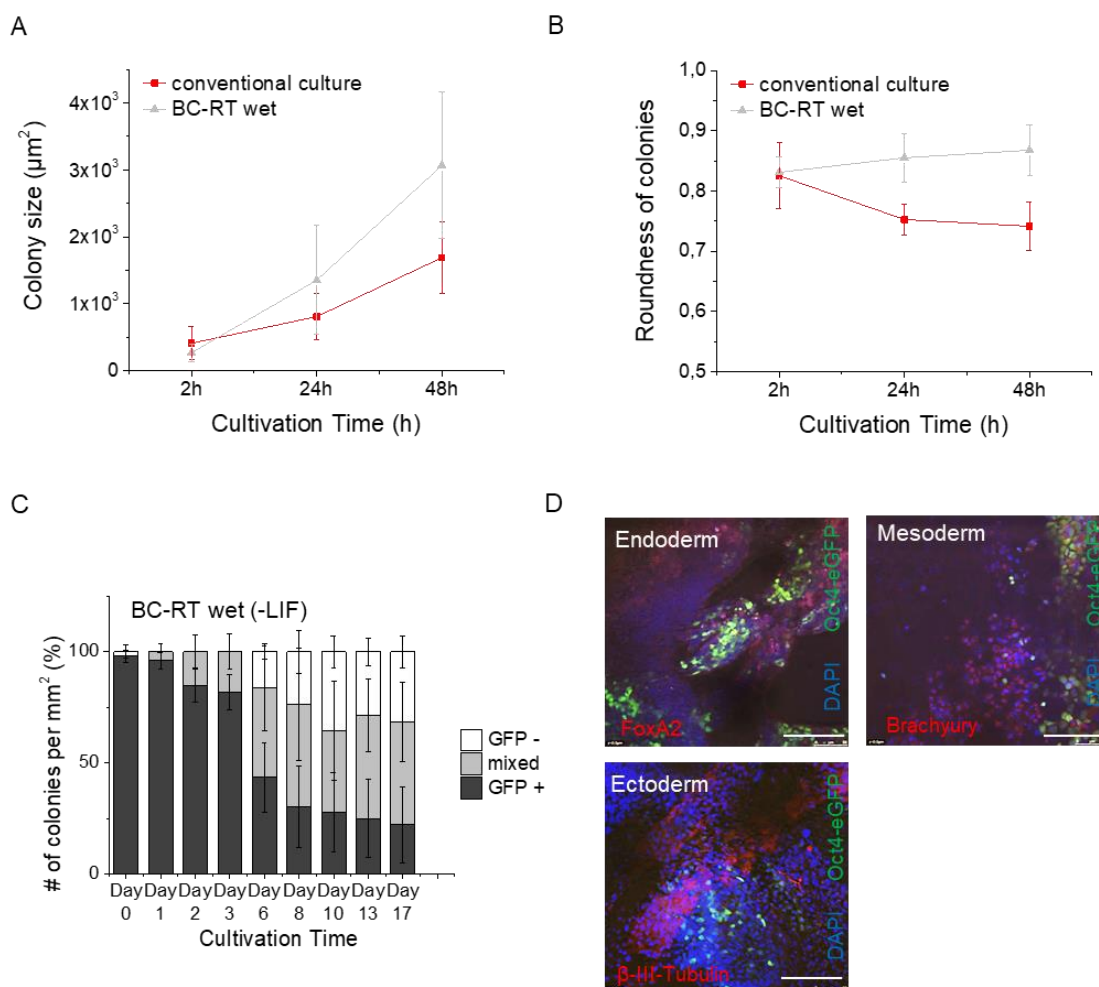
Figure A 1. Characterization of mESC Oct4-eGFP culture on BC-RT wet. (A) Assessment of colony size as indication for growth rate of mESC Oct4-eGFP under conventional culture and culture on BC-RT wet. (B) Roundness of mESC Oct4-eGFP colonies under conventional culture conditions (red line) and cultured on BC-RT wet (grey line). (C) Percentage of GFP+, mixed and GFP- colonies under culture on BC-RT wet in absence of LIF (Leukemia inhibitory factor). (D) Immunofluorescence staining showing potential of mESC Oct4-eGFP to differentiate into 3 germ layers (endo-, meso-, ectoderm) after being under conventional culture conditions. Cells were cultured for 6 days, detached and cultured for 48 h using "hanging drop" method to form embryoid bodies (EBs). EBs were transferred to fibronectin coated cover slips and cultured for 12 days. Subsequently immunofluorescence staining of endo-, meso- and ectoderm markers (FoxA2, Brachyury and β-III-Tubulin respectively) and cell nucleus (DAPI) was performed. Scale bar 100 μm.
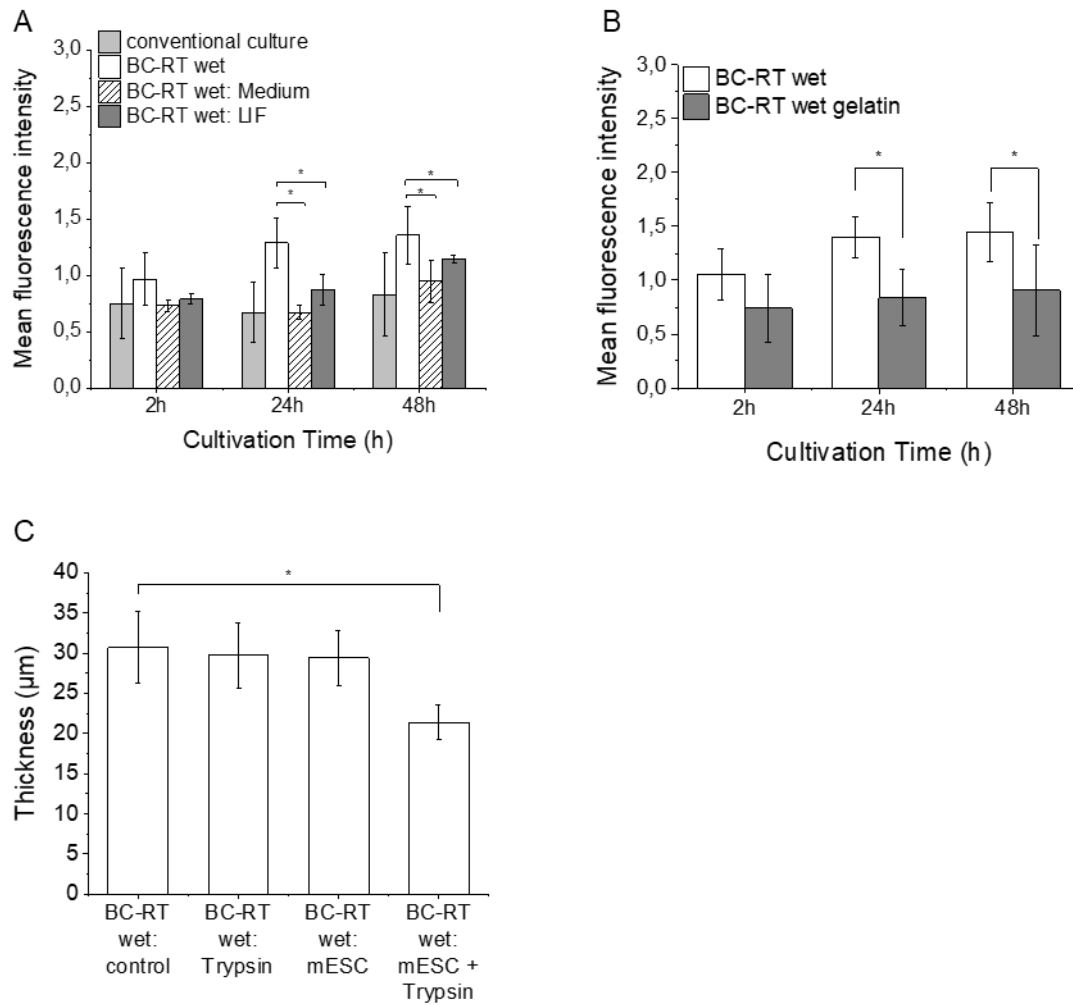
Figure A 2. Assessment of conditioning BC-RT wet. (A) Preconditioning of BC-RT wet with medium from 24 h culture of mESC Oct4-eGFP (BC-RT wet: Medium), with LIF alone (BC-RT wet: LIF) by incubation of BC with respective solutions before cell seeding. Mean fluorescence intensity measurement of mESC Oct4-eGFP when cultured under conventional conditions, on BC-RT wet, on with medium preconditioned BC-RT wet (BC-RT wet: Medium) and on with LIF preconditioned BC-RT wet (BC-RT wet: LIF). (B) Masking of surface structure and inhibiting direct cell contact *via* gelatin coating (BC-RT wet gelatin). Measurement of mean fluorescence intensity of mESC Oct4-eGFP cultured on gelatin masked BC-RT and untreated BC-RT wet. (C) Assessment of cellulose degradation through culture of mESC Oct4-eGFP on BC-RT wet. As control served cellulose that was never used for cell culture (BC-RT wet: control) and for 15 min with trypsin incubated BC (BC-RT wet: Trypsin). Thickness of the BC was measured before mESC Oct4-eGFP (BC-RT wet: mESC) detachment and after detachment using trypsin (BC-RT wet: mESC +Trypsin).

5.2 Droplet Microarray based on patterned superhydrophobic surfaces prevents stem cell differentiation and enables high-throughput stem cell screening

S1
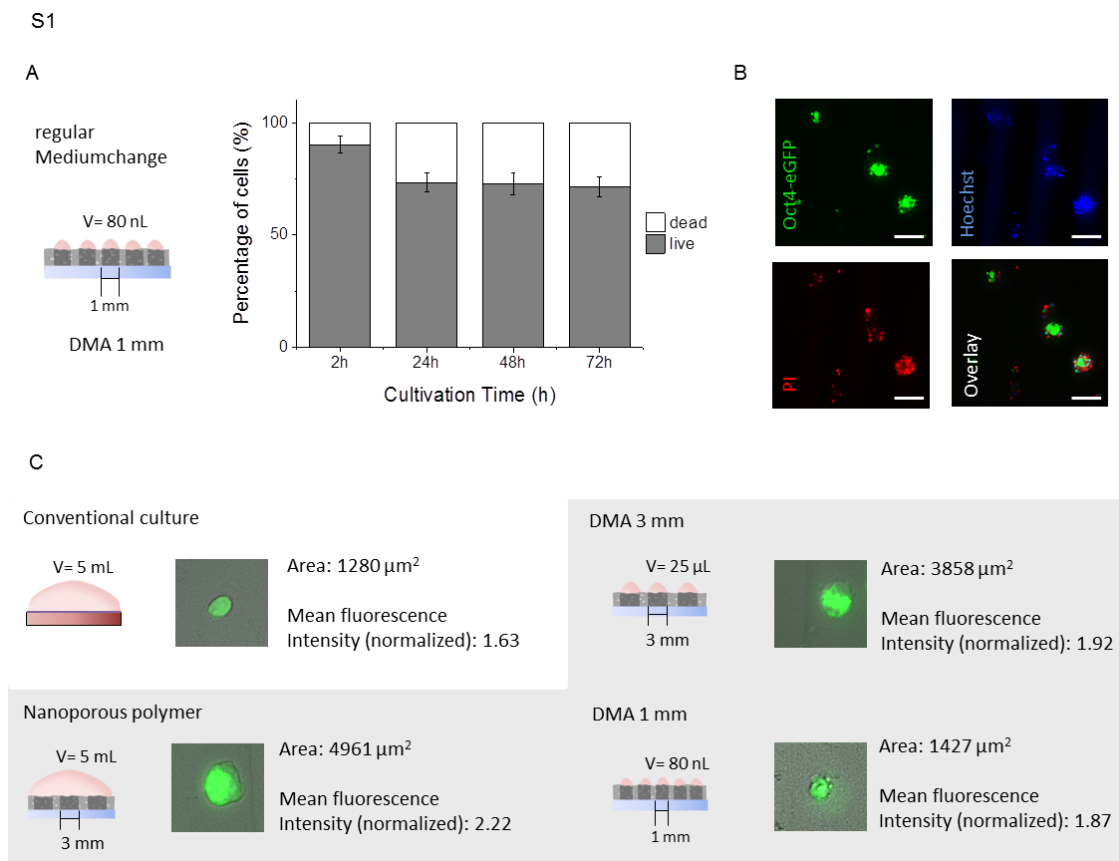
Figure A 3. Representative images showing viability staining and colony morphology upon different culture conditions. (A) Viability of mESC colonies grown in individual droplets on DMA with 1 mm spot size ~80 nL volume (-MEFs, +gelatin, +LIF) upon regular medium change. Medium was changed daily *via* rolling a drop of fresh medium over the array. Staining with propidium Iodide (PI) and Hoechst 33342 to assess the percentage and to count dead (PI+, Hoechst +) and live cells (PI-, Hoechst+). N=3; n >150 (B) Representative images of viability staining of mESC Oct4-eGFP with PI and Hoechst 33342. (C) Representative images showing mESC Oct4-eGFP colonies cultured under the different conditions. Area and mean fluorescence intensity of respective colonies is given and was measured using ImageJ. Mean fluorescence intensity was normalized to time point 0.
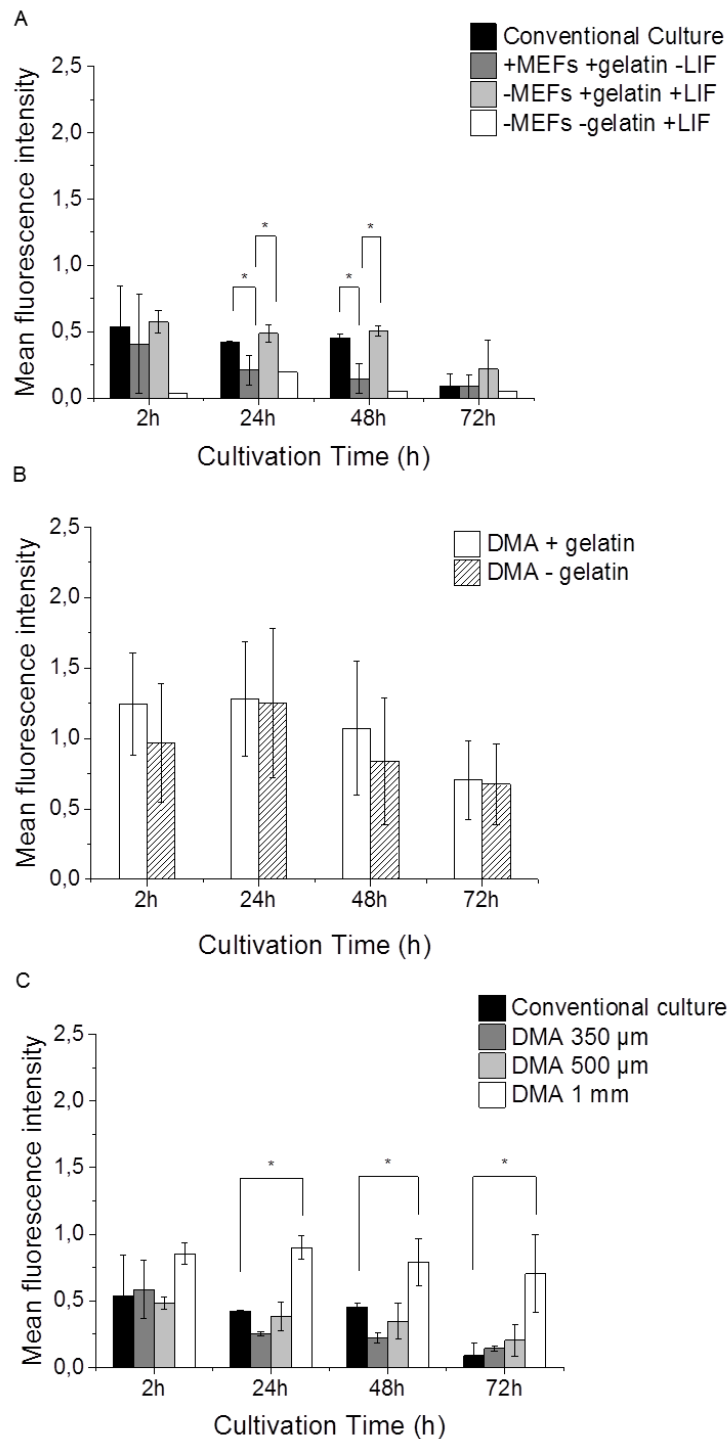
Figure A 4. Quantification of mESC Oct4-eGFP stemness. Measurement of the Oct4-eGFP mean fluorescence intensity obtained using image analysis software (ImageJ) (A) Mean fluorescence intensity of mESC upon culture under conventional conditions and in absence of LIF, MEFs or gelatin coating (B) Mean fluorescence intensity of mESC Oct4-eGFP culture on DMA 1 mm spot size with and without previous gelatin coating of polymer surface. (C) Mean fluorescence intensity of mESC Oct4-eGFP cultured on the DMA with 1 mm , 500 µm and 350 µm spot size in comparison to conventional culture conditions N=3; n >100 Statistical significance: t-test, *indicate p-value ≤0.05.
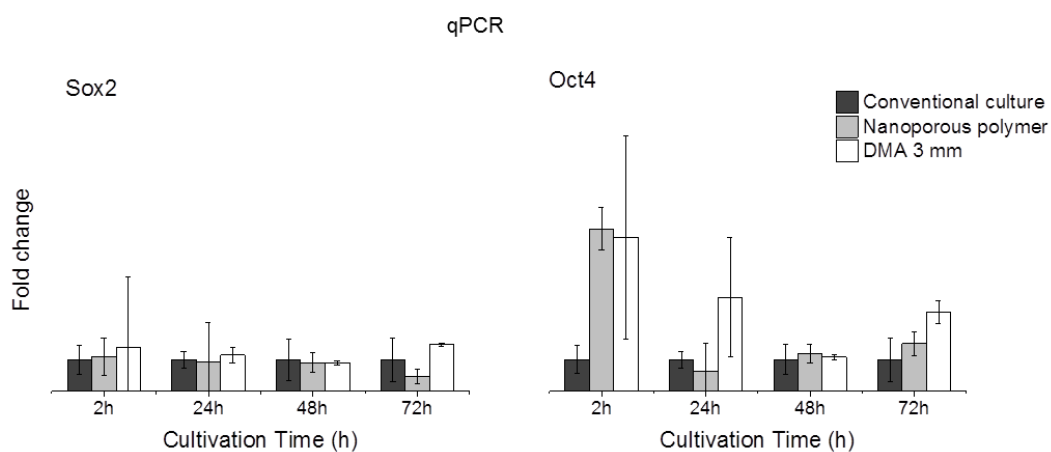
Figure A 5. Quantification of mESC stemness obtained through analysis of relative gene expression of pluripotency genes Sox2 and Oct4 using qPCR. Fold change normalized to conventional culture conditions. N=3

Table A 1. Gene specific primers used for amplification in qPCR experiment. Purchased from Metabion International AG (Planegg, Germany)

Gene	5' Primer	3' Primer
GAPDH	TCCCACTCTTCCACCTTCGATGC	GGGTCTGGGATGGAAATTGTGAGG
Oct4	GCAGGAGCACGAGTGGAAAGCAAC	CAAGGCCTCGAAGCGACAGATG
Sox2	CGAGATAAACATGGCAATCAAAT	AACGTTTGCCTTAAACAAGACCAC
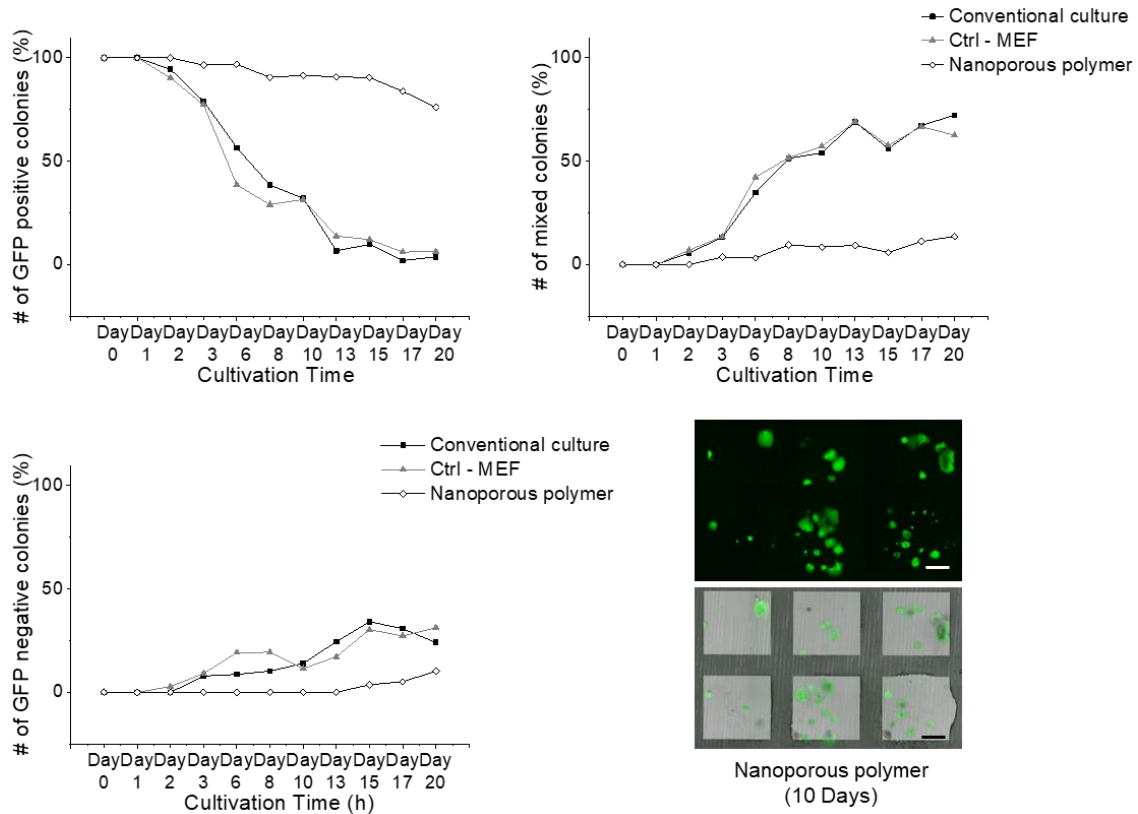
Figure A 6. Count of GFP+, mixed and GFP- colonies from the mESC Oct4-eGFP line long-term cultivated under conventional conditions, in absence of MEFs (Ctrl – MEF) and on the nanoporous polymer. Medium was changed every 48 h in all samples. 5 mL culture medium supplemented with LIF was used for all samples. Representative images (green channel and overlay with brightfield) showing mESC cultured on nanoporous polymer for 10 days. N=3, n > 100

5.3 Droplet Microarray: miniaturized platform for rapid formation and high-throughput screening of embryoid bodies

Table A 2. High-throughput screen (HTS): primary screen. Table showing results of 12 hit compounds from the primary screen with 774 FDA approved compounds. mESC Oct4-eGFP were cultured in hanging droplets using the DMA in presence of respective compounds for 72 h. mESC were stained with Hoechst 333442 (cell nucleus, for automated segmentation of embryoid bodies (EBs)) and propidium iodide (PI, dead cells). Evaluated and measured was the formation of EBs (yes/-), EB diameter (in µm), EB roundness, mean fluorescence intensity (MFI) of Oct4-eGFP of EBs as indication for differentiation and percentage of dead cells (PI positive) of total EB area as indication for toxicity.

Compound	EB formation	Diameter (µm)	Roundness (1-100)	Differentiation (MFI GFP)	Toxicity (% PI)
Control	Yes	85 ± 7	36 ± 3.5	71 ± 11	2
13-cis-retinoic acid	Yes	74 ± 21	23 ± 6	53 ± 23	29
lansoprazole	Yes	168 ± 2	19 ± 0	52 ± 11	0
meclizine dihydrochloride	Yes	41 ± 2	28 ± 15	29 ± 19	0
metaproterenol hemisulfate	Yes	45 ± 4	23 ± 15	23 ± 15	0
propafenone·HCl	Yes	172 ± 1	13 ± 8	77 ± 16	0
dutasteride	Yes	97 ± 21	51 ± 0	166 ± 84	20
eptifibatide	Yes	57 ± 9	40 ± 9	245 ± 84	22
mesna	Yes	74 ± 31	38 ± 18	13 ± 4	19
phentolamine·HCl	Yes	123 ± 34	16 ± 10	161 ± 72	36
busulfan	-	-	-	-	-
digoxin	-	-	-	-	-
mycophenolate mofetil	-	-	-	-	-
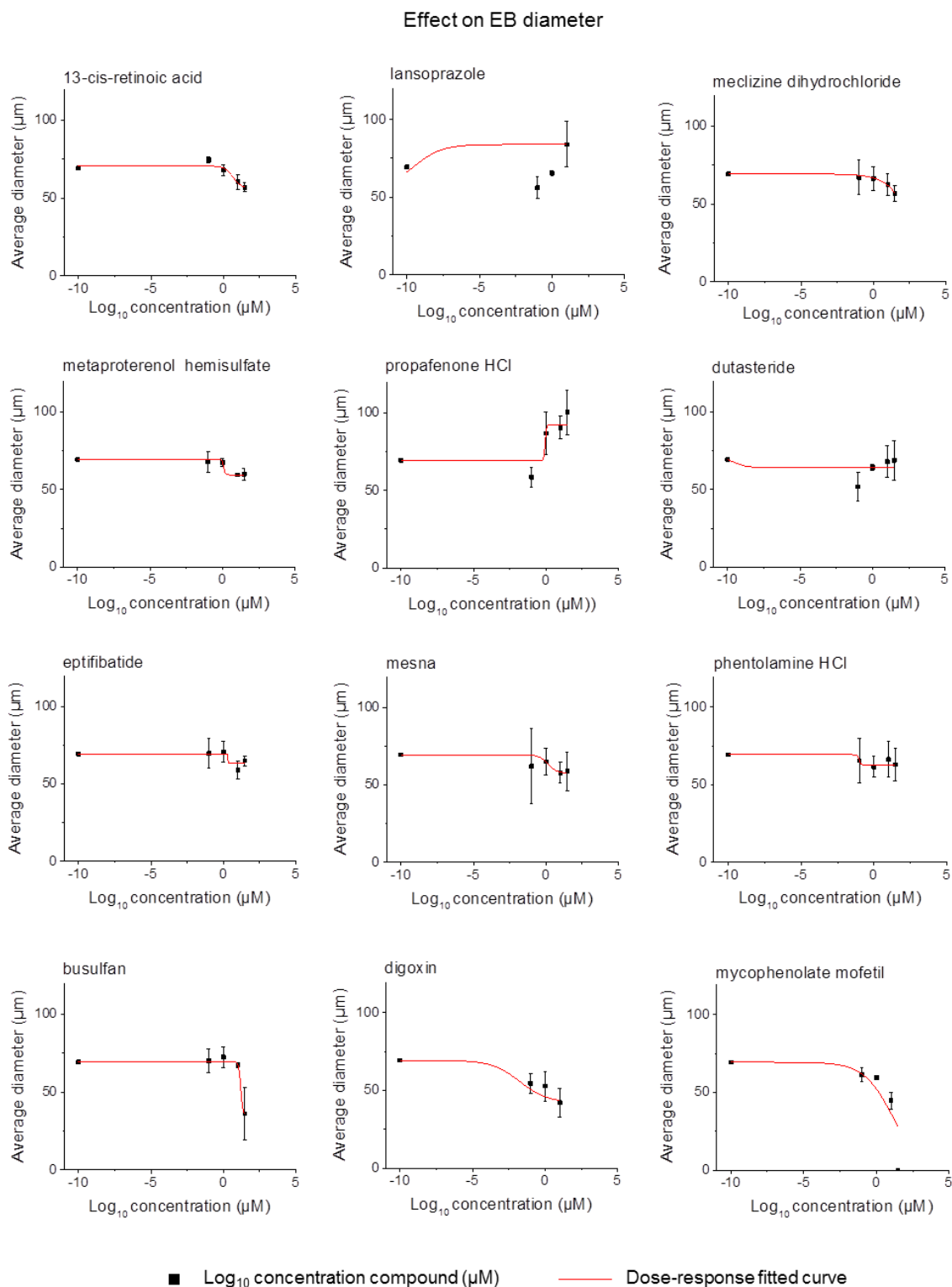
Figure A 7. Secondary screen: fitted dose-response-curve of 12 hit compounds (EB size). mESC Oct4-eGFP were cultured in presence of respective compounds in concentrations from 0.1 μM to 30 μM in hanging droplet using the DMA for 72 h. mESC were stained with Hoechst 333442 (cell nucleus, for automated segmentation of embryoid bodies (EBs)) and propidium iodide (PI, dead cells). Graphs show measured EB diameter (μm) for respective compounds and concentration. Fitted dose-response-curve is depicted as red line. n=4, N=3.

Effect on roundness
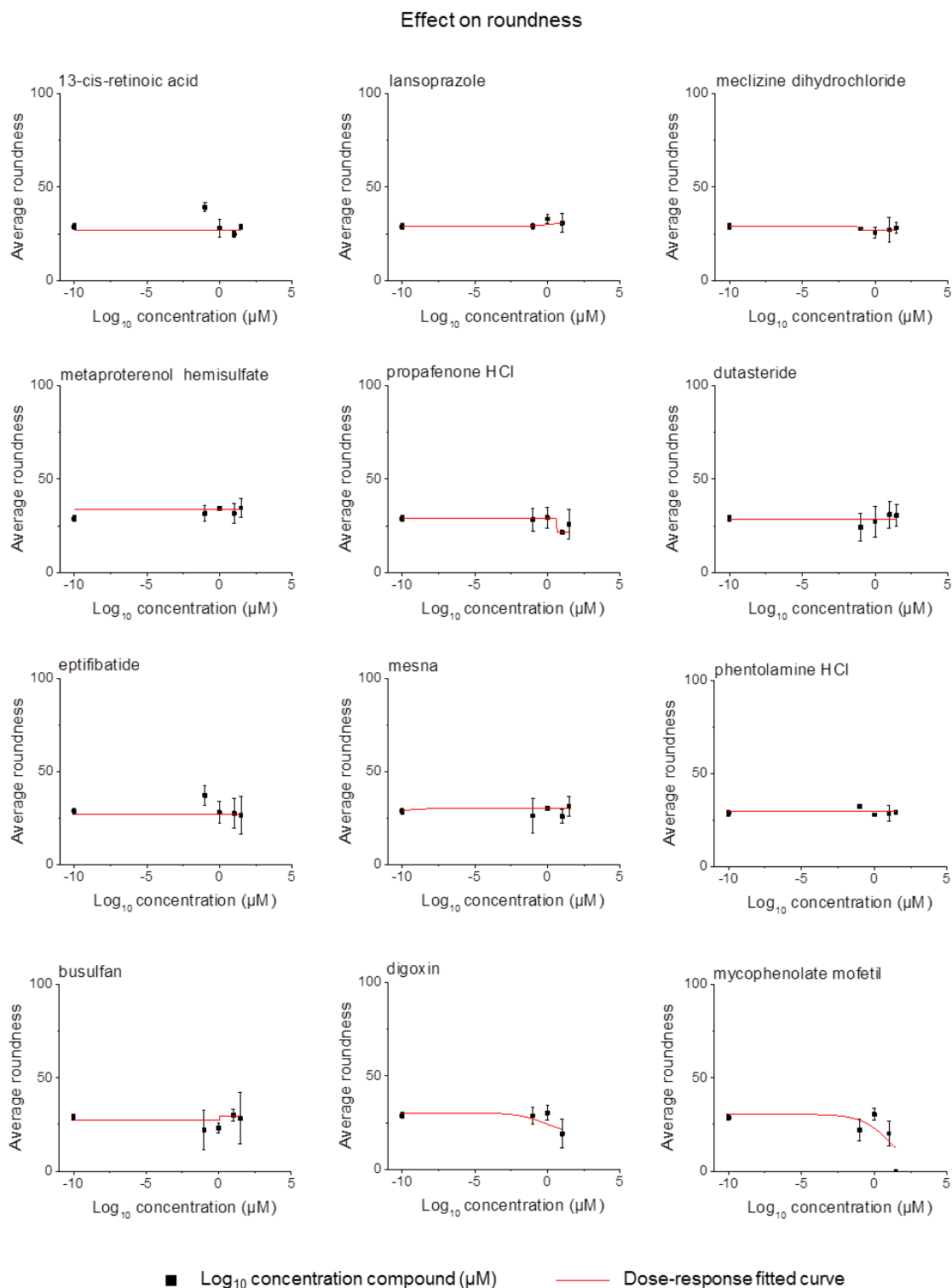
Figure A 8. Secondary screen: dose-response-curve of 12 hit compounds (roundness). mESC Oct4-eGFP were culture in presence of respective compounds in concentrations from 0.1 μM to 30 μM in hanging droplet using the DMA for 72 h. mESC were stained with Hoechst 333442 (cell nucleus, for automated segmentation of embryoid bodies (EBs)) and propidium iodide (PI, dead cells). Graphs show measured EB roundness (0-100) for respective compounds and concentration. Fitted dose-response-curve is depicted as red line. n=4, N=3.

Figure A 9. Secondary screen: dose-response-curve of 12 hit compounds (toxicity). mESC Oct4-eGFP were cultured in presence of respective compounds in concentrations from 0.1 µM to 30 µM in hanging droplet using the DMA for 72 h. mESC were stained with Hoechst 333442 (cell nucleus, for automated segmentation of embryoid bodies (EBs)) and propidium iodide (PI, dead cells). Graphs show toxicity of respective compounds in different concentrations (area fraction of PI positive cells from total EB area). n=4, N=3
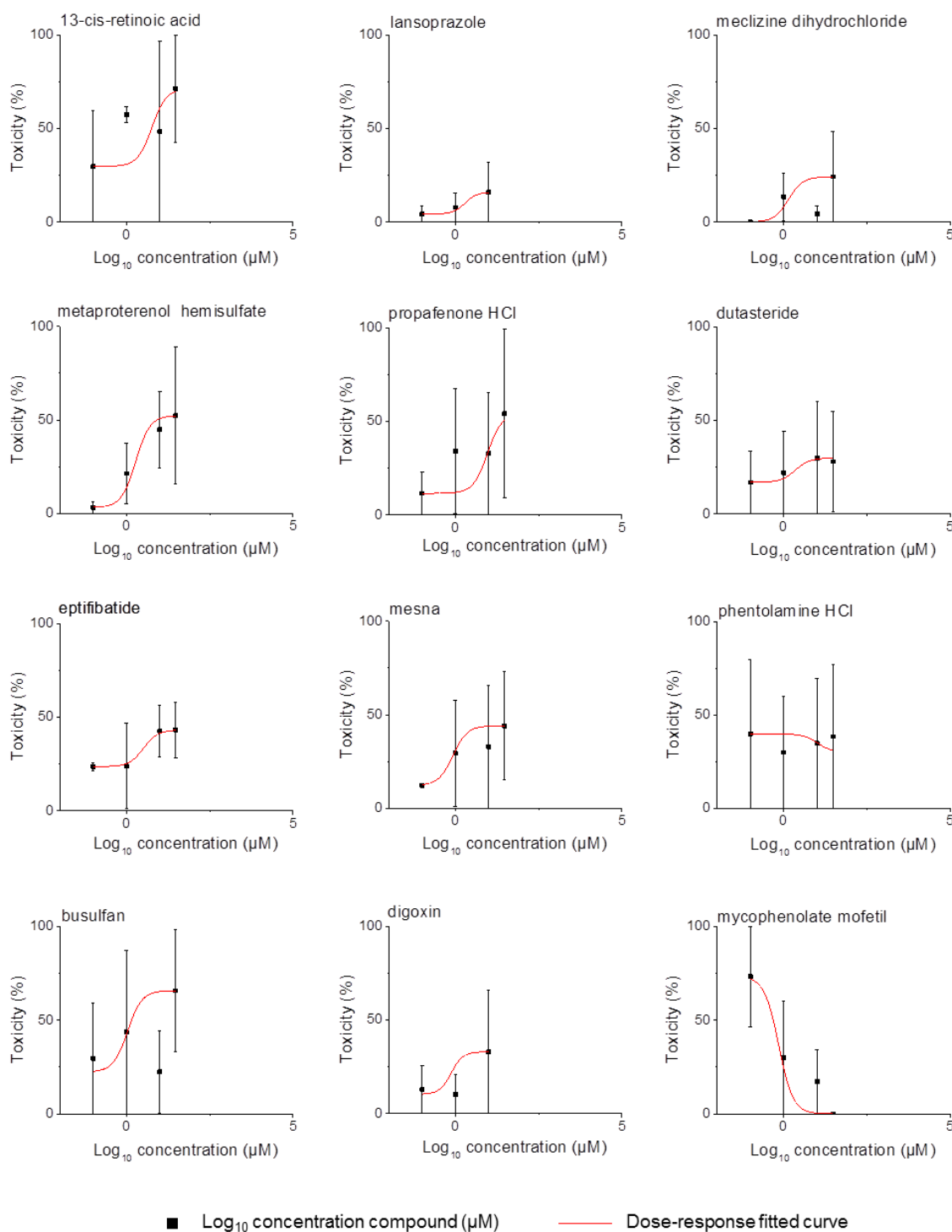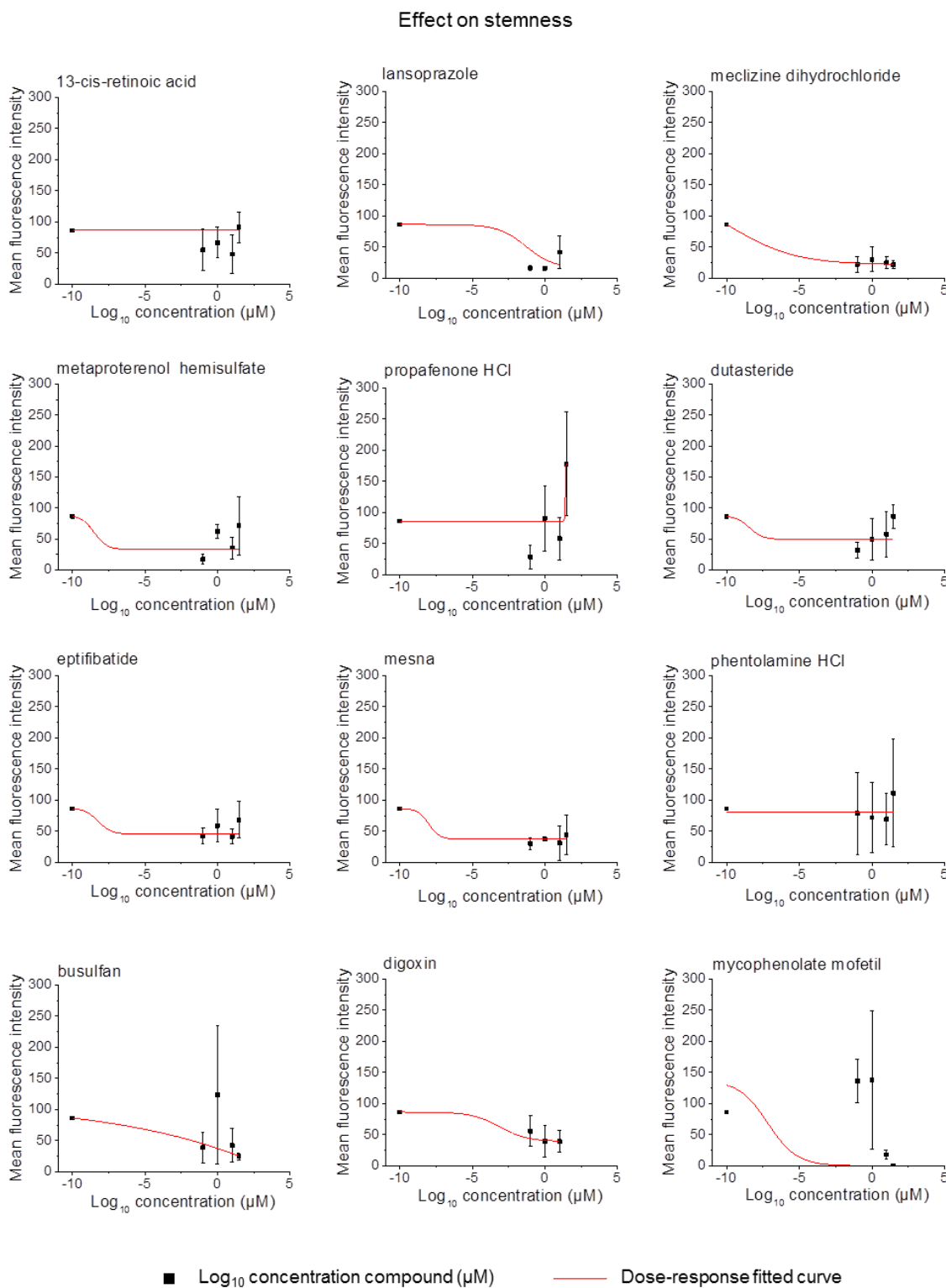
Figure A 10. Secondary screen: dose-response-curve of 12 hit compounds (stemness). mESC Oct4-eGFP were cultured in presence of respective compounds in concentrations from 0.1 μM to 30 μM in hanging droplet using the DMA for 72 h. mESC were stained with Hoechst 333442 (cell nucleus, for automated segmentation of embryoid bodies (EBs)) and propidium iodide (PI, dead cells). Graphs show mean fluorescence intensity of Oct4-eGFP signal for respective compounds and concentrations as indication for differentiation. Fitted dose-response-curve is depicted as red line. n=4, N=3.

References

Abdelalim, E. & Turksen, K. (2016). Stem Cell Biology and Regenerative Medicine.

Alberti, K., Davey, R. E., Onishi, K. & other authors (2008). Functional immobilization of signaling proteins enables control of stem cell fate. *Nat Methods* **5**, 645-650.

Ankam, S., Teo, B. K. K., Kukumberg, M. & Yim, E. K. F. (2013). High throughput screening to investigate the interaction of stem cells with their extracellular microenvironment. *Organogenesis* **9**, 128-142.

Arai, K., Eguchi, T., Rahman, M. M. & other authors (2016). A Novel High-Throughput 3D Screening System for EMT Inhibitors: A Pilot Screening Discovered the EMT Inhibitory Activity of CDK2 Inhibitor SU9516. *PLOS ONE* **11**, e0162394-e0162394.

Ardila, N., Medina, N., Arkoun, M., Heuzey, M. C., Ajji, A. & Panchal, C. J. (2016). Chitosan-bacterial nanocellulose nanofibrous structures for potential wound dressing applications. *Cellulose* **23**, 3089-3104.

Avior, Y., Sagi, I. & Benvenisty, N. (2016). Pluripotent stem cells in disease modelling and drug discovery. *Nat Rev Mol Cell Bio* **17**, 170-182.

Balikov, D. A., Crowder, S. W., Boire, T. C. & other authors (2017). Tunable Surface Repellency Maintains Stemness and Redox Capacity of Human Mesenchymal Stem Cells. *ACS Appl Mater Interfaces* **9**, 22994-23006.

Becavin, T., Kuchler-Bopp, S., Kokten, T., Huck, O., Messaddeq, N., Lesot, H., Deveaux, E., Benkirane-Jessel, N. & Laetitia, K. (2016). Well-organized spheroids as a new platform to examine cell interaction and behaviour during organ development. *Cell Tissue Res* **366**, 601-615.

Berthuy, O. I., Muldur, S. K., Rossi, F., Colpo, P., Blum, L. J. & Marquette, C. A. (2016). Multiplex cell microarrays for high-throughput screening. *Lab Chip* **16**, 4248-4262.

Bhardwaj, N. & Kundu, S. C. (2010). Electrospinning: A fascinating fiber fabrication technique. *Biotechnology Advances* **28**, 325-347.

Brafman, D. A., Phung, C., Kumar, N. & Willert, K. (2013). Regulation of endodermal differentiation of human embryonic stem cells through integrin-ECM interactions. *Cell Death Differ* **20**, 369-381.

Bratt-Leal, A. M., Carpenedo, R. L. & McDevitt, T. C. (2009). Engineering the Embryoid Body Microenvironment to Direct Embryonic Stem Cell Differentiation. *Biotechnol Progr* **25**, 43-51.

Buesen, R., Visan, A., Genschow, E., Slawik, B., Spielmann, H. & Seiler, A. (2004). Trends in improving the embryonic stem cell test (EST): an overview. *Altex-Altern Tierexp* **21**, 15-22.

Buesen, R., Genschow, E., Slawik, B., Visan, A., Spielmann, H., Luch, A. & Seiler, A. (2009). Embryonic Stem Cell Test Remastered: Comparison between the Validated EST and the New Molecular FACS-EST for Assessing Developmental Toxicity In Vitro. *Toxicol Sci* **108**, 389-400.

Ceriotti, L., Buzanska, L., Rauscher, H. & other authors (2009). Fabrication and characterization of protein arrays for stem cell patterning. *Soft Matter* **5**, 1406-1416.

Chagastelles, P. C. & Nardi, N. B. (2011). Biology of stem cells: an overview. *Kidney Int Suppl* **1**, 63-67.

Chen, Q. S., Wu, J., Zhuang, Q. C., Lin, X. X., Zhang, J. & Lin, J. M. (2013). Microfluidic isolation of highly pure embryonic stem cells using feeder-separated co-culture system. *Sci Rep-Uk* **3**.

Chien, S., Brafman, D. A. & Willert, K. (2011). Arrayed cellular microenvironments for identifying culture and differentiation conditions for stem, primary and rare cell populations. *Nature Protocols*.

Chung, B. G., Flanagan, L. A., Rhee, S. W., Schwartz, P. H., Lee, A. P., Monuki, E. S. & Jeon, N. L. (2005). Human neural stem cell growth and differentiation in a gradient-generating microfluidic device. *Lab Chip* **5**, 401-406.

Clausen, T. (2002). Acute stimulation of Na/K pump by cardiac glycosides in the nanomolar range. *J Gen Physiol* **119**, 295-296.

Clements, L. R., Wang, P. Y., Tsai, W. B., Thissen, H. & Voelcker, N. H. (2012). Electrochemistry-enabled fabrication of orthogonal nanotopography and surface chemistry gradients for high-throughput screening. *Lab Chip* **12**, 1480-1486.

Corradi, S., Dakou, E., Yadav, A., Thomassen, L. C., Kirsch-Volders, M. & Leyns, L. (2015). Morphological observation of embryoid bodies completes the in vitro evaluation of nanomaterial embryotoxicity in the embryonic stem cell test (EST). *Toxicol in Vitro* **29**, 1587-1596.

Costa-Rodrigues, J., Reis, S., Teixeira, S., Lopes, S. & Fernandes, M. H. (2013). Dose-dependent inhibitory effects of proton pump inhibitors on human osteoclastic and osteoblastic cell activity. *Febs J* **280**, 5052-5064.

Coyle, R., Jia, J. & Mei, Y. (2016). Polymer microarray technology for stem cell engineering. *Acta Biomaterialia* **34**, 60-72.

Darcy, A., Meltzer, M., Miller, J., Lee, S., Chappell, S., Donck, K. V. & Montano, M. (2012). A novel library screen identifies immunosuppressors that promote osteoblast differentiation. *Bone* **50**, 1294-1303.

Das, M., Ithychanda, S., Qin, J. & Plow, E. F. (2014). Mechanisms of talin-dependent integrin signaling and crosstalk. *Biochim Biophys Acta* **1838**, 579-588.

Deiss, F., Matochko, W. L., Govindasamy, N., Lin, E. Y. & Derda, R. (2014). Flow-Through Synthesis on Teflon-Patterned Paper To Produce Peptide Arrays for Cell-Based Assays. *Angewandte Chemie International Edition* **53**, 6374-6377.

Desbordes, S. C., Placantonakis, D. G., Ciro, A., Socci, N. D., Lee, G., Djaballah, H. & Studer, L. (2008). High-throughput screening assay for the identification of compounds regulating self-renewal and differentiation in human embryonic stem cells. *Cell Stem Cell* **2**, 602-612.

Du, G. S., Fang, Q. & den Toonder, J. M. J. (2016). Microfluidics for cell-based high throughput screening platformsd-A review. *Anal Chim Acta* **903**, 36-50.

Duffy, C., Venturato, A., Callanan, A., Lilienkampf, A. & Bradley, M. (2016). Arrays of 3D double-network hydrogels for the high-throughput discovery of materials with enhanced physical and biological properties. *Acta Biomaterialia* **34**, 104-112.

Dumont, C. M., Karande, P. & Thompson, D. M. (2014). Rapid Assessment of Migration and Proliferation: A Novel 3D High-Throughput Platform for Rational and Combinatorial Screening of Tissue-Specific Biomaterials. *Tissue Eng Part C-Me* **20**, 620-629.

Efe, J. A. & Ding, S. (2011). The evolving biology of small molecules: controlling cell fate and identity. *Philos T R Soc B* **366**, 2208-2221.

Esa, F., Tasirin, S. M. & Rahman, N. A. (2014). Overview of Bacterial Cellulose Production and Application. *Agriculture and Agricultural Science Procedia* **2**, 113-119.

Evans, M. J. & Kaufman, M. H. (1981). Establishment in Culture of Pluripotential Cells from Mouse Embryos. *Nature* **292**, 154-156.

Favi, P. M., Ospina, S. P., Kachole, M., Gao, M., Atehortua, L. & Webster, T. J. (2016). Preparation and characterization of biodegradable nano hydroxyapatite–bacterial cellulose composites with well-defined honeycomb pore arrays for bone tissue engineering applications. *Cellulose* **23**, 1263-1282.

Feng, W. Q., Li, L. X., Ueda, E., Li, J. S., Heissler, S., Welle, A., Trapp, O. & Levkin, P. A. (2014). Surface Patterning via Thiol-Yne Click Chemistry: An Extremely Fast and Versatile Approach to Superhydrophilic-Superhydrophobic Micropatterns. *Adv Mater Interfaces* **1**.

Fernandes, T. G., Diogo, M. M., Clark, D. S., Dordick, J. S. & Cabral, J. M. (2009). High-throughput cellular microarray platforms: applications in drug discovery, toxicology and stem cell research. *Trends Biotechnol* **27**, 342-349.

Flaim, C. J., Chien, S. & Bhatia, S. N. (2005). An extracellular matrix microarray for probing cellular differentiation. *Nat Methods* **2**, 119-125.

Floren, M. & Tan, W. (2015). Three-dimensional, soft neotissue arrays as high throughput platforms for the interrogation of engineered tissue environments (vol 59, pg 39, 2015). *Biomaterials* **67**, 204-204.

Gaharwar, A. K., Arpanaei, A., Andresen, T. L. & Dolatshahi-Pirouz, A. (2016). 3D Biomaterial Microarrays for Regenerative Medicine: Current State-of-the-Art, Emerging Directions and Future Trends. *Adv Mater* **28**, 771-781.

Geisel, N., Clasohm, J., Shi, X., Lamboni, L., Yang, J., Mattern, K., Yang, G., Schäfer, K. H. & Saumer, M. (2016). Microstructured Multilevel Bacterial Cellulose Allows the Guided Growth of Neural Stem Cells. *Small* **12**, 5407-5413.

Ghaemi, S. R., Harding, F., Delalat, B., Vasani, R. & Voelcker, N. H. (2013). Surface Engineering for Long-Term Culturing of Mesenchymal Stem Cell Microarrays. *Biomacromolecules* **14**, 2675-2683.

Gieseck, R. L., Colquhoun, J. & Hannan, N. R. F. (2015). Disease modeling using human induced pluripotent stem cells: Lessons from the liver. *Bba-Mol Cell Biol L* **1851**, 76-89.

Giobbe, G. G., Zagallo, M., Riello, M., Serena, E., Masi, G., Barzon, L., Di Camillo, B. & Elvassore, N. (2012). Confined 3D microenvironment regulates early differentiation in human pluripotent stem cells. *Biotechnol Bioeng* **109**, 3119-3132.

Gobaa, S., Hoehnel, S., Roccio, M., Negro, A., Kobel, S. & Lutolf, M. P. (2011). Artificial niche microarrays for probing single stem cell fate in high throughput. *Nat Methods* **8**, 949-955.

Gobaa, S., Hoehnel, S. & Lutolf, M. P. (2015). Substrate elasticity modulates the responsiveness of mesenchymal stem cells to commitment cues. *Integr Biol-Uk* **7**, 1135-1142.

Gracz, A. D., Williamson, I. A., Roche, K. C. & other authors (2015). A high-throughput platform for stem cell niche co-cultures and downstream gene expression analysis. *Nat Cell Biol* **17**, 340-+.

Gupta, K., Kim, D. H., Ellison, D., Smith, C., Kundu, A., Tuan, J., Suh, K. Y. & Levchenko, A. (2010). Lab-on-a-chip devices as an emerging platform for stem cell biology. *Lab Chip* **10**, 2019-2031.

Gupta, P. B., Onder, T. T., Jiang, G., Tao, K., Kuperwasser, C., Weinberg, R. A. & Lander, E. S. (2009). Identification of Selective Inhibitors of Cancer Stem Cells by High-Throughput Screening. *Cell* **138**, 645-659.

Harink, B., Le Gac, S., Truckenmuller, R., van Blitterswijk, C. & Habibovic, P. (2013). Regeneration-on-a-chip? The perspectives on use of microfluidics in regenerative medicine. *Lab Chip* **13**, 3512-3528.

Hayashi, Y., Furue, M. K., Okamoto, T. & other authors (2007). Integrins regulate mouse embryonic stem cell self-renewal. *Stem Cells* **25**, 3005-3015.

Heo, J., Lee, J. S., Chu, I. S., Takahama, Y. & Thorgeirsson, S. S. (2005). Spontaneous differentiation of mouse embryonic stem cells in vitro: Characterization by global gene expression profiles. *Biochem Bioph Res Co* **332**, 1061-1069.

Higuchi, A., Ling, Q. D., Kumar, S., Munusamy, M., Alarfajj, A. A., Umezawa, A. & Wu, G. J. (2014). Design of polymeric materials for culturing human pluripotent stem cells: Progress toward feeder-free and xeno-free culturing. *Prog Polym Sci* **39**, 1348-1374.

Horváth, L., Umehara, Y., Jud, C. & other authors (2015). Engineering an in vitro air-blood barrier by 3D bioprinting. *Sci Rep-Uk* **5**, 7974-7974.

Hu, J. Q., Gondarenko, A. A., Dang, A. P. & other authors (2016). High-Throughput Mechanobiology Screening Platform Using Micro- and Nanotopography. *Nano Letters* **16**, 2198-2204.

Huang, Y., Wang, J., Yang, F., Shao, Y., Zhang, X. & Dai, K. (2017). Modification and evaluation of micro-nano structured porous bacterial cellulose scaffold for bone tissue engineering.

Jackman, R. J., Duffy, D. C., Ostuni, E., Willmore, N. D. & Whitesides, G. M. (1998). Fabricating large arrays of microwells with arbitrary dimensions and filling them using discontinuous dewetting. *Anal Chem* **70**, 2280-2287.

Jaggy, M., Zhang, P., Greiner, A. M., Autenrieth, T. J., Nedashkivska, V., Efremov, A. N., Blattner, C., Bastmeyer, M. & Levkin, P. A. (2015). Hierarchical Micro-Nano Surface Topography Promotes Long-Term Maintenance of Undifferentiated Mouse Embryonic Stem Cells. *Nano letters* **15**, 7146-7154.

Jang, W. D., Hwang, J. H., Kim, H. U., Ryu, J. Y. & Lee, S. Y. (2017). Bacterial cellulose as an example product for sustainable production and consumption. *Microb Biotechnol* **10**, 1181-1185.

Jeon, J. S., Bersini, S., Gilardi, M., Dubini, G., Charest, J. L., Moretti, M. & Kamm, R. D. (2015). Human 3D vascularized organotypic microfluidic assays to study breast cancer cell extravasation (vol 112, pg 214, 2014). *P Natl Acad Sci USA* **112**, E818-E818.

Jeon, K., Oh, H. J., Lim, H., Kim, J. H., Lee, D. H., Lee, E. R., Park, B. H. & Cho, S. G. (2012). Self-renewal of embryonic stem cells through culture on nanopattern polydimethylsiloxane substrate. *Biomaterials* **33**, 5206-5220.

Jin, L., Xu, Q., Kuddannaya, S., Li, C., Zhang, Y. & Wang, Z. (2017). Fabrication and Characterization of Three-Dimensional (3D) Core–Shell Structure Nanofibers Designed for 3D Dynamic Cell Culture. *Acs Appl Mater Inter* **9**, 17718-17726.

Joddar, B. & Ito, Y. (2013). Artificial niche substrates for embryonic and induced pluripotent stem cell cultures. *J Biotechnol* **168**, 218-228.

Jones, G. (2015). Fitting and handling dose response data. *J Comput Aid Mol Des* **29**, 1-11.

Kang, L. F., Hancock, M. J., Brigham, M. D. & Khademhosseini, A. (2010). Cell confinement in patterned nanoliter droplets in a microwell array by wiping. *J Biomed Mater Res A* **93a**, 547-557.

Kang, P. H., Kumar, S. & Schaffer, D. V. (2017). Matrix degradation: Making way for neural stemness. *Nat Mater* **16**, 1174-1176.

Keller, G. (2005). Embryonic stem cell differentiation: emergence of a new era in biology and medicine. *Gene Dev* **19**, 1129-1155.

Kirchhof, N., Carnwath, J. W., Lemme, E., Anastassiadis, K., Scholer, H. & Niemann, H. (2000). Expression pattern of Oct-4 in preimplantation embryos of different species. *Biol Reprod* **63**, 1698-1705.

Kitambi, S. S. & Chandrasekar, G. (2011). Stem cells: a model for screening, discovery and development of drugs. *Stem Cells Cloning* **4**, 51-59.

Kobel, S. & Lutolf, M. P. (2010). High-throughput methods to define complex stem cell niches. *Biotechniques* **48**.

Kondo, M., Wagers, A. J., Manz, M. G., Prohaska, S. S., Scherer, D. C., Beilhack, G. E., Shizuru, J. A. & Weissman, I. L. (2003). Biology of hematopoietic stem cells and progenitors: Implications for clinical application. *Annu Rev Immunol* **21**, 759-806.

Kumar, A., Singh, S. K., Kumar, V., Kumar, D., Agarwal, S. & Rana, M. K. (2015). Huntington's disease: An update of therapeutic strategies. *Gene* **556**, 91-97.

Kurosawa, H., Imamura, T., Koike, M., Sasaki, K. & Amano, Y. (2003). A simple method for forming embryoid body from mouse embryonic stem cells. *J Biosci Bioeng* **96**, 409-411.

Kurosawa, H. (2007). Methods for inducing embryoid body formation: In vitro differentiation system of embryonic stem cells. *J Biosci Bioeng* **103**, 389-398.

Lanza, R. P. (2009). Essentials of stem cell biology, 2nd ed. edn. San Diego, Calif. ; London: Academic.

Laustriat, D., Gide, J. & Peschanski, M. (2010). Human pluripotent stem cells in drug discovery and predictive toxicology. *Biochem Soc Trans* **38**, 1051-1057.

Lee-Thedieck, C. & Spatz, J. P. (2014). Biophysical regulation of hematopoietic stem cells (vol 2, page 1796, 2014). *Biomater Sci-Uk* **2**, 1796-1796.

Lin, Y. T., Wang, C. K., Yang, S. C. & other authors (2017). Elimination of undifferentiated human embryonic stem cells by cardiac glycosides. *Sci Rep* **7**, 5289.

Liu, F. K., Huang, J., Ning, B., Liu, Z. X., Chen, S. & Zhao, W. (2016). Drug Discovery via Human-Derived Stem Cell Organoids. *Front Pharmacol* **7**.

Llames, S., Garcia-Perez, E., Meana, A., Larcher, F. & del Rio, M. (2015). Feeder Layer Cell Actions and Applications. *Tissue Eng Part B Rev* **21**, 345-353.

Lodish, H. F. a., Berk, A. a., Kaiser, C. a., Krieger, M. a., Bretscher, A. a., Ploegh, H. L. a., Amon, A. a. & Scott, M. P. a. Molecular cell biology, Seventh edition, International edition. edn.

Luo, W. & Yousaf, M. N. (2011). Developing a self-assembled monolayer microarray to study stem cell differentiation. *J Colloid Interf Sci* **360**, 325-330.

Lutolf, M. P., Gilbert, P. M. & Blau, H. M. (2009). Designing materials to direct stem-cell fate. *Nature* **462**, 433-441.

Macarron, R., Banks, M. N., Bojanic, D. & other authors (2011). Impact of high-throughput screening in biomedical research. *Nat Rev Drug Discov* **10**, 188-195.

Manganelli, G., Masullo, U. & Filosa, S. (2014). HTS/HCS to Screen Molecules Able to Maintain Embryonic Stem Cell Self-Renewal or to Induce Differentiation: Overview of Protocols. *Stem Cell Rev Rep* **10**, 802-819.

Martin, G. R. (1981). Isolation of a Pluripotent Cell-Line from Early Mouse Embryos Cultured in Medium Conditioned by Teratocarcinoma Stem-Cells. *P Natl Acad Sci-Biol* **78**, 7634-7638.

Mayr, L. M. & Fuerst, P. (2008). The future of high-throughput screening. *J Biomol Screen* **13**, 443-448.

Mehta, A., Konala, V. B. R., Khanna, A. & Majumdar, A. S. (2008). Assessment of drug induced developmental toxicity using human embryonic stem cells. *Cell Biol Int* **32**, 1412-1424.

Mei, Y., Saha, K., Bogatyrev, S. R. & other authors (2010). Combinatorial development of biomaterials for clonal growth of human pluripotent stem cells. *Nature Materials* **9**.

Mei, Y. (2012). Microarrayed materials for stem cells. *Mater Today* **15**, 444-452.

Mertaniemi, H., Escobedo-Lucea, C., Sanz-Garcia, A., Gandia, C., Makitie, A., Partanen, J., Ikkala, O. & Yliperttula, M. (2016). Human stem cell decorated nanocellulose threads for biomedical applications. *Biomaterials* **82**, 208-220.

Mishima, K., Kitoh, H., Ohkawara, B., Okuno, T., Ito, M., Masuda, A., Ishiguro, N. & Ohno, K. (2015). Lansoprazole Upregulates Polyubiquitination of the TNF Receptor-Associated Factor 6 and Facilitates Runx2-mediated Osteoblastogenesis. *Ebiomedicine* **2**, 2046-2061.

Moraes, C., Chen, J. H., Sun, Y. & Simmons, C. A. (2010). Microfabricated arrays for high-throughput screening of cellular response to cyclic substrate deformation. *Lab Chip* **10**, 227-234.

Murdter, T. E., Coller, J., Claviez, A., Schonberger, F., Hofmann, U., Dreger, P. & Schwab, M. (2001). Sensitive and rapid quantification of busulfan in small plasma volumes by liquid chromatography-electrospray mass spectrometry. *Clin Chem* **47**, 1437-1442.

Murphy, W. L., McDevitt, T. C. & Engler, A. J. (2014). Materials as stem cell regulators. *Nat Mater* **13**, 547-557.

Nagaoka, M., Koshimizu, U., Yuasa, S., Hattori, F., Chen, H., Tanaka, T., Okabe, M., Fukuda, K. & Akaike, T. (2006). E-Cadherin-Coated Plates Maintain Pluripotent ES Cells without Colony Formation. *Plos One* **1**.

Nam, S. H., Lee, H. J., Son, K. J. & Koh, W. G. (2011). Non-positional cell microarray prepared by shape-coded polymeric microboards: A new microarray format for multiplex and high throughput cell-based assays. *Biomicrofluidics* **5**.

Neto, A. I., Correia, C. R., Custodio, C. A. & Mano, J. F. (2014). Biomimetic Miniaturized Platform Able to Sustain Arrays of Liquid Droplets for High-Throughput Combinatorial Tests. *Adv Funct Mater* **24**, 5096-5103.

Niakan, K. K., Han, J. N., Pedersen, R. A., Simon, C. & Pera, R. A. R. (2012). Human pre-implantation embryo development. *Development* **139**, 829-841.

Nierode, G. J., Perea, B. C., McFarland, S. K., Pascoal, J. F., Clark, D. S., Schaffer, D. V. & Dordick, J. S. (2016). High-Throughput Toxicity and Phenotypic Screening of 3D Human Neural Progenitor Cell Cultures on a Microarray Chip Platform. *Stem Cell Rep* **7**, 970-982.

Nirmalanandhan, V. S. & Sittampalam, G. S. (2009). Stem cells in drug discovery, tissue engineering, and regenerative medicine: emerging opportunities and challenges. *J Biomol Screen* **14**, 755-768.

Paquette, J. A., Kumpf, S. W., Streck, R. D., Thomson, J. J., Chapin, R. E. & Stedman, D. B. (2008). Aassessment of the Embryonic Stem Cell Test and application and use in the pharmaceutical industry. *Birth Defects Res B* **83**, 104-111.

Patel, A. K., Tibbitt, M. W., Celiz, A. D., Davies, M. C., Langer, R., Denning, C., Alexander, M. R. & Anderson, D. G. (2016). High throughput screening for discovery of materials that control stem cell fate. *Curr Opin Solid St M* **20**, 202-211.

Pattinson, S. W. & Hart, A. J. (2017). Additive Manufacturing of Cellulosic Materials with Robust Mechanics and Antimicrobial Functionality. *Adv Mater Technol-Us* **2**.

Pettinato, G., Wen, X. J. & Zhang, N. (2015). Engineering Strategies for the Formation of Embryoid Bodies from Human Pluripotent Stem Cells. *Stem Cells Dev* **24**, 1595-1609.

Pieters, T. & van Roy, F. (2014). Role of cell-cell adhesion complexes in embryonic stem cell biology. *J Cell Sci* **127**, 2603-2613.

Popova, A. A., Schillo, S. M., Demir, K., Ueda, E., Nesterov-Mueller, A. & Levkin, P. A. (2015). Droplet-Array (DA) Sandwich Chip: A Versatile Platform for High-Throughput Cell Screening Based on Superhydrophobic-Superhydrophilic Micropatterning. *Adv Mater* **27**, 5217-5222.

Popova, A. A., Demir, K., Hartanto, T. G., Schmitt, E. & Levkin, P. A. (2016). Droplet-microarray on superhydrophobic-superhydrophilic patterns for high-throughput live cell screenings. *Rsc Adv* **6**, 38263-38276.

Popova, A. A., Depew, C., Permana, K. M., Trubitsyn, A., Peravali, R., Ordiano, J. A. G., Reischl, M. & Levkin, P. A. (2017). Evaluation of the Droplet-Microarray Platform for High-Throughput Screening of Suspension Cells. *Slas Technol* **22**, 163-175.

Raic, A., Rodling, L., Kalbacher, H. & Lee-Thedieck, C. (2014). Biomimetic macroporous PEG hydrogels as 3D scaffolds for the multiplication of human hematopoietic stem and progenitor cells. *Biomaterials* **35**, 929-940.

Ran, J., Jiang, P., Liu, S., Sun, G., Yan, P., Shen, X. & Tong, H. (2017). Constructing multi-component organic/inorganic composite bacterial cellulose-gelatin/hydroxyapatite double-network scaffold platform for stem cell-mediated bone tissue engineering. *Materials Science & Engineering C* **78**, 130-140.

Rodin, S., Antonsson, L., Hovatta, O. & Tryggvason, K. (2014). Monolayer culturing and cloning of human pluripotent stem cells on laminin-521-based matrices under xeno-free and chemically defined conditions. *Nat Protoc* **9**, 2354-2368.

Rosowski, K. A., Mertz, A. F., Norcross, S., Dufresne, E. R. & Horsley, V. (2015). Edges of human embryonic stem cell colonies display distinct mechanical properties and differentiation potential. *Sci Rep* **5**, 14218.

Seki, T. & Fukuda, K. (2015). Methods of induced pluripotent stem cells for clinical application. *World J Stem Cells* **7**, 116-125.

Shah, N., Ul-Islam, M., Khattak, W. A. & Park, J. K. (2013). Overview of bacterial cellulose composites: A multipurpose advanced material. *Carbohyd Polym* **98**, 1585-1598.

Shariati, S. R. P., Moeinzadeh, S. & Jabbari, E. (2016). Nanofiber Based Matrices for Chondrogenic Differentiation of Stem Cells. *Journal of Nanoscience and Nanotechnology* **16**, 8966-8977.

Simon, C. G. & Lin-Gibson, S. (2011). Combinatorial and High-Throughput Screening of Biomaterials. *Adv Mater* **23**, 369-387.

Sulaeva, I., Henniges, U., Rosenau, T. & Potthast, A. (2015). Bacterial cellulose as a material for wound treatment: Properties and modifications. A review. *Biotechnology Advances* **33**, 1547-1571.

Sultana, N. & Zainal, A. (2016). Cellulose acetate electrospun nanofibrous membrane: fabrication, characterization, drug loading and antibacterial properties. *B Mater Sci* **39**, 337-343.

Sun, Y., Chen, C. S. & Fu, J. (2012). Forcing stem cells to behave: a biophysical perspective of the cellular microenvironment. *Annu Rev Biophys* **41**, 519-542.

Takahashi, K. & Yamanaka, S. (2006). Induction of pluripotent stem cells from mouse embryonic and adult fibroblast cultures by defined factors. *Cell* **126**, 663-676.

Tarunina, M., Hernandez, D., Kronsteiner-Dobramysl, B. & other authors (2016). A novel high throughput screening platform reveals an optimised cytokine formulation for human hematopoietic progenitor cell expansion. *Stem Cells and Development* **25**, scd.2016.0216-scd.2016.0216.

Theunissen, T. W., Powell, B. E., Wang, H. & other authors (2014). Systematic Identification of Culture Conditions for Induction and Maintenance of Naive Human Pluripotency. *Cell Stem Cell* **15**, 524-526.

Thomson, J. A., Itskovitz-Eldor, J., Shapiro, S. S., Waknitz, M. A., Swiergiel, J. J., Marshall, V. S. & Jones, J. M. (1998). Embryonic stem cell lines derived from human blastocysts. *Science* **282**, 1145-1147.

Titmarsh, D. M., Ovchinnikov, D. A., Wolvetang, E. J. & Cooper-White, J. J. (2013). Full factorial screening of human embryonic stem cell maintenance with multiplexed microbioreactor arrays. *Biotechnol J* **8**, 822-+.

Tong, Z. X., Solanki, A., Hamilos, A., Levy, O., Wen, K., Yin, X. L. & Karp, J. M. (2015). Application of biomaterials to advance induced pluripotent stem cell research and therapy. *Embo J* **34**, 987-1008.

Tronser, T., Popova, A. A., Jaggy, M., Bastmeyer, M. & Levkin, P. A. (2017). Droplet Microarray Based on Patterned Superhydrophobic Surfaces Prevents Stem Cell Differentiation and Enables High-Throughput Stem Cell Screening. *Adv Healthc Mater*.

Tumarkin, E., Tzadu, L., Csaszar, E. & other authors (2011). High-throughput combinatorial cell co-culture using microfluidics. *Integr Biol-Uk* **3**, 653-662.

Ueda, E., Geyer, F. L., Nedashkivska, V. & Levkin, P. A. (2012). Droplet Microarray: facile formation of arrays of microdroplets and hydrogel micropads for cell screening applications. *Lab Chip* **12**, 5218-5224.

Ueda, E., Feng, W. & Levkin, P. A. (2016). Superhydrophilic-Superhydrophobic Patterned Surfaces as High-Density Cell Microarrays: Optimization of Reverse Transfection. *Adv Healthc Mater* **5**, 2646-2654.

Ullah, H., Wahid, F., Santos, H. A. & Khan, T. (2016). Advances in biomedical and pharmaceutical applications of functional bacterial cellulose-based nanocomposites. *Carbohyd Polym* **150**, 330-352.

van der Sanden, B., Dhobb, M., Berger, F. & Wion, D. (2010). Optimizing stem cell culture. *J Cell Biochem* **111**, 801-807.

Vince Z Beachley, M. T. W. K. S. S. S. M. H. J., Michael R Blatchley, J. S. B. A. P. D. P. & Jennifer, H. E. (2015). Tissue matrix arrays for high-throughput screening and systems analysis of cell function. *Nature*.

Viswanathan, P., Gaskell, T., Moens, N., Culley, O. J., Hansen, D., Gervasio, M. K. R., Yeap, Y. J. & Danovi, D. (2014). Human pluripotent stem cells on artificial microenvironments: a high content perspective. *Front Pharmacol* **5**.

Vrij, E. J., Espinoza, S., Heilig, M., Kolew, A., Schneider, M., van Blitterswijk, C. A., Truckenmuller, R. K. & Rivron, N. C. (2016). 3D high throughput screening and profiling of embryoid bodies in thermoformed microwell plates. *Lab Chip* **16**, 734-742.

Walker, M. R., Patel, K. K. & Stappenbeck, T. S. (2009). The stem cell niche. *J Pathol* **217**, 169-180.

Wang, L. N. & Kisaalita, W. S. (2010). Characterization of micropatterned nanofibrous scaffolds for neural network activity readout for high-throughput screening. *J Biomed Mater Res B* **94b**, 238-249.

Warkus, E. L., Yuen, A. A., Lau, C. G. & Marikawa, Y. (2016). Use of In Vitro Morphogenesis of Mouse Embryoid Bodies to Assess Developmental Toxicity of Therapeutic Drugs Contraindicated in Pregnancy. *Toxicol Sci* **149**, 15-30.

Watt, F. M. & Hogan, B. L. (2000). Out of Eden: stem cells and their niches. *Science* **287**, 1427-1430.

Williams, D. R., Kim, G.-H., Lee, M.-R. & Shin, I. (2008). Fluorescent high-throughput screening of chemical inducers of neuronal differentiation in skeletal muscle cells. *Nature Protocols*.

Wobus, A. M. & Loser, P. (2011). Present state and future perspectives of using pluripotent stem cells in toxicology research. *Arch Toxicol* **85**, 79-117.

Xiao, B., Ng, H. H., Takahashi, R. & Tan, E. K. (2016). Induced pluripotent stem cells in Parkinson's disease: scientific and clinical challenges. *J Neurol Neurosur Ps* **87**, 697-702.

Yu, J. Q., Huang, T. R., Lim, Z. H., Luo, R. C., Pasula, R. R., Liao, L. D., Lim, S. & Chen, C. H. (2016). Production of Hollow Bacterial Cellulose Microspheres Using Microfluidics to Form an Injectable Porous Scaffold for Wound Healing. *Advanced Healthcare Materials* **5**, 2983-2992.

Zeng, M., Laromaine, A. & Roig, A. (2014). Bacterial cellulose films: influence of bacterial strain and drying route on film properties. *Cellulose* **21**, 4455-4469.

Zhang, P., Zhang, J., Bian, S. & other authors (2016). High-throughput superhydrophobic microwell arrays for investigating multifactorial stem cell niches. *Lab Chip* **8**, 949-955.

Zhou, Q., Kuhn, P. T., Huisman, T., Nieboer, E., van Zwol, C., van Kooten, T. G. & van Rijn, P. (2015a). Directional nanotopographic gradients: a high-throughput screening platform for cell contact guidance. *Sci Rep* **5**, 16240.

Zhou, Q., Kühn, P. T., Huisman, T. & other authors (2015b). Directional nanotopographic gradients: a high-throughput screening platform for cell contact guidance. *Scientific Reports* **5**, 16240-16240.

Zonca, M. R., Yune, P. S., Heldt, C. L., Belfort, G. & Xie, Y. (2013). High-Throughput screening of substrate chemistry for embryonic stem cell attachment, expansion, and maintaining pluripotency. *Macromolecular Bioscience* **13**, 177-190.

Acknowledgements

I'm grateful for my supervisor Dr. Pavel Levkin, who gave me the opportunity to work on this interesting project within his group broadening my knowledge in the field of stem cell research and technology development. Thanks for the help and feedback during the numerous discussion throughout the whole PhD work.

I'm very thankful to Prof. Dr. Martin Bastmeyer for his supervision as "Erstgutachter" as well as for his guidance and help during our various discussions.

Furthermore, a special thanks to Dr. Cornelia Lee-Thedieck for being my TAC member and for all the valuables scientific discussion and advises.

Thanks to Dr. Mona Jaggy, Dr. Markus Reischl, Dr. Anna Laromaine and Dr. Anna Roig for their collaborative work, help, suggestions and expertise.

Thanks to all my colleagues, in particular: Dr. Anna Popova, Konstantin Demir, Dr. Wenqian Feng, Dr. Ana Isabel Morais Neto, Zheqin Dong, Marius Brehm, Dr. Lei Li, Farid Behboodi Sadabad, Alisa Rozenfeld, Maximilian Benz, Yanxi Liu, Wenxi Lei and Dorothea Paulssen. Thanks for the nice working atmosphere and all the discussion, both scientific and private.

Special thanks to my husband Tillmann Tronser, my parents, Armando and Irene Cruz, and my brother Tom Cruz, for always being there for me, encouraging me and supporting me in everything I did. I'm grateful to have such a wonderful and loving family.

Curriculum Vitae

Personal data

Name:	Tina Tronser (née Correia da Cruz)
Date of birth:	18.02.1990
Place of birth:	Pforzheim, Germany

Education

January 2015 - present	Karlsruhe Institute of Technology (KIT), Campus Nord, Institute of Toxicology and Genetics (ITG) PhD
October 2012 - October 2014	Eberhard-Karls University Tübingen, Master's degree in biology: molecular cell biology and immunology
October 2009 - August 2012	Eberhard-Karls University Tübingen, Bachelor's degree in biology
2000 – 2009	Hebel-Gymnasium Pforzheim, Abitur – university entrance qualification

Poster presentation

May 2017	Droplet Microarray - a superhydrophobic-hydrophilic microarray maintaining undifferentiated state of mESCs and enabling high-throughput screening of stem cells
	Advances in stem cells and regenerative medicine, EMBO conference, Heidelberg, Germany
February 2017	Droplet-Microarray: miniaturized, superhydrophobic-hydrophilic microarray maintaining undifferentiated mESCs via nanoporous surface enabling high-throughput screening of stem cells
	UMM-KIT Symposium
May 2016	Investigation of mouse embryonic stem cell (mESC) differentiation using the Droplet Microarray
	High content and phenotypic screening 2016, SELECTBIO conference, Cambridge, UK (poster prize)

<u>Publications</u>

Publications related to PhD thesis:

2017 / 2018

Tina Tronser, Anna A. Popova, Mona Jaggy, Martin Bastmeyer, Pavel A. Levkin
Droplet microarray based on patterned superhydrophobic surfaces prevents stem cell differentiation and enables high-throughput stem cell screening, Advanced Healthcare Materials, 2017, 1700622

Tina Tronser, Konstantin Demir, Markus Reischl, Martin Bastmeyer, Pavel A. Levkin
Droplet Microarray: miniaturized platform for rapid formation and high-throughput screening of embryoid bodies
-under preparation-

Tina Tronser, Anna Laromaine, Anna Roig, Pavel Levkin
Bacterial Cellulose promotes long-term stemness of mESC, ACS Applied Materials & Interfaces, 2018 10 (19), 16260-16269

Other Publications during PhD:

2017/2018

Tina Tronser, Anna A. Popova, Pavel A. Levkin
Miniaturized platform for high-throughput screening of stem cells, Curr Opin Biotechnol 46 (2017) 141-149

Anna Laromaine, **Tina Tronser**, Ivana Pini, Sebastià Parets, Pavel A. Levkin, Anna Roig

Free-standing three-dimensional hollow bacterial cellulose structures with controlled geometry via patterned hydrophobic-hydrophilic surfaces, Soft Matter, 2018, 14, 3955-3962

Lei Li, **Tina Tronser**, Connor Long, Konstantin Demir, Pavel A. Levkin

Inherently photodegradable polymethacrylate hydrogels for microfabrication -submitted-

2016

Gabriella E. Jogia, **Tina Tronser**, Anna A. Popova, Pavel A. Levkin

Droplet Microarray based on superhydrophobic-superhydrophilic patterns for single cell analysis, Microarrays 5(4) (2016)